# Processing of Interpenetrating Composites

by

## Suresh Talluri

A Thesis submitted
in partial fulfilment of the requirements
for the award of Degree of Master of Philosophy
of Loughborough University

December 2005

# ABSTRACT

Interpenetrating composites are emerging as a new class of materials due to their potential for displaying multifunctional properties. They consist of 3-dimensionally interpenetrating matrices of two different phases. In the present work the primary focus has been on ceramic/polymer composites though some work has also been done on ceramic/metal systems.

The ceramic/polymer composites have been produced by infiltrating alumina foams with polyester resin. The foams are made by mechanically agitating ceramic suspensions to entrain gases and then setting the structure via the *in-situ* polymerisation of the organic monomers. This resulted in the foams having a very open and interconnected structure that could be easily infiltrated using simple, low pressure systems. Both positive and negative pressures have been investigated, the former yielded higher final densities since the later encouraged the entrapment of gas within the liquid polymer that remained in the composite. A suitable polymer squeeze casting process was developed and processing parameters were optimised. To date, densities >95% of theoretical have been achieved using the positive pressure infiltration process; it is expected that this can be improved further as the processing is increasingly optimised. The resulting composites have been characterised by a range of microscopy techniques followed by mechanical testing. In addition to the practical investigations, an extensive literature survey was performed to find potential fields of application for the resulting composites.

The research work was also focused on the potential for developing piezoelectric devices with a lower modulus of elasticity than the pure ceramic phase by infiltrating $BaTiO_3$ preforms with a piezoelectric polymer, polyvinylidenefluoride. This involved investigating the production of $BaTiO_3$ foams. However, this was limited as the foams suffered from severe cracking. The reason for the cracking was not determined; further experiments would be needed and no further work was done on the infiltration of these foams with any of the polymers.

Interpenetrating ceramic/metal composites were successfully produced by infiltrating alumina foam preforms with LM25 alloy using squeeze casting. Densities >98% of theoretical and hardness increases of up to 43% over the component alloy were achieved. The pressure used in the squeeze casting trials was very high; values in the range of 100-150 MPa were required.

# ACKNOWLEDGEMENTS

# TABLE OF CONTENTS

# LIST OF TABLES

# LIST OF FIGURES

# CHAPTER 1:

# INTRODUCTION

## 1.1    History

In the centuries before Christ, our ancestors invented composites by mixing straw and clay to make bricks. The straw was the fibre reinforcement and the clay was the matrix. Today, in parts of the world, homes are made with the same material, using straw and vegetable fibre for reinforcement. We all remember the plaster ceilings and walls made in the past century with small rows of wooden slats to hold the plaster. Reinforcement of concrete with steel bars for construction has been used now for 150 years in bridge construction and buildings, in art and statues, etc [1].

The position of the reinforcement, orientation of the fibre in all of these products is very important in how they are engineered and developed. The properties of the composite depend on the matrix, the reinforcement and the boundary layer between the two, called the "interphase". Consequently, there are many variables to consider when designing a composite. These include the type of matrix, the type of reinforcement, their relative proportions, geometry of the reinforcement and the nature of the interphase [1]. Each of these variables must be carefully controlled in order to produce a structural material optimised for the conditions under which it is to be used.

## 1.2    A definition

A composite material is one that has a chemically and/or physically distinct phase distributed within a continuous phase [2]. The composite generally has characteristics better than or at least different from those of either component. The matrix phase is the continuous phase, while the distributed phase, commonly called the reinforcement phase, can be in the form of particles, whiskers or short fibres, continuous fibres or sheet. Figure 1.1 shows the types of composite based on the form of reinforcement. Composite materials are developed to reach properties that single materials cannot provide.
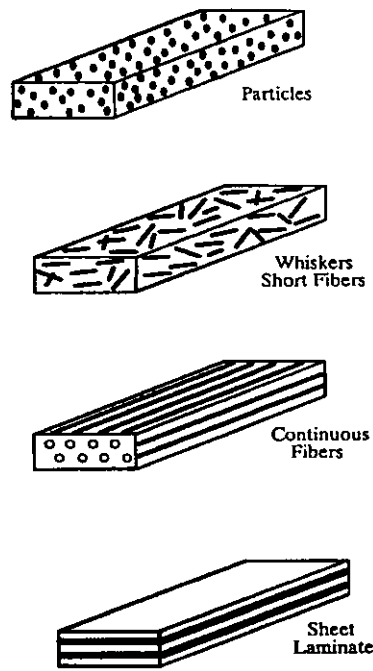
Figure 1.1: Types of composite based on the form of reinforcement [2].

Often it is convenient to classify different types of composites as per the matrix material characteristics, e.g. polymer matrix composites (PMCs), metal matrix composites (MMCs) and ceramic matrix composites (CMCs). The function of the reinforcement is more or less given with its name. The reinforcement has to support most of the external applied loads. The reinforcement in any matrix can be polymeric, metallic or ceramic. Polymer matrix composites containing reinforcement fibres such as carbon, glass or aramid are quite commonly used as engineering materials. Metals containing ceramic particles, whiskers or fibres (short or long) are also gaining importance. The ceramic matrix composites are the newest entrants in the composite field [2].

In most common cases composite materials have a chemically and/or physically distinct phase distributed within a continuous phase to improve its properties. The continuous basic material is called the matrix and the added material is described as the reinforcement, because the property improvement very often leads to a higher strength. The matrix holds the reinforcement material aligned while simultaneously keeping the reinforcements apart from each other. The reinforcement parts can be arranged in the best way to support the expected loads, e.g. fibres parallel to the tensile stress and the matrix makes sure that they act as separate entities. This is

important due to the following reasons. First, most of the reinforcement materials have a high strength because they are very small particles, whiskers, fibres or sheets. Especially ceramics, which are often used for reinforcement, develop their highest strength as fibres. Whiskers for example are produced as single crystals that have a theoretically perfect shape and dimensions. The remarkable increase in strength at small scales is in part a statistical phenomenon: the probability that a sample of material will contain a flaw large enough to cause brittle failure goes down as the sample size is reduced [3]. Clusters of reinforcement material inside the matrix would act as defects inside the matrix rather than strengthen it. Further the properties of the material would vary over the part, if the particles are not equally dispersed. Another reason is that the failure of one separated reinforcement does not affect the others, while a crack in a cluster or a fibre bundle could easily propagate through it. Further the matrix has to protect the reinforcement material from mechanical damage and chemical attack, like abrasion, oxidation and corrosion. Last but not least the matrix must transmit and distribute the external loads to the reinforcement.

Next to these two phases there is a third component in a composite that is of great importance for its quality – the interface between the matrix and the reinforcement. The interface between two solids, especially when thermal or chemical processes have been involved in putting them together, is rarely a simple boundary between two materials of quite different character. Over a certain range, which will vary in dimensions depending upon the chemical and physical natures of the fibres and the matrix, there will be some modification of either chemical or physical characteristics, or both, resulting in a region, perhaps only of molecular dimensions, perhaps many microns, which has properties quite different from those of either of the two major components [4]. The interface properties determine the manner in which stresses are transferred from matrix to fibres and in consequence, many of the chemical, physical and mechanical properties of the composite itself. Control of this interface or interface region, is a major concern to developers and suppliers of commercial composite materials. The strength of the interfacial bond between the fibres and the matrix may make all the difference between a satisfactory material and an inadequate one [4].

It becomes clear that the quality of the bond between the components of the composite defines the quality of the composite itself. If the bond is too weak the reinforcement material can easily act as a defect inside the matrix rather than

3

reinforcement, leading to worse properties than the matrix material itself. In the case of fibres, an elongation of the composite would lead to an elongation of the matrix while the fibres would just be pulled out of the matrix instead of supporting any load. On the other hand a strong bond is not the only thing that matters. For example, the combination of carbon-fibres as reinforcement and an aluminium-silicon alloy as matrix achieves a very high bond but the properties of the fibres are destroyed afterwards. The reaction between the carbon and the silicon is too strong to keep the structure of the carbon-fibres. The development of a composite must therefore also include an investigation of the reaction of the components under the given circumstances.

After the selection of the component phases of the composite, the second most important variable is the way the components are connected to each other. A different kind of connectivity can change the properties of composites drastically. For example, a composite material that is used to conduct current or heat in one spatial direction and simultaneously insulates it in the other directions. If the connectivity of the conducting material in one direction is disrupted the property of the material would change significantly. On the other hand, if the connectivity of the conducting material is diverted to another direction, the flow of the current or heat can reach other areas that may not bear it.

Another example is a fibre reinforced material where continuous fibres lie in the direction of the applied stress. A disconnection of them in one direction would decrease the strength of the material. It would also make no sense to increase the connectivity to another direction because if the applied stress acts perpendicular to the fibres it would just pull them apart.

Newnham et al. [5] describe the different levels of connectivity. Each component of a composite can be self-connected in zero, one, two or three dimensions. For a composite with two phases this leads to ten different kinds of connectivity from 0-0 to 3-3. These ten kinds of connectivity are shown in Figure 1.2. For composites with more than two phases the distribution of the connectivity is similar, but far more numerous. For three phase composites there are 20 different kinds of connectivity and for four phase composites there are 35. The number of connectivity patterns for n-phase composites can be calculated with the following equation [6]:

$$\frac{(n+3)!}{3!n!} \qquad\qquad 1.1$$
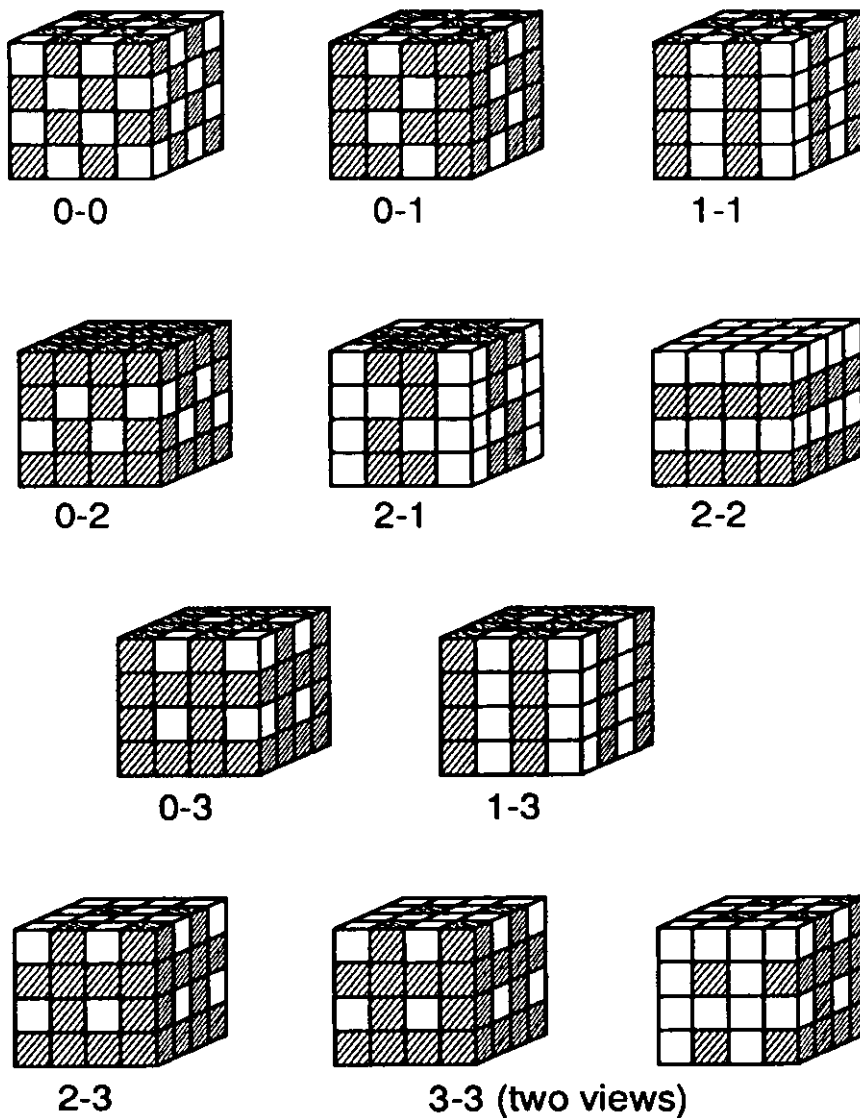
Figure 1.2: Ten different kinds of connectivity [6].

Some examples give an idea how some of these connectivities can be realised. Particles dispersed in a matrix have a 3-0 connectivity, e.g. SiC-particle strengthened alumina. Fibre reinforced material, where the fibres are arranged parallel to each other and in the direction of the expected stress, has a 3-1 connectivity. An example for a 2-2 connectivity is a composite that consists of two alternating layers.

The 3-3 connectivity is a great challenge for materials scientists, where the two phases form an interpenetrating three-dimensional network. This kind of composite has the advantage of a continuous second phase with high volume fraction. This is of great interest for applications where two different properties must be combined, e.g. a high

electrical conductivity together with a high strength. However, before these interpenetrating composites are produced and their properties are systematically investigated, the effect of the interpenetration and another continuous phase on the properties of the composite can only be assumed. At the very least, the development of these materials would also seem to offer opportunities for testing the detailed scientific understanding of composite materials, the processing issues involved, and the characterisation of the materials [6].

Although this kind of connectivity is relatively common in natural composites, e.g. coral and bones, there have been only a few attempts of creating this kind of composite synthetically.

The ceramic foam, with a complete pore interconnectivity, so that every pore is accessible from all other pores, possesses this 3-3 connectivity. The first phase is the three dimensional network of the ceramic material that builds the foam and the second phase is the air that is inside the pores. Using the infiltration process, the air will be replaced by the infiltration material, and a 3-3 connected composite will be achieved. Therefore, a ceramic foam used as a preform provides an encouraging basis for the production of a 3-3 connected composite.

## 1.3    Interpenetrating composites

The traditional approaches to making composite materials usually result in materials with microstructures consisting of discrete, dispersed, and isolated phases embedded in an otherwise homogeneous matrix material. Unless considerable ingenuity is taken, only dilute concentrations of a second phase can usually be incorporated. Reflecting the convergence of two of the dominant themes in material science today, recent developments in processing, aimed primarily at increasing the volume fraction of second phases, have raised the possibility of deliberately making composite materials in which each phase is continuous and interpenetrating through the microstructure [6]. In the terminology of percolation theory [7, 8, 9], each phase spans or percolates throughout the microstructure. In a practical sense, the size of regions of continuous phase becomes commensurate with the size of a piece of the material. The ability to fabricate, by design, such a three dimensional microstructure raises the possibility of developing materials with truly multifunctional characteristics: each phase contributing its own properties to the macroscopic properties of the composite. For instance, one

phase might provide strength to the material (high strength or wear resistance) and the other phase could provide the required property (electrical conductivity).

Although materials having an interpenetrating microstructure are relatively common in biology, for instance, as bones in mammals and the trunks and limbs of many plants, there are only relatively few that are synthetic. Among those that derive their properties from having an interpenetrating microstructure are certain spinodal alloys, for instance the Vycor$^{TM}$ glasses (Corning, Inc., Corning, NY), polycrystalline ceramics containing grain-boundary phases, some of the DIMOX$^{TM}$ materials from Lanxide Corporation (Newark, DE), and a number of carbon/carbon composites. Micrographs of two such materials are produced in Figure 1.3.
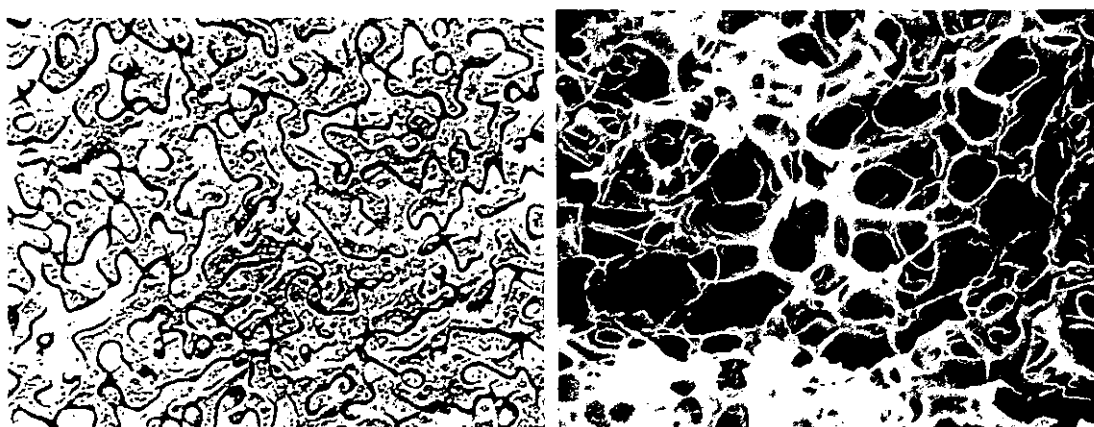


Figure 1.3: Examples of two materials having an interpenetrating microstructure [6]: (a) Replica TEM micrograph of a spinodally decomposed Vycor glass after leaching away the boron rich phase and (b) SEM micrograph of a zinc oxide-based varistor material after etching away the zinc oxide phase to reveal the remnant interpenetrating skeleton of bismuth oxide phase.

These microstructures also provide visual direction of some of approaches that may be contemplated in fabricating interpenetrating composites.

# 1.4    Aims and objectives of the project

This research aims to develop a process route for the successful production of ceramic-polymer and ceramic-metal interpenetrating composites. In order to achieve this goal, the specific objectives of the research were:

1. To develop an inexpensive and effective production process that was suitable for the infiltration of ceramic foams using vacuum/pressure assisted infiltration process for polymers and squeeze casting for low melting point metals.

2. To design and develop a suitable die for the successful infiltration of a selected polymer resin and alloy.

3. To characterise the preforms prior to the infiltration trials for porosity, cell and window size analysis and the end-products achieved, using a range of techniques such as electron microscopy, x-ray diffraction, impact and three point bend test, etc.

4. To investigate the effects of the structure and properties of the ceramic preforms, i.e. cell size and density, on the vacuum/pressure assisted infiltration parameters (polymer viscosity, gel time, temperature, etc.) and squeeze infiltration parameters (pressure, temperature, molten metal viscosity, preform preheating temperature, etc.).

5. To learn how to infiltrate successfully with one polymer and one alloy and to produce a sound composite, which was free from voids and defects.

6. To investigate, via the literature, potential applications for polymer and metal infiltrated foam ceramics.

# CHAPTER 2:

# LITERATURE SURVEY

## 2.1 Introduction

The physical and mechanical properties of any composite are strongly influenced by its final structure. Understanding a material's properties, the effect of processing parameters on the structure of the composite and how its behaviour changes when subject to different regimes is imperative in the design, operation and optimisation of all composite processing techniques.

This chapter describes in detail the history and evolution of polymer matrix and metal matrix composites, common production techniques for them, materials for their production, processing of interconnected porous ceramics and various infiltration principles. The effects of permeability, fluid flow, wettability, surface tension and also the effect of processing parameters like melt temperature, melt quality, die temperature, infiltration speed (metal velocity) and pressure applied on the structure, physical and mechanical properties of composites are addressed, followed by an extensive literature review of the conceivable applications for ceramic-polymer and ceramic-metal interpenetrating composites.

## 2.2 Porous ceramics

Since the earliest of times, ceramics have made the transition from simple utilitarian products, graduating into the first mass storage containers for wines and grains, to highly sought after ornamental treasures like service sets from Roman, Chinese and English artisans. Today's ceramics have moved from the dinner table and storage cabinet to the forefront of technology providing advanced superconducting wires, specialized space shuttle tiles that protect astronauts from the heat of re-entry, to the turbine blades that will lift your next jet flight into the air. For the most part, ceramics are thought of as dense, hard, extremely strong, functional shapes that fit the needs of man. These generic ceramic types are found in everything from cabinet pull

knobs and electric wire insulators to optical glass fibres, fine china and keepsakes such as dolls and figurines [10].

There are other ceramics, however, that are developed for their porous natures, that are "hydrophilic" (water loving) and provide capillary wicking and transport of polar substances like water. This unique class of ceramics has become extremely important in finding and measuring the fundamental relationships of liquid/gas/material interactions found in many naturally occurring environments. A porous ceramic is akin to many natural substances like plants, soils, rocks, outcrops, even bone. Such natural materials have crevices and pathways (pores) that allow liquids and gases to mix, migrate and flow. It is this unique porous structure of our ceramics that makes them ideal for instruments, processes or procedures that can replicate, measure or monitor these complex, long term interactions and relationships in our natural world.

Early porous ceramics were developed from high temperature porcelain "bisqueware" the ("fired" but unglazed) ceramic used in fine china. Other common recipes called for lower firing temperatures associated with talc/clay mixtures to produce a similar porous structure.

Porous ceramics can be grouped in two general categories: reticulate ceramics and foam ceramics [11]. A reticulate ceramic is a porous material comprised of interconnected voids surrounded by a web of ceramic; a foam ceramic has closed voids within a continuous ceramic matrix. These porous network structures have relatively low mass, low density, and low thermal conductivity.

Reticulate and foam ceramics differ in the property of permeability. Permeability is high in reticulate ceramics and low in foam ceramics. The difference is due to the open- versus closed cell structure. By combining the proper ceramic materials and processing, porous ceramics can also have high strength, high resistance to chemical attack, high-temperature resistance, and high structural uniformity. These properties make porous ceramics suitable for a variety of applications. The most common applications for open-cell (reticulate) porous ceramics are molten-metal and diesel engine exhaust filters. Reticulate ceramics are also used as catalyst supports and industrial hot-gas filters. Both reticulate and foam ceramics are used as light-structure plates, thermal-insulating materials, fire protection materials and gas combustion burners.

The interest in porous ceramics has increased concurrently with new processes and new applications. Porous ceramics have traditionally been used for thermal

insulation purposes and as building materials. Applications such as filters, catalyst support and membranes are currently rapidly growing markets owing to, among other things, environmental aspects. Porous ceramics are produced within a wide range of porosities and pore sizes depending on the application intended. Filters for molten metals often have pore sizes of 300-800 $\mu$m, whereas membranes for reverse osmosis have pore sizes of a few tenths of a nanometre [12].

## 2.2.1 Processing of interconnected porous ceramics

Although far from new, considerable interest has recently been generated in the fabrication of porous ceramics and polymers. Apart from their traditional use as refractories (because of their superior thermal shock resistance), porous ceramics have found widespread application as filters (for molten metals and fuels); light weight, impact-resistant materials; sound insulators; and catalyst supports. Porous, semi conducting oxides, such as stannic oxide and chromite spinel, are also widely used as humidity and gas sensors. By virtue of their lower dielectric constants, a number of interconnected porous ceramic are also now the subject of intensive research for substrate and radome applications.

The general development and the aims of investigation in the field of ceramics usually have been in the direction of producing dense and flaw free materials. This is due to the characteristic of brittle materials where the largest defect determines the strength of the material. However, the development and production of porous ceramics has recently been increased because of several interesting properties, which lead to various applications.

Although the fabrication of porous ceramics can be relatively straight forward, for instance, by sintering particles together to the desired density or alternatively, by foaming a ceramic slip, the central problem has been to produce materials having both high strength and low density. As in other brittle materials strength is generally determined by the largest flaw sizes, which in porous materials often corresponds to the extreme of the pore size distribution. In the context of the current paradigm relating strength to processing, greater control of both the rheology of the starting suspensions and their packing in the "green" state will be required to increase strength reliability and has already been widely discussed in the ceramics-processing literature [13,14].

Within the term porous ceramics, two different kinds can be distinguished. This difference has its origins in the type of porosity.

The microstructural porosity is the porosity that usually appears in ceramic materials if they are not completely densified during forming and sintering. This is characterised by voids between the ceramic grains, which are called pores. These pores are the kind of defects that have been tried to avoid during ceramic processing to increase the strength and reliability of ceramic parts. However, there are also some applications where this microporosity is desired, e.g. membranes.

The macroporosity is based on hollow cells inside the ceramic material that are produced during the forming process. These cells can vary in their form and size and further they can be connected to each other or separated. These appearances are described as open and closed cells, which lead to open or closed macroporosity. The areas between these cells consist of the ceramic material, which further can have a microstructural porosity or can be fully dense.

This report deals with the type of porous ceramics that is characterised by an open macroporosity. These ceramic foam structures are interesting for infiltration with metals or polymers because thereby an interconnected three-dimensional network of two different phases can be achieved. Therefore the following chapters describe only processing methods to produce cell like structures within a ceramic material. The main problem is the production of highly porous materials with a low density that simultaneously provide an acceptable strength.

## 2.2.1.1 Gel casting

This technique is based on the generation of a foam from an aqueous suspension of ceramic powder and the subsequent stabilisation of the structure by in situ polymerisation of organic monomers [15, 16]. The production of ceramic foams by this technique is outlined in the flowchart in Figure 2.1.

The aqueous suspension is prepared by blending the ceramic powder with an organic monomer and dispersing agent in water. Commonly applied types of organic monomers are methyl metacrylate, butyl acrylate, acryl amide, and other acrylates [15]. The mixture is thoroughly dispersed and homogenised. To stabilise the foamed structure a surfactant is added to the suspension. The molecular configuration of the surfactants consists of a hydrophilic part and a hydrophobic part. Therefore the

.molecules settle at the interfaces between the liquid and the gas phases and reduce the surface tensions of these interfaces. This stabilises the existing bubbles for the long time that is required for setting.

```
┌─────────────────────────────────────────────────────────┐
│      Ceramic Powder, Organic Monomers, Water and Dispersants      │
└─────────────────────────────────────────────────────────┘
                              │
                              ▼
                  ┌───────────────────────┐
                  │   Ceramic Suspension   │
                  └───────────────────────┘
                              │
                              ▼
                      ┌───────────────┐
                      │    Forming     │
                      └───────────────┘
                              │
                              ▼
                  ┌───────────────────────┐
                  │    Polymerisation      │
                  └───────────────────────┘
                              │
                              ▼
              ┌───────────────────────────────┐
              │      Removal from Mould         │
              └───────────────────────────────┘
                              │
                              ▼
              ┌───────────────────────────────┐
              │      Drying and Sintering       │
              └───────────────────────────────┘
```
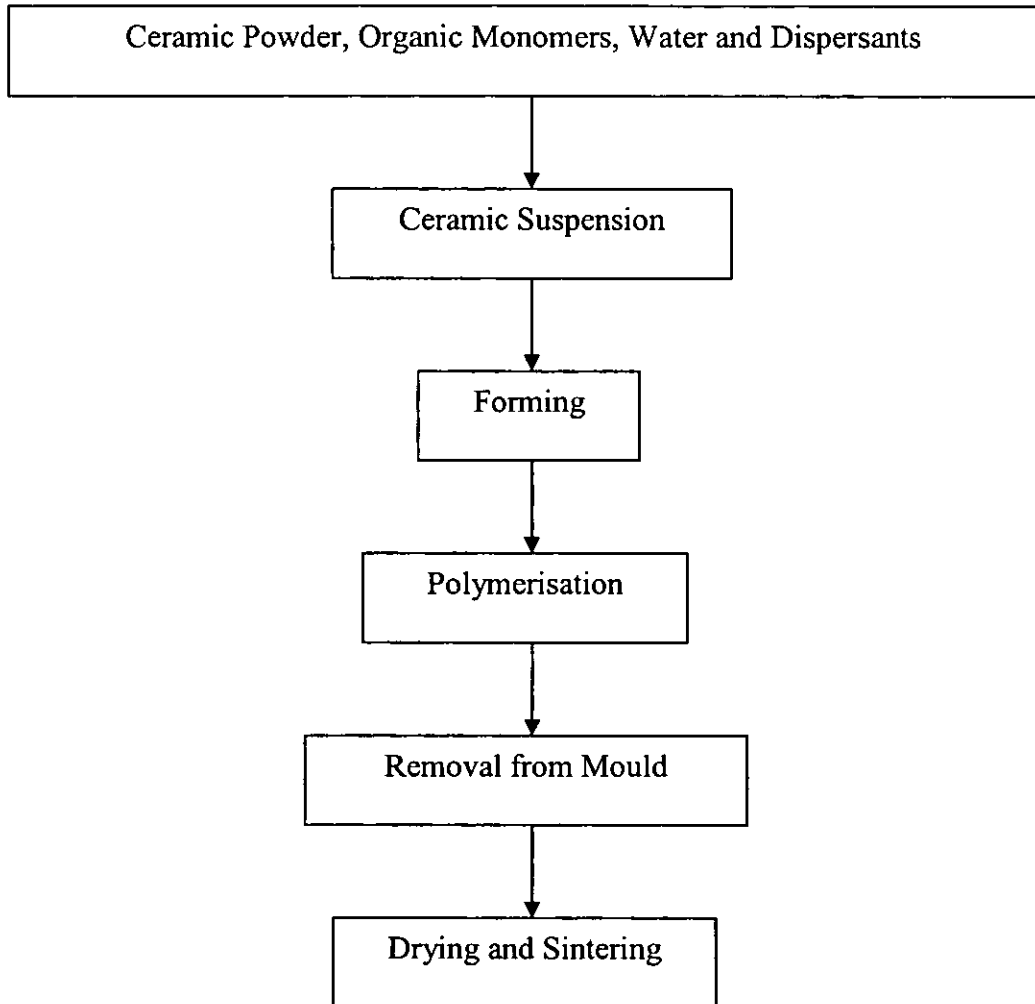
Figure 2.1: Flowchart of the production of ceramic foams by the gelcasting technique [15].

The suspension is then foamed by mechanical frothing or the injection of gases under a controlled nitrogen atmosphere. During the foaming process the initiator and catalyst are added to start the setting process. The time between the addition of the reagents and the beginning of the polymerisation process is characterised by an induction time. The polymerisation process is an exothermic reaction that makes it easy to define the beginning of setting. The induction time is very important during the production process because it describes the time available for the casting of the foamed

suspension. Further, the length of this time influences the final structure of the ceramic foam. After the suspension is foamed and cast, the existing bubbles may transform. They could either shrink, disappear, or merge to form larger bubbles. The reasons for this transformation are forces that occur in the structure. These forces include gravity, capillary forces and surface tension. These forces mainly try to concentrate the material into the cell edges. That means that the struts between bubbles will become thinner at their direct contact points while the material fills the larger voids. If the time is short only a small transformation takes place and the films around the bubbles remains intact. This will lead to closed cells within the final ceramic. At longer times more films between bubbles will collapse. Further there is more time for bubble enlargement. If the time is too long the foam structure can be completely destroyed. With a short induction time cell sizes in the range of 30 to 300 $\mu$m can be achieved together with a narrow cell size distribution. With an increasing time both the mean cell size and the cell size distribution increase. This shows that the induction time is very important for the final cell size, cell size distribution and strut thickness and therefore for the final properties of the ceramic foam. The induction time can be adjusted by altering the concentration of the initiator and the catalyst. However, other parameters such as the temperature and the pH-value are also important [15]. After the setting reaction the samples are dried and finally sintered to obtain the rigid ceramic foam.

The density of the final foam can be changed by two different methods. First, by the level of foaming. The foaming entrains gas into the suspension and leads to an increase in the volume. This volume increase is limited by a minimum thickness of film that can sustain a stable foam. A longer foaming procedure would not further increase the volume and therefore lower the density [15]. However, the density can be further lowered by the previously described expansion of the foam by reducing the pressure. If the foam is expanded before setting, the cells are enlarged and new windows are created. The struts become thinner as the foam expands, and results in large windows between the cells, together with the interconnectivity. Foam densities in the range of 7 to 50 % of the theoretical densities were produced.

The gelcasting method is able to produce parts with high degrees of complexity and good mechanical properties. The complexity can be achieved due to the casting process that makes it possible to shape foams without additional machining. If further structures are required, such as holes, the cast and dried green foams are strong enough

to handle but easy to machine. The good mechanical properties are retained by the structure of foams. The struts between the cells provide a high level of densification and contain minimal defects.

## 2.2.1.2 Replication

The replication of polymeric foams was one of the first production techniques developed for materials with a controlled macroporosity. The first patent was obtained in 1963 where Schwartzwalder et al. [17] described the polymeric-sponge technique. This production technique involves the coating of a flexible open-cell polymer foam with ceramic slurries. After drying, the polymer is burned out and the ceramic sintered to achieve a replica of the original foam. Some further patents that describe this kind of production technique are given in [18,19]. A flow chart, which represents this technique, is shown in Figure 2.2.

A lot of different polymers are suitable as materials for the basic foam. The main factor is that the polymer volatises at a temperature below that required to sinter the ceramic. Some possible materials are polyurethane, cellulose, PVC, and polystyrene. The polymeric foam structure and pore size determines the structure of the resulting ceramic foam. Usually the polymer foam can be shaped into almost any shape, however it has to be considered that there are several construction rules for ceramics that could limit the shape. If these rules are not followed, the part may be produced as a green body but is likely to break during burn out, sintering or usage.

The ceramic slurry does not differ much from other slurry production routes and has to be adjusted to the final desired properties of the ceramic foam. In some cases flocculating agents are added to improve the adherence of the slurry to the polymeric material. Generally, any ceramic material can be used that is obtainable as a slurry. To receive a homogeneous coating, a pure, fine ceramic powder with a narrow particle size distribution should be used. The solid weight percentage of the slurries usually lies in a range between 50 and 70 wt. %. A higher solid concentration leads to a higher viscosity that might cause difficulties for the infiltration.

After the polymeric foam and ceramic slurry are ready the coating process can be carried out. Therefore the foam is immersed into the slurry and compressed to remove air. While still in the slurry the foam is allowed to expand again. Thereby the slurry is sucked into the open cells of the foam. This step can be repeated several times

to achieve the desired density. After the foam is infiltrated with the ceramic slurry excess slurry that completely fills the pores has to be removed. There are several methods used but usually they all end up with a defined compression of the foam. When the foam has been coated and infiltrated in the desired way it is dried at room temperature or in an separate oven to solidify the ceramic structure.
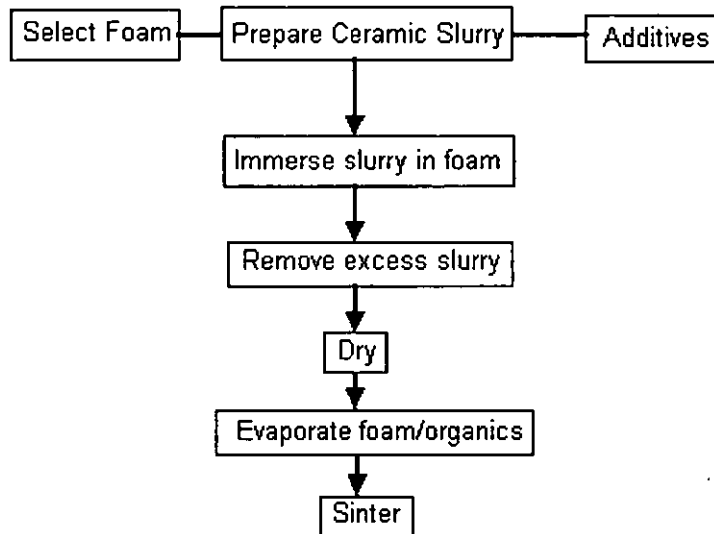


Figure 2.2: Flowchart of the production of ceramic foams by the replica process [17].

After the foam is prepared and dried the last two steps are firing processes. The first one is at lower temperatures to remove the additives from the ceramic and to volatilise the polymeric foam. Therefore the dried foam is heated to a temperature in the range of 350°C to 800°C. This process can be carried out under air or if necessary under a defined atmosphere. The temperature required depends on the polymeric material that was chosen for the basic foam. Usually the temperature should be as low as possible and the heating rate should be very low and carefully controlled. This is to prevent the induction of residual stresses and breaking of the ceramic network due to the volatilisation of the polymer.

After the polymer material is completely removed the final consolidation of the ceramic material is carried out by sintering. This process can be included in the burn out process or performed separately. The sinter temperature mainly depends on the

16

ceramic material chosen and its sintering characteristics. This step must also be very carefully controlled to prevent the destruction of the ceramic structure.

A variation of the replication process is the pyrolysis process where the polymeric material is not burned out but pyrolysed to a carbonaceous material. The pyrolysed porous network can then be infiltrated by a ceramic slurry to obtain a composite foam like material. Sherman et al. [20] describe a further replication method. They also start with a polymeric foam that is then pyrolysed to obtain a carbonaceous structure. For the infiltration process they do not use ceramic slurry but the chemical vapour deposition (CVD) / chemical vapour infiltration (CVI) technique. Thereby the three dimensional network is heated to a suitable deposition temperature and then flowed with a reactant gas. The gaseous precursor compound is reduced or decomposed at the foam surfaces, forming a uniform deposit throughout the internal structure of the foam. Any material that can be deposited by the CVD process can be used for the infiltration and deposited material densities of up to 50% of the theoretical density can be achieved.

## 2.2.1.3 Pore-formers

This technique describes the production of porous ceramic structures from ceramic powders where the porosity is achieved by so called pore-formers. Ceramic powders are blended with inorganic pore-formers and then fabricated by conventional forming techniques. Inorganic pore-formers consist of alkaline earth metals, alkali metals and/or metal oxides, nitrides or carbides, e.g. $SiO_2$, $Al_2O_3$, MgO, CaO, $Na_2O$, SiC or $Si_3N_4$, and/or metals, especially perlite [21]. Pore-formers consist of natural or synthetically produced porous or hollow bodies that have a volume that is several times that of their actual constituent material. One example could be hollow spheres made of glass or perlite. After forming and drying, the green bodies are fired. During this firing process the pore-formers melt partially or completely and can further react with the ceramic powders.

The structure and porosity of the final porous ceramic can be adjusted by the shape, size, porosity and amount of the pore-formers. The final pore size of these structures can be in the range of a few micrometers up to several centimetres. The use of inorganic pore-formers that do not vaporise has the advantage that they do not pollute the environment.

## 2.2.1.4 Other production techniques

Another production technique for porous ceramic structures is the bubble generation method. In the majority of these cases, a chemical mixture containing the desired constituents is treated to evolve a gas, which creates bubbles and causes the material to foam.

The ceramic particles and some additives are mixed together with the blowing agents. Then the mixture is formed by conventional methods. In a further specific thermal treatment, the blowing agents expand and the green bodies transform into a highly porous ceramic. This porous green structure is sintered to create the final rigid ceramic.

Williams et al. [22] describe manufacturing low-density ceramic foams by applying the procedures used for expanded polystyrene. Alumina powder was blended with polystyrene and small pellets were produced. The pellets were immersed in pentane and then moulded into the desired shape. The mouldings were then heat-treated with steam and the material expanded. The remaining polystyrene was pyrolysed to a ceramic material during the final firing process to consolidate the porous ceramic material.

Tuck et al. [23] used food-grade reagents as foaming agents. The suspension was stirred until the achieved foam was stiff. Then the material was moulded, dried and sintered to generate the porous ceramic materials.

## 2.2.1.5 Different foaming methods

Sunderman et al. [24] described a foaming technique for producing reticulate ceramics in a patent in 1973. In this approach preswelled ball-shaped granules of clay were placed in a mould that had the shape of the final product. The mould was then passed through a furnace at 900° to 1000°C in an oxidising environment. The heat and high-pressure air first caused the clay balls to bind to one another. When sufficient heat was transferred throughout the clay particles, growth occured and the mould was filled. The resulting ceramic foam was then cooled.

In Sunderman's technique, suitable clays included common clay, brick clay, and slate clay. Propellants such as calcium carbide, calcium hydroxide, aluminium sulphate, and hydrogen peroxide were used to preswell the clay granules.

A 1974 patent by Wood et al. [25] described a unique alternative to the polymeric-sponge method. In Wood's method, a poly(urethane) "sponge" polymer network was produced simultaneously with the foaming of a ceramic–filled slurry. A hydrophilic crosslinked poly(urethane) foam was produced by reacting an isocyanate-capped poly(oxyethylene) polyol with a slurry of finely divided ceramic particles. The carbon dioxide generated when the reactants were mixed produced a poly(urethane) foam with ceramic material uniformly distributed throughout. Virtually any ceramic powder capable of being suspended in aqueous or organic vehicles can be used in this process. Examples were alumina, magnesium silicate, barium titanate, and zirconia. Metal, such as aluminium or nickel, can also be used with a binder and other additives to produce a foam structure. Typical quantities of ceramic materials were 20% to 80% by weight. The foamed material must also be dried. The final steps were burn out of the organic crosslinked network and sintering. These were typically accomplished by heating at a rate of 100 to 200°C/h to a temperature of 500° to 2000°C (depending on the material) and holding for 0.5 to 5 h.

Motoki [26] described a porous ceramic produced by a room temperature, atmospheric-pressure process in a 1978 patent. In this approach, four components were mixed together: an aqueous solution of pH $\leq 2.0$ containing an acid and an acidic phosphate, one or more cement materials and anhydrous alkali-metal silicates, a metal blowing agent, and foaming stabilizer.

Once the components were mixed, the acidic solution reacted with the metal blowing agent in the presence of the cement material, hydrogen gas was evolved and the mixture foamed and hardened simultaneously. The result of this concurrent foaming and hardening was a foam ceramic with a predominantly closed cellular structure, imparting the property of very low permeability. Porous ceramics produced by this method typically have a very uniform cell structure, with the cell size ranging from 0.5 to 10 mm in diameter.

A 1985 patent by Jackson [27] described a process for making a high-strength ceramic foam by careful control of the cell-size. Jackson found compressive strengths as high as 1.4 MPa with layer-silicate derived ceramic foams which have a mean cell

diameter below 60 μm. In this method, a suspension of one or more of the layer – silicate minerals plus other additives is aerated by whisking or beating to form a "wet foam or froth." The stable wet foam structures does not collapse or lose appreciable volume after 5 to 6 hrs. The density of wet foam controls the cell size of the resulting ceramic foam. The aeration process may be repeated several times to produce optimal density for achieving the 60 μm mean cell size.

Any layer-silicate materials, such as kaolin, vermiculate, china clay and calcium montmarillonite clay, can be used. The amount varies from 15% to 60% by weight. Additives, such as binders, foaming agents, and fillers may be added to the silicate suspension. The wet foam is heated to approximately 1000°C to sinter the resulting high-strength ceramic foam.

One novel alternative to forming a ceramic foam is described in a 1990 patent by Nakajima et al. [28]. A porous alumina structure is produced by partially reacting coarse alumina particles with ultrafine silica particles. Mullite $(3Al_2O_3.2SiO_2)$, formed on the surface of the alumina particles during firing, binds the alumina particles together and leaves pores between them. This porous body must be produced at a temperature no higher that 1700°C, the proper temperature range for the formation of mullite. The process was developed in a response to the undesirably low porosity and high production costs of porous alumina made by more conventional methods. In the conventional process, alumina powder is combined with a binder and a flux and heated to greater than 2000°C. The high sintering temperature results in both low porosity and high costs. The lower firing temperature of Nakajima's process provides the advantage.

Meek, Blake, and Gregory [29] describe the fabrication of ceramic foams by microwave heating of glass and metal microballoons. The microballoons range between 30 and 130 μm in diameter for glass and 400 to 600 μm for metal. In this process, about 25% by weight of glass balloons is mixed with 2% by weight of metal balloons and 73% by weight of potassium silicate binder. A microwave-coupling agent was also added to the mixture to improve energy absorption at room temperature. Examples of coupling agents were glycerol, nitrates, and potassium silicate. This mixture was then placed inside a microwave oven and heated for 5 to 30 min in air. Fibres can also be added to improve the strength of the ceramic foam.

## 2.3 Polymer matrix composites

Polymer matrix composites, or PMCs, originated through efforts in the aerospace community during World War II to produce materials with specific strength and stiffness values that were significantly higher than existing structural materials. In addition, existing aerospace structural alloys, such as those based on aluminium, were subject to corrosion and fatigue damage, and PMCs provided an approach to overcome these issues. By the end of the war, glass-fibre reinforced plastics had been used successfully in filament-wound rocket motors and demonstrated in various other prototype structural aircraft applications. These materials were put into broader use in the 1950s and provided important improvements in structural response and corrosion resistance. Commercial applications in consumer sporting equipment in the 1960s provided a larger market, which improved design and production capabilities, established consumer familiarity and confidence and lowered costs [30].

Defence spending during the Cold War ensured sufficient resources for research and development of new, high-technology materials and a market for their application. The significant number of new military aircraft, and the large numbers of systems ordered, provided an ideal environment for the development and insertion of high-performance PMCs. The energy crisis during the 1970s provided a significant incentive for the introduction of PMCs into commercial aircraft and the successful experience in military aircraft was an important factor in their acceptance in the commercial industry. Dramatic improvements in structural efficiency became possible during this period through the introduction of high-performance carbon fibres. Improved manufacturing capabilities and design methodologies provided the back ground for significant increases in PMC use for military and commercial aircraft and spacecraft structures.

Over the past 30 years, PMCs have won an increasing mass fraction of aircraft and spacecraft structures. This is demonstrated by the fact that the vintage 1970s application of PMCs to fighter aircraft was typically confined to tailskins and other secondary or "noncritical" flight structures. For example, only 2% of the F-15 E/F was comprised of PMCs [30]. During the subsequent years, significant government and private investments were made toward research, development, fabrication, testing, and flight service demonstration of composite materials and structures. Parallel programmes were also ongoing for the use of composites in military and civilian land and naval vehicles. For example, the development of fibreglass structures for boats and other

marine applications was extremely successful and now accounts for a significant portion of composite production volume. During these years confidence in using composite materials increased dramatically. This was also a period of great innovation in manufacturing, assembly and repair method development.

The advantages demonstrated by composites, in addition to high stiffness, high strength, and low density, include corrosion resistance, long fatigue lives, tailorable properties (including thermal expansion, critical to satellite structures), and the ability to form complex shapes. An example of recent PMC application is the next-generation U.S. tactical fighter aircraft, the F-22. Over 24% of the F-22 structure is PMCs. The B-2 bomber is constructed using an even higher percentage of composites, as are current helicopter and vertical lift designs. For example, the tilt-rotor V-22 Osprey is over 41% composite materials. The upper-use temperature of PMCs has also increased dramatically: early epoxies were considered useable (for extended periods) up to 121°C (252°F). Current generation polymers, such as bismaleimides, have increased that limit to around 204°C (400°F), and the use of polyimide-matrix composites has extended the range to 288°C (550°F) [30].

Once considered premium materials only to be used if their high costs could be justified by increased performance, PMCs can now often "buy their way onto" new applications. This is due not only to a dramatic drop in materials costs, but also to advances in the ability to fabricate large, complex parts requiring far less hand labour to manually assemble. A recent example of this is the addition of large composite structures in the tail and landing gear pods on the C-17 cargo aircraft. Clearly, the applications, technology, confidence, and other considerations of high-performance PMCs have expanded dramatically since the 1980s. Perhaps the most dramatic example of this is the growing use of high-performance PMCs in the commodity market infrastructure.

## 2.3.1 Materials

The materials that are used for the production of polymer matrix composites can be distinguished into thermosets and thermoplastics.

## 2.3.1.1 Thermosets

These are the most frequently used matrix materials, especially for the infiltration of porous performs. The final matrix material of duroplastics is produced by a reaction of two components, the resin and the catalyst. This reaction is called 'curing' and is usually an exothermic reaction. During this reaction the monomers build cross-links between each other, which leads to a solid material. The cross-linking reaction is not reversible, this means that the material cannot be melted, formed or dissolved afterwards.

## 2.3.1.2 Thermoplastics

These polymers have recently begun to be used. They melt and their solidification is reversible. They have a much higher elongation at fracture and therefore they provide very high impact characteristics. The problems are that they are difficult to process and tend to creep. The high viscosity melts of thermoplastic materials cause difficulties with the infiltration and wetting of the preforms. Therefore, they are more often used in the form of prepregs that are pre-coated and then pressed to produce the final parts.

## 2.3.1.3 Polymer matrices for commercial applications

Polymer matrices for commercial applications include polyester and vinyl ester resins; epoxy resins are used for some "high-end" applications. Polyester and vinyl ester resins are the most widely used of all matrix materials. They are used in commercial, industrial and transportation applications, including chemically resistant piping and reactors, truck cabs and bodies, appliances, bathtubs, showers, and automobile hoods, decks, and doors. The very large number of resin formulations, curing agents, fillers, and other components provides a tremendous range of possible properties.

The development of highly effective silane coupling agents for glass fibres allowed the fabrication of glass-fibre-reinforced polyester and vinyl ester composites that have excellent mechanical properties and acceptable environmental durability.

These enhanced characteristics have been the major factors in the wide spread uses of these composites today.

The problems of attaining adequate adhesion to carbon and aramid fibres have discouraged the development of applications for polyester or vinyl ester composites that use these fibres. Although there are applications of high-performance fibreglass composites in military and aerospace structures, the relatively poor properties of advanced composites of polyester and vinyl ester resins when used with other fibres, combined with the comparatively large cure shrinkage of these resins, have generally restricted such composites to lower-performance applications.

**Other Resins**

When property requirements justify the additional costs, epoxies and other resins, as discussed subsequently, are used in commercial applications, including high-performance sporting goods (such as tennis rackets and fishing rods), piping for chemical processing plants and printed circuit boards.

## 2.3.1.4 Polymer matrices for aerospace applications

These include epoxy, bismaleimide and polyimide resins. Various other thermoset and thermoplastic resins are in development or use for specific applications.

Epoxy resins are presently used far more than all other matrices in advanced composite materials for structural aerospace applications. Although epoxies are sensitive to moisture in both their cured and uncured states, they are generally superior to polyesters in resisting moisture and other environmental influences and offer lower curing shrinkage and better mechanical properties. Even though the elongation-to-failure of most cured epoxies is relatively low, for many applications epoxies provide an almost unbeatable combination of handling characteristics, processing flexibility, composite mechanical properties and acceptable cost. Modified "toughened" epoxy resin formulations (typically via the addition of thermoplastic or rubber additives) have improved elongation capabilities.

Moisture absorption decreases the glass transition temperature ($T_g$) of an epoxy resin. Because a significant loss of epoxy properties occurs at the $T_g$, the $T_g$ in most

cases describes the upper-use temperature limit of the composite. To avoid subjecting the resins to temperatures equal to or higher than this so-called wet $T_g$ (the wet $T_g$ is the $T_g$ measured after the polymer matrix has been exposed to a specified humid environment and allowed to absorb moisture until it reaches equilibrium), epoxy resins are presently limited to a maximum service temperature of about 120°C (250°F) for highly loaded, long term applications and even lower temperatures (80 to 105°C, or 180 to 220°F) for toughened epoxy resins [30]. Although this limit is conservative for some applications, its imposition has generally avoided serious thermal-performance difficulties. Considerable effort continues to be expended to develop epoxy resins that will perform satisfactorily at higher temperatures when wet. However, progress in increasing the 120°C (250°F) limit has been slow.

Bismaleimide resins possess many of the same desirable features as do epoxies, such as fair handleability, relative ease of processing and excellent composite properties. They are superior to epoxies in maximum hot/wet use temperature, extending the safe in-service temperature to 177 to 230°C (350 to 450°F) [30]. Unfortunately, BMIs also tend to display the same deficiencies (or worse) as do epoxies: they have an even lower elongation-to-failure and are quite brittle. Damage tolerance is generally comparable to commercial aerospace epoxy resins. Progress has been made to formulate BMIs with improved toughness properties.

Polyimide resins are available with a maximum hot/wet in service temperature of 232°C (450°F) and above (up to 370°C, or 700°F, for single use short periods). Unlike the previously mentioned resins, these cure by a condensation reaction that releases volatiles. This poses a problem, because the released volatiles produce voids in the resulting composite. Substantial effort has been made to reduce this problem and there are currently several polyimide resins in which the final cure occurs by an addition reaction that does not release volatiles. These resins will produce good-quality, low void content composite parts. Unfortunately, like BMIs, polyimides are quite brittle.

## 2.3.1.5 Other thermosetting resins

The attempt to produce improved thermosetting resins is ongoing, with major efforts focusing on hot/wet performance and/or impact resistance of epoxies, BMIs and

polyimides. Other resins are constantly in development and some are in commercial use for specialized applications. Phenolic resins, for example, have been used for years in applications requiring very high heat resistance and excellent char and ablative performance. These resins also have good dielectric properties, combined with dimensional and thermal stability. Unfortunately, they also cure by a condensation reaction, giving off water as a byproduct and producing a voidy laminate. However, they also produce low smoke and less toxic by-products upon combustion and are therefore often used in such applications as aircraft interior panels where combustion requirements justify the lower properties. Cyanate esters are also used as matrix materials. Their low-moisture absorption characteristics and superior electrical properties allow them to see applications in satellite structures, radomes, antennas, and electronic components.

## 2.3.1.6    Resin comparison summary

The polyesters, vinylesters and epoxies discussed here probably account for some 90% of all thermosetting resin systems used in structural composites. In summary the main advantages and disadvantages of each of these types are [31]:

| Resin Type | Advantages | Disadvantages |
|---|---|---|
| **Polyesters** | Easy to use<br>Lowest cost of resins available (£1-2/kg) | Only moderate mechanical properties<br>High styrene emissions in open moulds<br>High cure shrinkage<br>Limited range of working times |
| **Vinylesters** | Very high chemical/environmental resistance<br>Higher mechanical properties than polyesters | Postcure generally required for high properties<br>High styrene content<br>Higher cost than polyesters (£2-4/kg)<br>High cure shrinkage |
| **Epoxies** | High mechanical and thermal properties<br>High water resistance<br>Long working times available<br>Temperature resistance can be up to 140°C wet / 220°C dry<br>Low cure shrinkage | More expensive than vinylesters (£3-15/kg)<br>Critical mixing<br>Corrosive handling |

## 2.3.1.7 Other resin systems used in composites

Besides polyesters, vinylesters and epoxies there are a number of other specialised resin systems that are used where their unique properties are required [31].

## Phenolics

Primarily used where high fire-resistance is required, phenolics also retain their properties well at elevated temperatures. For room temperature curing materials, corrosive acids are used which leads to unpleasant handling. The condensation nature of their curing process tends to lead to the inclusion of many voids and surface defects, and the resins tend to be brittle and do not have high mechanical properties. Typical costs: £2-4/kg.

## Cyanate esters

Primarily used in aerospace industry. The material's excellent dielectric properties make it very suitable for use with low dielectric fibres such as quartz for the manufacture of radomes. The material also has temperature stability up to around 200°C wet. Typical costs: £40/kg.

## Silicones

Synthetic resin using silicone as the backbone rather than the carbon of organic polymers. Good fire-resistant properties, and able to withstand elevated temperatures. High temperature cures needed. Used in missile applications. Typical costs: >£15/kg.

## Polyurethanes

High toughness materials, sometimes hybridised with other resins, due to relatively low laminate mechanical properties in compression. Uses harmful isocyanates as curing agent. Typical costs:2-8/kg.

27

## Bismaleimides (BMI)

Primarily used in aircraft composites where operation at higher temperatures (230°C wet/250°C dry) is required. e.g. engine inlets, high speed aircraft flight surfaces. Typical costs: >£50/kg.

## Polyimides

Used where operation at higher temperatures than bismaleimides can stand is required (use up to 250°C wet/300°C dry). Typical applications include missile and aero-engine components. Extremely expensive resin (>£80/kg), which uses toxic raw materials in its manufacture. Polyimides also tend to be hard to process due to their condensation reaction emitting water during cure, and are relatively brittle when cured.

### 2.3.2 Polymer infiltration techniques

There are three main polymer infiltration techniques that are commercially used for the infiltration of preforms.

- The Resin Transfer Moulding Process (RTM)
- The Vacuum Infiltration Technique and
- The Structural-Reaction-Injection-Moulding Process (S-RIM)

All these techniques have in common that a separately produced preform is placed into a mould and infiltrated with a matrix material. The two most used techniques are outlined in the following sections.

### 2.3.2.1 Resin transfer moulding

The common standard process for Polymer-Matrix-Composites is the infiltration of performs assisted by pressure. The Resin Transfer Moulding Process (RTM) was developed at the beginning of the 1950s. The technique is often used for automotive applications such as convertible hard tops, bonnets and cab roofs, aerospace applications such as propeller blades and airframe components and also the sports and

leisure industry with boats, bike frames and rackets.

During the process a preform is placed into a mould and then infiltrated by the matrix material. The process consists of six steps, Figure 2.3, that are:

1) Placing the preform into the mould

2) Closing of the mould

3) Injection of the matrix material

4) Curing or solidifying of the matrix material

5) Removing the composite

6) Reworking and finishing

In the beginning of the process the preform is placed into an open mould that is usually coated with a mould release oil or paste. This prevents the resin, which is very adhesive, sticking the part to the mould. Most of the resins are injected at room temperature and then cured by external heating. Some other resins require cooling during the curing process because of a strong exothermic reaction.
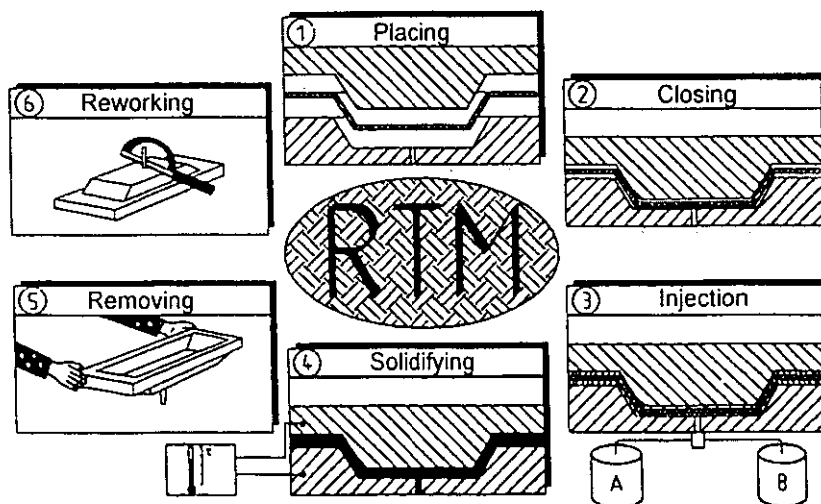


Figure 2.3: The Resin Transfer Moulding Process [32].

Thermoplastic matrix materials must be heated to melt them and to attain a suitable viscosity. After the complete injection the mould is then cooled to solidify the matrix material again. These differences show clearly that the process depends very much on the materials used. As mentioned before, the most used matrix materials for

the Resin Transfer Moulding Process are thermoset materials that react in cross-linking processes. The resin and the hardener (catalyst) are mixed before injection in a separate container or directly during the infiltration process just before entering the mould. Usually after the mould is completely filled and the preform is infiltrated the mould is heated to speed the curing process. Sometimes the resin is injected into a preheated mould but then unfilled areas and voids are very likely. After the composite part is cured and solidified enough to be handled, the mould is opened and the part is removed. The final curing is often carried out in a separate oven or just by storing it for a defined time. For some parts a final step is necessary in reworking and finishing the 'near net shape'-produced part. For the next cycle the mould must be cleaned and coated again.

The quality of the composite parts depends on the parameters that control the production process. These parameters are:

➤ Viscosity of the matrix material
➤ Injection velocity
➤ Pressure during the injection and curing
➤ Temperature during the injection and curing

The resin transfer moulding process should be suitable for the infiltration of ceramic foams with polymers. The ceramic foams must be shaped to the required form and then placed into the mould. The main difference between a fibre preform and a ceramic foam preform is that the fibre preform can be deformed up to a defined degree whereas the ceramic foam is rigid and would break if the applied load exceeds its strength. But with the right choice of parameters this should not be a problem for the infiltration process. The sequence of the process should be the same as with conventional fibre performs; only the parameters have to be adjusted to the new material.

## 2.3.2.2 Vacuum infiltration

Another commonly used infiltration technique is the Vacuum Injection Process (see Figure 2.4). Kotte [32] describes this process as the easiest method to produce continuous fibre reinforced parts because next to the mould only a vacuum pump and a

resin basin is needed. The process is similar to the Resin Transfer Moulding Process (RTM); the main difference is that the pressure force used for infiltration is replaced by a vacuum to suck the resin into the mould. The main difficulty exists in the correct placement of the inlet and outlet ports to make sure that the mould will be completely filled by the resin. Just like the RTM process, the resin should start gelling and curing after the complete filling of the mould and impregnation of the preform. The composite can be removed from the mould if the resin is solid and no longer sticky. Tengler [33] received satisfying results with fibre volume fractions up to 35% and found out that vacuum injection is also suitable for more complex geometries.

Just as for RTM, the mould is coated with a mould release material. Then the perform is placed into the mould. The mould is closed and vacuum is applied. The matrix material can now be applied either just out of an open container from which it is sucked into the mould, or pressure assisted. After the mould is completely filled and the preform infiltrated, the supply is closed while the vacuum is still applied. The vacuum must be held until the matrix is completely solidified. This leads to a pore free, dense composite.



a - overflow basin
b - lower mould
c - upper mould
d - valves
e - resin basin
f - vacuum pump
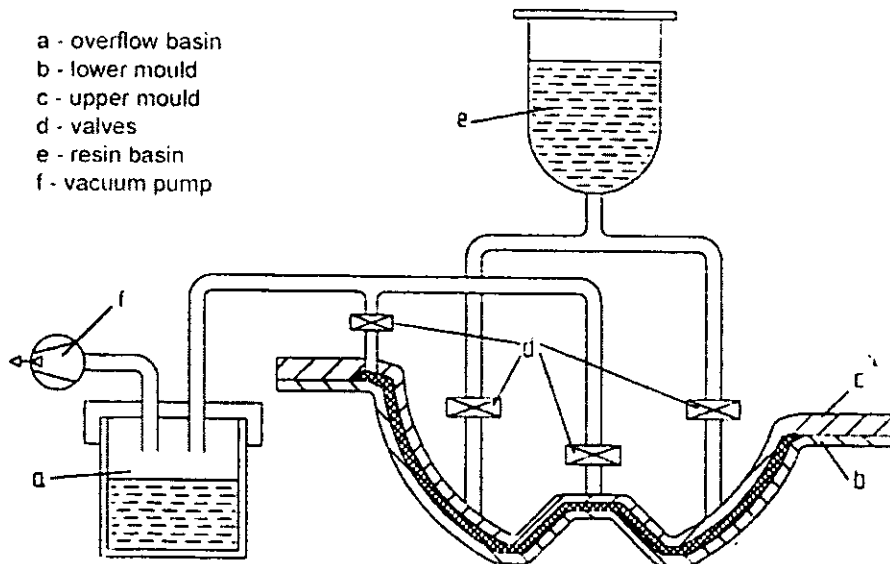
Figure 2.4: The Vacuum Injection Process [33].

Some guidelines for the construction of the vacuum infiltration tools are given by Tengler [33]. The resin supply should be at the lowest point of the tool while the

vacuum connection should be at the highest point. This prevents sucking out the resin before the mould is completely filled and ensures a complete evacuation of the air and a complete and void free infiltration. Eventually required ejectors may not hinder the resin flow and have to be sealed. The thickness of the supply channel has to be adjusted to the dimensions of the part and the viscosity of the matrix material. In some cases several supplies or a ring-shaped supply may be better to receive a complete and equal filling of the mould. Behind the vacuum connection of the mould there must be an overflow basin to prevent the resin entering the vacuum pump. The overflow basin must be big enough for the necessary amount of resin and has to be designed for low pressure resistance.

These facts lead to the assumtion that the vacuum infiltration technique should also work if the three dimensional fibre performs are replaced by ceramic foam performs with open porosity. The main difference is again that the ceramic preform is not flexible and compressible and this may lead to holes or bubbles during the shrinkage of the resin while curing. On the other hand the shape of the preform and therefore also of the resulting parts does not change and low tolerances could be received. Another advantage of the non-compressible ceramic foam preform is that the pore size stays the same during infiltration and cannot be closed by compression. Therefore the permeability of the preform depends only on the pore size and varies not with the compression of the preform. The experiments have to show which pore sizes are infiltratable and if there are bubbles and unfilled pores in the ceramic foam.

## 2.3.3 Polymer matrix composite applications

Based on their high-performance properties, reduced-cost manufacturing methods and the high level of confidence among users, the use of PMC materials has expanded greatly since the mid-1980s. High-performance composites were born of the need for extremely high-performance aircraft structures during the days of the Cold War. The military aerospace markets still constitute a major user of the higher-end performance materials. For example, the B-2 bomber, F-22 fighter, Joint Strike Fighter, F-18E/F air craft, Eurofighter, Gripen aircraft, and Rafale aircraft in production, on the books, or in prototype form are all constructed using high percentages of PMCs [30]. Current-production helicopters are now largely composite. On the commercial side,

PMCs constitute a significant portion of the new large Boeing 777 and planned Airbus A380, which reportedly will contain the first carbon fibre wing centre section in a large commercial aircraft, in addition to extensive PMC use in tail surfaces, bulkheads and fuselage keel and floor beams. Space applications for PMCs have flourished, from satellite structures (where low CTE, in addition to low weight, is a major advantage of PMCs) to the use of PMCs in booster fairings, shrouds and tanks. The maturity of high-temperature PMC structures has afforded the use of PMCs in many engine applications for both air and space vehicles.

The sports and recreation market continues to be one of the primary consumers of composite raw materials. Golf clubs, bicycles, snowboards, water skis, tennis rackets, hockey sticks, and so on - the list of consumer products now produced using PMCs is extensive and common place. On the marine side, the consumer use of fibreglass PMCs in low- to high-end boats is the norm. Military ships have seen several applications of PMCs, primarily topside structures and minesweepers. Carbon-fibre composites can be seen in high-performance engine-powered, sail powdered, and human-powered racing boats.

A potentially huge market exists for composite materials in the upgrading of the infrastructure needs. For example, 31% of the highway bridges in the United States are categorized as structurally deficient [30]. To address this, many activities are underway at national, state, and local levels to use composites to repair and, in some cases replace, deficient bridges. Figure 2.5 shows an example of an all-fibreglass bridge being installed in Butler County, Ohio. This bridge is fully instrumented to detect structural performance loss. The bridge has completed four years of service with almost no maintenance required. Composites have also been used for seismic enhancement of existing highways and bridges.

Land vehicles have also benefited greatly from the application of PMCs. Military armored vehicles have been demonstrated that offer ballistic protection of their occupants in addition to light weight. The demand for energy-efficient and low-maintenance vehicles has spurred composites use in advanced automobile, truck, bus, and train commercial products. Production parts include everything from small linkage assemblies to very large exterior structural panels.

Rounding out the PMC application discussion are a host of products. For example, the medical industry has applied PMCs to products ranging from implanted orthopedic devices to X-ray tables and lightweight assistance devices, an example is

shown in Figure 2.6. Industrial applications include electronic housings, large rollers, tanks, robotic arms, etc. Spoolable piping for oil wells allows deeper wells due to the increased strength and reduced "hang weight" of composite tubular products. In short, the development and use of PMCs were initially spurred by early investments based on military need, and, based on those successes, have now dramatically taken off in the private sector, based solely on their commercial merits.
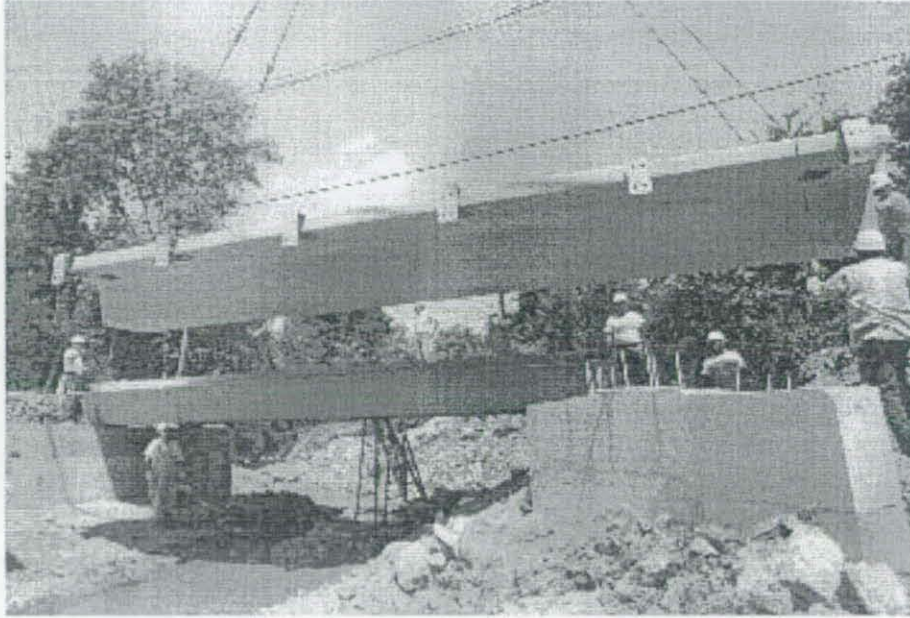


Figure 2.5: All-composite bridge in Butler County, Ohio. Factory-constructed primarily using glass fibre, the bridge was trucked to the site and installed in less than one day [30].
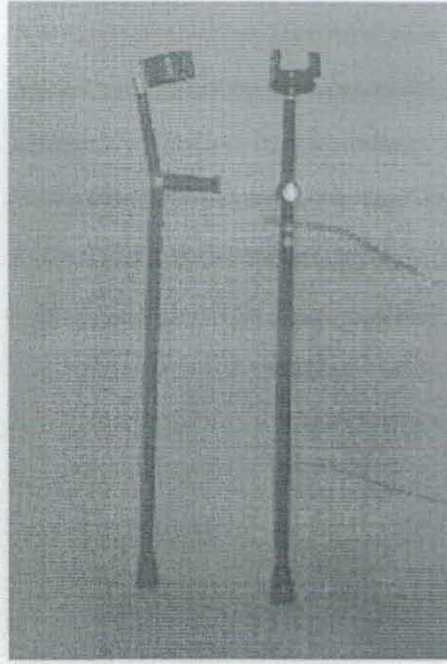
Figure 2.6: Carbon/epoxy composite crutch. This crutch is stronger than its aluminium counterpart yet weighs 50% less, is quieter, and is more aesthetically pleasing [30].

## 2.3.4 Applications for polymer infiltrated foam ceramics

Conceivable applications for polymer infiltrated ceramic foams could be found in the building industry, the automotive industry, the transport industry and for sensor applications.

A very broad area for polymer infiltrated ceramic foams is the use as building materials in the civil engineering industry. Applications that are conceivable could reach from thick construction elements for walls and ceilings, like bricks or large plates, to smaller parts, like trim and cladding panels or tiles, and last but not least they might be used for roofing tiles.

All these applications depend on the lightweight structure of the composite, combined with insulation, fire resistance, waterproofness, low cost and the possibility to machine them via cutting and drilling. Both ceramic foams and polymer resins provide very low heat conductivity that suits their use as insulation materials. Further they have also a low sound conductivity that makes them suitable for noise absorption and insulation. Another advantage is that with the right choice of the resin they will be

non-flammable and in case of fire they would not lead to fast fire spread. Generally most resins could be adjusted to be non-flammable or at least difficult to burn. A resin that is usually linked with the application and production of non-flammable polymer composites is the phenolic resin. Most polymer resins are waterproof which enables them for the use in boats or automobile roofs. A waterproof composite consisting of a combination of ceramic foam and polymer resin could also be used as roofing tiles or panelling. Because the production process of the ceramic foams is a casting process, it is easy to cast more complex shapes like the shapes of roofing tiles. The infiltration of these shapes with vacuum infiltration technique or the Resin Transfer Moulding technique is also no problem by using them as preforms in a fitting mould. The casting, firing and infiltration process is not very cost intensive and no further reworking is necessary.

At the 1980 SAE conference in Detroit the Polimotor Research Corporation introduced an engine where most parts had been built of PMCs. Metal was only used where the temperatures exceeded 260°C [34]. Polymer infiltrated foam ceramics could provide similar properties. Parts already made of PMCs [35] and conceivable for polymer infiltrated ceramic foams are the crankshaft, water jacket, inlet manifolds and carburettor parts.

The following paragraphs give some examples for Polymer-Matrix-Composites that are used in the fields mentioned above. Most of these applications are conceivable with polymer infiltrated ceramic foams.

In 1985 Plastic Industry News, described the development of a wall panel for building applications [36]. The phenolic resin plates cannot burn out but only char to carbon. The company expects their product to replace foamed building materials. The phenolic resin is further used to produce sound-proof wall panels by combining the foamed phenolic resin sheet with another sheet material.

In 1987 in European Plastic News, Acell Holding originated a process which produces a structural composite phenolic based foam with tailorable properties for the end user [37]. Using this process ceiling tiles and panels were produced that were fibre-free and offer excellent thermal, acoustic and fire properties. Further they are light, strong and dimensionally stable and provide moisture resistance.

In 1996 Reinforced Plastics introduced a fire-safe flooring material (Figure 2.7), that was non-conducting and strong [38]. The material is produced in sheet form and has the appearance of ceramic tiles. It is made of phenolic infiltrated woven and non-woven glass. The production of phenolic impregnated ceramic foams in this shape is easily possible and the replacement of the glass fibres could lead to a further cost reduction.



Figure 2.7: Flooring made of phenolic infiltrated glass [38].

In 1994 Reinforced Plastics introduced two further cladding panels [39,40]. Both panels are produced as a sandwich construction, where a porous material is coated or infiltrated with a phenolic resin to achieve the fire protection properties (Figure 2.8). The panels are used in transport industry for internal panelling, as tunnel linings, as hygienic lining in industrial and food processing and further in the building industry for cladding of walls, doors, ceilings, walkways, power stations and for insulation.

Two additional applications of mineral filled resins are come in to the picture in the year 1995-96 [41,42]. A filled epoxy resin was used as a synthetic granite for machine tool beds and precision instrument panels because it provides a high stiffness, a high damping factor, superior corrosion resistance and a very low coefficient of thermal expansion. A mineral filled polyester resin was also used for the wall sections of high quality speakers. The advantage lies in the superior damping characteristics and the high accuracy and casting flexibility.
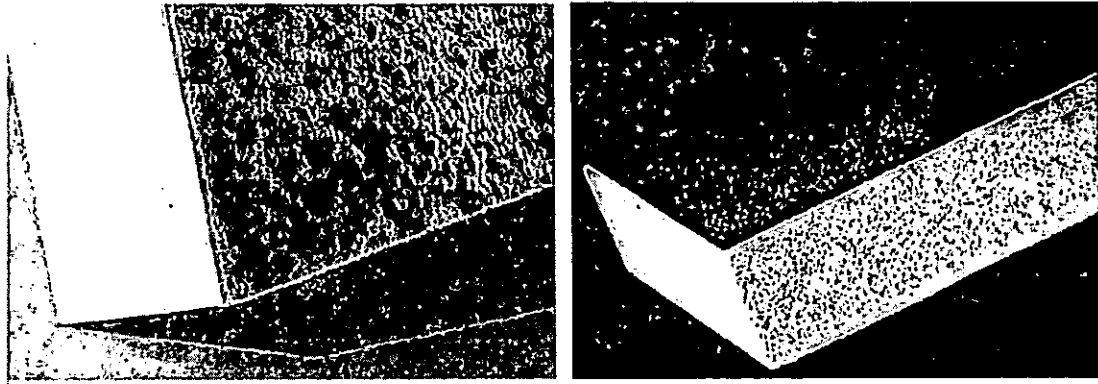
Figure 2.8: Cladding panels made with phenolic resins [39.40].

Another conceivable application for polymer infiltrated ceramic foam was found in the electronic industry for the use as piezoelectric sensors. Piezoelectric materials have the ability to change their dimensions when an electric field is applied and, similarly, develop a voltage when mechanical forces are applied that lead to the material being strained. By polarising the material and connecting electrodes, the piezoelectric property can be used for transducers, actuators, sensors and many other applications. Recently, piezoelectric materials are integrated into body panels of cars to prevent vibrations by reacting against local strains.

Many piezoelectric applications are based on the use of dense piezo electric ceramics. However, in the case of hydrophones for sonar, ceramic/polymer composites have been found to be better suited since a larger piezoelectric coefficient can be achieved. The two parameters describing the quality and suitability of a material for this application are the hydrostatic voltage coefficient, $g_h$, which relates the voltage appearing across the transducer to the applied pressure, and the hydrostatic charge coefficient, $d_h$, which relates the charge developed to the applied stress [43]. Therefore for hydrostatic material the $d_h g_h$ product is considered to be an all-encompassing "figure of merit" [44].

The hydrostatic charge coefficient is given by: $d_h = d_{33} + 2d_{31}$      2.1

where the subscripts are the reduced notation for designated directions in an orthogonal axis system [44]. For lead zirconate-titanate (PZT), the most commonly used piezoelectric ceramic, $d_{31}$ is opposite in sign to $d_{33}$ and about one half of it in value. In

addition, the permittivity of PZT is high and because the hydrostatic voltage coefficient is derived by dividing the hydrostatic charge coefficient by the permittivity, the former becomes very low. Another disadvantage of dense ceramic materials is that they are poorly matched to water.

Skinner et al. [45] described the basic requirements of a suitable material as follows. A low-density piezoelectric should have better acoustic coupling to water and have its buoyancy more easily adjusted than a high-density PZT ceramic. Further, a more complaint material is more resistant towards mechanical shock and has a higher damping, both of which are desirable in a passive device.

Skinner et al. [45] calculated, via comparison of a parallel with a series connection, that the highest piezoelectric values should be achieved by having a continuous piezoelectric phase from one electrode to the other, providing the connectivity of electric flux required for saturation poling. The ceramic phase should also be oriented normal to the electroded surface for the transmission of mechanical stresses and high piezoelectric responses. A composite of this type would have a 1-3 connectivity and is very often obtained by piezoelectric rods placed into a three dimensional polymer matrix. Examples therefore are given in [43,45,46].

Newnham et al. [5] described the different appearances of connectivity. Each component of a composite can be self-connected in zero, one, two or three dimensions. For a composite with two phases this leads to ten different kinds of connectivity from 0-0 to 3-3.

The most complicated, and in many ways the most interesting pattern, is the 3-3 connectivity [5]. Here two phases form an interpenetrating three dimensional network. This kind of composite is very often found in natural materials such as wood, bones or corals. Coral skeletons, for instance, are characterised by the following structure [45]:

- A narrow pore size distribution
- A pore volume approximately equal to the solid phase volume
- Complete pore interconnectivity, making every pore accessible from all other pores

This description sounds very similar to that achieved by infiltrating a ceramic foam, therefore these applications will be discussed in more detail.

The first development of a 3-3 connected composite was made by the 'replamineform' process, which stands for 'replicated life forms'. This process is described in [47] and consists of a technique for duplicating the microstructure of carbonate skeletal components in ceramic, metal or polymer materials. It was developed for making prosthetic materials having a controlled microstructure, an end result that was not achievable with artificial technique at that time. The process starts with the selection of a suitable natural material with the desired microstructure. The organic material is then removed by dissolution. The carbonate skeleton is dried and can be machined very easily to the shape of the desired preform, e.g. cylinders, screws, nuts, etc. the preform is then vacuum infiltrated with a polymer or a wax depending on whether a positive or negative form is needed. The original calcinate can be leached away with 5 – 20 % HCl and the remaining voids back-filled with the desired material to produce a composite consisting of the two phases needed for the application.

Skinner et al. [45] used this replamine form process to produce piezoelectric composites and investigated their properties. They first vacuum impregnated the coral skeleton with wax. Thereafter they leached away the skeleton with HCl and infiltrated the voids again with a PZT slip by vacuum and vibration assistance. The wax negative was burned out at 300°C leaving a coral structure of PZT. This structure was sintered and again infiltrated by a suitable polymer, in this case a high purity silicone rubber. The resultant composite was connected with electrode layers and poled in an electric field. After poling the replica was still a rigid structure because of three dimensional connectivity of the ceramic phase. If a flexible composite was desired the body could be crushed to break the ceramic struts by reducing the sample height to 80% and simultaneously shearing the sample 20% of the sample height about an axis perpendicular to the crushing force direction. The breaking of the ceramic phase lowered the permittivity by interrupting the electric flux. But because the pieces were still held in position by the polymer matrix, stress was still transmitted. This resulted in a high coefficient, whilst the permittivity was lowered and therefore the piezoelectric voltage coefficient was greatly enhanced. If the composite was not broken, a rigid polymer, e.g. epoxy or polyester, could be used and a low density, high coupling resonator could be fabricated.

Shrout et al. [48] investigated a PZT/polymer composite with a 3-3 connectivity that was produced by burning out plastic spheres (BURPS). Here a PZT powder was

mixed with polymethyl metacrylate (PMM) spheres in 30/70 volume ratios. The spheres ranged from 50 to 150 μm in diameter. The mixture was pressed to form green bodies, which were then slowly heated to 400°C to volatilise the spheres. Thereafter the highly porous ceramic structure was sintered and vacuum infiltrated with a polymer. They also used silicone rubber and further an epoxy resin for the infiltration to compare the properties with the properties of the composites achieved by the replamine form process but the microstructure was more randomly orientated. The main advantage of this process lies in the fewer steps required.

Whilst these two processing technologies were developed in the late seventies, two patents of the late nineties were found which also describe the production of 3-3 connected piezoelectric ceramic/polymer composites. The US patent PA 559 13 72 [49], (which is connected to US PA 566 08 77 [50] and EP 0 764 994 [51]), describes a piezoelectric composite with anisotropic 3-3 connectivity developed by the General Electric Company. A ceramic perform of interconnected lamella, where the connectivity of the lamella in z-direction is greater than in other directions, was produced by the freeze drying or gelling of a ceramic slurry. The anisotropic connectivity was achieved by using an unidirectional heat flow. The preform was then sintered and vacuum infiltrated with a polymer, a low acoustic impedance glass or low acoustic impedance cement. Poling and the addition of the electrodes lead to the final usable composite material.

A second patent that describes a method for novel ceramic composites is US PA 600 45 00 [52]. The method is also further described by Bandyopadhyay et al. [53]. The composites were produced by using the novel technique of rapid prototyping. This method uses a CAD-file to describe the complex shape of the microstructure, which is then converted into a solid part by sintering, curing or solidifying a material with laser, UV-light or other energy beams. The CAD-file allows the easy variation of the structure and the realisation of any complex shapes. It further provides an excellent reproducibility and accuracy. The process distinguishes a direct and an indirect route. In the direct route a green 3D structure was built by rapid curing a ceramic slurry containing a polymer binder. Afterwards the green body was heat-treated and sintered and then again infiltrated by a suitable polymer. In the indirect route a 3D negative structure of a polymer mould was built by rapid curing of a polymer. This mould was then filled with a ceramic slurry. After drying, the polymer mould was burned out and

the ceramic structure sintered. Then the structure was infiltrated with a suitable polymer to achieve the composite.

## 2.3.5 Trends in PMCs

The main trends in the structural composite field are related to the reduction of cost which cannot only be related to the improvement in the manufacturing technology, but needs an integration between design, material, process, tooling, quality assurance and manufacturing [54]. Moreover high-tech industries, such as telecommunications, where specific functional properties are the principal requirements, will take advantages by the composite approach in the next future. The control of filler size, shape, and surface chemical nature has a fundamental role in the development of materials that can be utilized to develop sensors and actuators based on the tailoring of functional properties such as optical, chemical, mangneto-elastic, piezo electric etc. Finally, a future technological challenge will be the development of a new class of smart composite materials whose elasto-dynamic response can be adopted in real time in order to significantly enhance the performance of structural and mechanical systems under a diverse range of operating conditions.

Over a long period, countries like U.S. and Japan believe that advances in the materials area would prompt new breakthroughs in the area of composites. In fact, the current research emphasizes "fourth-generation" materials, i.e. those that are designed by controlling the behaviour of atoms and electrons and which provide carefully tailored functional gradients [54].

## 2.3.6 Expectation and needs for future PMCs

The composite materials market is expected to expand in areas where costs are today a strong limitation. The expected reduction of manufacturing costs of the structural composites will expand applications of such materials to large scale markets such as civil supplies and goods.

Expected breakthroughs are related to the development of multi-component materials with anisoptropic and non-linear properties, able to impart unique structural and functional properties. Applications include smart systems, able to recognize and to

adapt to external stimuli, as well as anisotropic and active composite systems to be used as scaffolds for tissue engineering and other biomedical applications [54].

Significant breakthroughs are expected in new composite materials, especially in those applications, such as electronic, optic and biomedical, where functionality is the most relevant technical need. Relevant developments will be expected in the area of interpenetrating phase composite synthesis and interpenetrating composite manufacturing technology. However, further optimisation studies are required to implement large-scale production.

## 2.4 Metal matrix composites

A metal matrix composite (MMC) combines into a single material a metallic base with a reinforcing constituent, which is usually non-metallic and is commonly a ceramic. By definition, MMCs are produced by means of processes other than conventional metal alloying. Like their polymer matrix counterparts, these composites are often produced by combining two pre-existing constituents (e.g. a metal and a ceramic fibre). Processes commonly used include powder metallurgy, diffusion bonding, liquid phase sintering, squeeze infiltration and stir casting [55]. Alternatively, the typically high reactivity of metals at processing temperatures can be exploited to form the reinforcement and/or the matrix in situ, i.e. by chemical reaction within a precursor of the composite.

MMCs come in several distinct classes, generally defined with reference to the shape of their reinforcement [56,57,58]:

**Particle-Reinforced Metals (PRMs):** These contain approximately equiaxed reinforcements, with an aspect ratio less than about 5. These are generally ceramic (SiC, $Al_2O_3$, etc.). PRMs commonly contain below 25 vol% ceramic reinforcement when used for structural applications, but can have as much as 80 vol% ceramic when used for electronic packaging. They are produced using both solid state (powder metallurgy) and liquid metal techniques (stir casting, infiltration). Their mechanical properties, while often inferior to those of fibre-reinforced metals, are more or less isotropic and often represent at moderate cost, significant improvements over those of corresponding unreinforced metals.

**Short Fibre-and Whisker-Reinforced Metals:** These contain reinforcements which have an aspect ratio of greater than 5, but are not continuous. These composites are commonly produced by squeeze infiltration. They often form part of a locally reinforced component, generally produced to net or near net shape. Their use in automotive engines is well established.

**Continuous Fibre-Reinforced Metals:** These contain continuous fibres (of alumina, SiC, carbon, etc.) with a diameter below about 20 μm. The fibres can either be parallel, or pre-woven before production of the composite; this is generally achieved by squeeze infiltration.

**Monofilament-Reinforced Metals:** These contain fibres that are relatively large in diameter (typically around 100 μm), available as individual elements. Due to their thickness, the bending flexibility of monofilaments is low, which limits the range of shapes that can be produced. Monofilament reinforced metals can be produced by solid state processes requiring diffusion bonding: they are commonly based in titanium alloy matrices, which are well-suited to such techniques.

**Interpenetrating Composites:** These are composites in which the metal is reinforced with a three-dimensional percolating phase, for example a ceramic foam. It is the open porous structure of the foams that allows them to be infiltrated relatively easily at low pressures with either molten metals such as aluminium or magnesium or any number of polymeric materials via a simple low pressure system.

Metal Matrix Composites (MMCs) are often reinforced by particles, short fibres and long fibres. A directional reinforcement becomes possible by using fibre preforms from long fibres. But there are some problems regarding the homogenity of particles, the manufacture, strength, handling and costs of preforms. The advantage of ceramic reinforcements is the application-orientated modification of mechanical and thermal properties of the metals. Application fields may be heat sinks (in this case the thermal expansion is decreased and the thermal conductivity is kept at a high level) or low weight metal-product MMCs (increase of the abrasion resistance and the Young's Modulus).

44

In comparison to unreinforced metals, MMCs have the advantage of improved strength and stiffness, increased hardness, wear and abrasion resistance and a better resistance against creep and fatigue. But next to these properties that are mainly due to the reinforcement, the matrix keeps its properties of ductility, electrical and thermal conductivity, oxidation resistance and impact resistance. All this is combined with higher operation temperatures and a light weight. Another important advantage for MMCs is that the combination of reinforcement and matrix material influences the thermal expansion coefficient. The sometimes high expansion coefficient of pure metal is reduced by the right selection and volume fraction of reinforcement material and this allows the designer a better matching of high-temperature engine parts, like turbine blades. Most developments have been done in the field of aluminium and aluminium alloy matrices, primarily due to the light weight, low cost, and ease of fabrication of aluminium. Magnesium and titanium matrices and some special applications, like super alloy matrices combined with tungsten fibres, have also been developed.

The development of the metal matrix composites (MMCs) goes back to the 1960s. It was stimulated by the performance needs of the aerospace and defence industries which place performance ahead of price, at least in development programmes [59]. By this time pure metals had reached their limits, especially in high temperature properties, and the great success of reinforced polymer matrix composites (PMCs) attracted the engineers gave them the idea of copying them in the metal area. The development of boron carbon fibers marked the beginning of the MMC manufacturing technology. Boron filament was developed for both metal and polymeric matrix applications. The early carbon fibres could only be applied to resin-matrix composites due to fibre strength degradation and poor wettability in molten aluminium alloys [59]. Thus, although the development had indicated that the potential was great, the manufacturing problems and the high production costs reduced the first attractiveness of these materials [60]. Twenty years of testing and investigations followed, where numerous matrix and reinforcement combinations and processing technologies were developed, but without the result of a significant application. To minimise the high reaction between matrix material and reinforcement during the liquid-state processing, other production techniques with lower temperatures have been developed. These solid-state processes (diffusion bonding (DB), hot isostatic pressing (HIP) and powder metallurgy (PM)) have been most successful but on the other hand are very cost intensive. It was realised that the success of metal matrix composites could only be

achieved by the invention of lower-cost production techniques. Because the liquid-state processes had the potential to be more economical, further attempts were made to overcome the problems of high reaction or non-wetting. One development in this direction was the introduction in 1984 of a low-cost short-fibre reinforcement, called Saffil™. These fibres consist of δ-alumina with a small amount of silica. Their strength was about 45% higher than other α-alumina fibres and their advantage was that they could be much more easily wetted by a range of aluminium alloys [61,62].

There are many ways to produce MMCs, Figure 2.10 depicts the various production techniques [61,63].
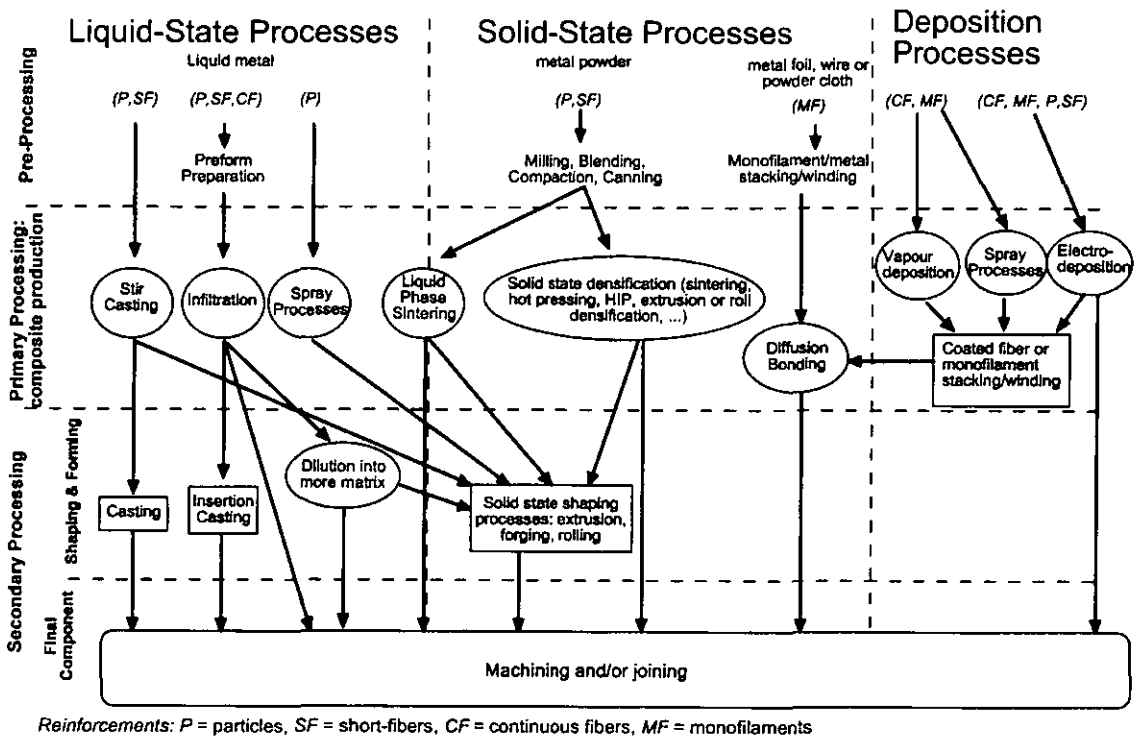


Figure. 2.9: Various production techniques for Metal Matrix Composites [64].

The following paragraph outlines most common production techniques for metal matrix composites [61,64]:

Diffusion bonding (DB):

The matrix material in form of foils or powder is combined with the reinforcement under high pressure and temperature below the melting point of the matrix metal. The diffusion of atoms unifies the material and although the temperature is lower, a reaction between the two phases takes place to realise a good chemical contact. Diffusion bonding is usually used for the production of continuous fibre reinforced composites.

Hot isostatic pressing (HIP):

Reinforcement and matrix material are blended and put into a can. The can is then vacuum degassed and consolidated by high pressure combined with a high temperature that lies below the melt temperature of the metal. After consolidation the part can be shaped and machined. Hot isostatic pressing can be used for all types of reinforcement.

Casting technologies:

Casting technologies, like die casting, squeeze casting or compocasting, are more or less simple casting technologies as used for pure metal alloys. The main difference here is that the reinforcement material, in form of particles or short fibres, is mixed into the melt. After solidification the material can be further processed by rolling, extrusion, forging and drawing. The advantages of the casting technologies are simplicity and economical productivity, the possibility to produce complex shapes and near-net-shape parts, the ease of fabricating selectively reinforced parts and the suitability for various kinds of metal matrices and reinforcements [65]. Possible difficulties include non-wetting, agglomeration of the particles, gravity setting of the particles and unwanted reinforcement/matrix interactions.

Spray co-deposition:

The matrix alloy is induction-melted and broken into droplets by a stream of inert gas (nitrogen). The reinforcement material is injected into this stream and the mixture builds a layer on a former that is placed into the stream. This method is only used for coatings and thin films. The composite material has a fine grain structure because of rapid cooling.

Liquid metal infiltration:

During liquid metal infiltration, like squeeze infiltration or pressure infiltration, a preheated porous perform consisting of the reinforcement material, is placed in a mould and then infiltrated with the liquid metal alloy by pressure or vacuum forces. Recent investigation has developed a spontaneous pressureless infiltration technique, known as PRIMEX$^{TM}$. The infiltration is achieved by the right combination of the atmosphere, the temperature, the alloy composition and the reinforcement material [66].

Obviously the type of reinforcement also influences the method of manufacture. Continuous fibres or woven performs need different production techniques than particles and short fibres. Generally two kinds of reinforcement can be distinguished in the Metal Matrix Composites. Fibre reinforced MMCs made with either continuous or discontinuous fibres (the latter often in the form of a preform), and particulate reinforced MMCs where particles or short fibres are dispersed in the matrix. Continuous fibre reinforced MMCs offer a greater potential for improved properties, but the high cost of the fibres and their anisotropic structure require further development before they will be widely accepted [67]. Discontinuously reinforced MMCs have more isotropic properties and they can be produced with traditional casting techniques, followed by conventional metal working processes such as extrusion and forging. This improves the economy of these composites compared to that of other composites, which are more expensive and labour intensive. G. Curran [68] wrote in his report about Metal-Matrix-Composites in 1998 that powder MMCs will be used in the near term, as they are the only price/performance relevant source of MMCs at the moment.

One of the first particulate MMCs was a class of materials known as 'cermets'. These are metal-bonded carbides and other ceramic materials that are used for cutting tools. In comparison with the recent MMCs, cermets contain only a very small volume fraction of metal.

As mentioned before, the primary support for the MMCs came from the aerospace and defence industries. Many projects were made to develop airframe and space aircraft structures, compressor bodies, vanes and rotors, etc. Hooker et al. [69] outline the benefits and potential applications of Al-MMCs and Ti-MMCs for use in aeroengines.

With the development of cheaper fibres and production technologies the area of application extended also to the automobile, transport, electronic and leisure industry.

There, metal matrix composites above all, were used for engine parts, e.g. pistons, cylinder blocks, connecting rods, etc. In 1982 Toyota commercialised an engine piston that was reinforced in the head with a perform made of short alumina fibres [70]. The composite was produced via the squeeze casting technology.

MMCs have reached an important and exciting phase of development and the future market size should increase faster than before. The first hurdle that still has to be overcome is the substitution of low-cost materials. Despite proven performance improvements, large weight savings and extended service lives, which appear to adequately justify the increased costs, the end use customers still hesitate to invest the initial higher prices to obtain the lower operation costs [71].

## 2.4.1 Infiltration principles

The infiltration process is characterised by the following procedure. A liquid material penetrates a porous solid structure to replace the gas medium within the pores and forms a composite. Usually a complete exchange is desired which means a complete infiltration and a dense material. Infiltration can only take place if the porosity of the host material is open, which means that the pores are interconnected to each other and to the surface of the part. There is extensive literature about the fluid flow aspects. But in the case of the infiltration of ceramic foams with metals further aspects have to be taken into account. The pressure required to infiltrate the porous material with the liquid depends also on the wetting characteristics of the different materials. Further, additional heat flow and solidification aspects have to be considered. All these characteristics have their own influence on the infiltration process and therefore on the quality of the final composite.

Figure 2.10 shows different infiltration conditions in a schematic illustration of the injection of a liquid metal into a mould containing a preform. Generally the temperature of the melt, $T_0$, the temperature of the mould, $T_i$, and the temperature of the perform, $T_f$, are different. Where the superheated metal enters the perform (region 3), the metal is still liquid. Further inside the perform (region 1), the usually cooler perform temperature causes the metal to solidify at the surface. There both liquid and solid metal coexist together with the reinforcement material. The solidification of the metal narrows also the pores of the preform and therefore influences the permeability and the liquid flow. Next to the mould surface (region 2) a further heat flow occurs

which leads to a faster cooling of the metal. In this region the metal first solidifies completely. In the uninfiltrated portion of the perform (region 4), existing gas is pushed and heated by the oncoming metal. These different regions explain the complex correlation of the infiltration kinetics.
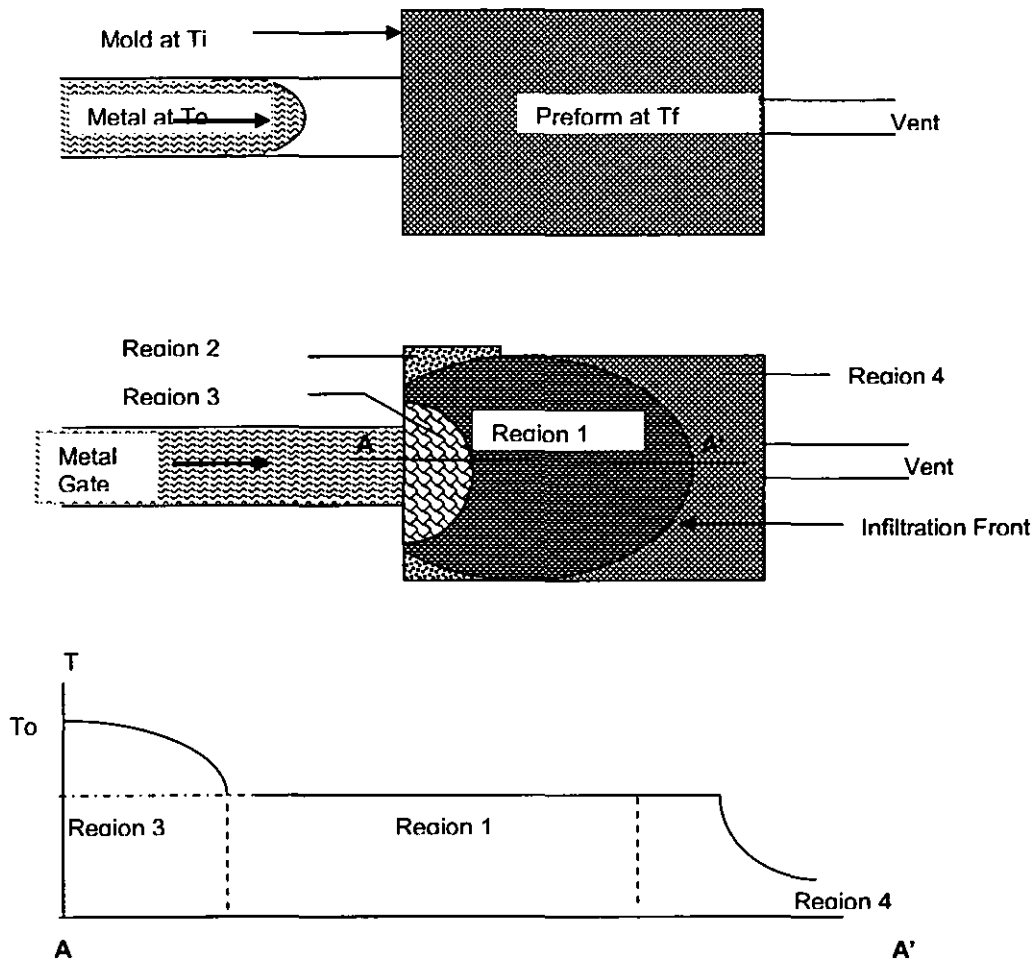


Figure 2.10: Schematic illustration of different infiltration conditions [72].

A lot of investigations have been carried out to combine all these characteristics and to model the complex kinetics of the infiltration of porous materials. Especially with the increasing significance of metal matrix composites several people tried to develop theoretical models of the process. Some of these theories are described by Mortensen et al. [59,72,73,74,75], Alonso et al. [76,77], Jonas et al. [78], Acosta et al. [79,80], Martins et al. [81] and Lacoste et al. [82]. Although there has been so much

50

research in this field, the complex combination of all characters and their influence is not completely discovered. The following topics shall outline the most important parameters.

## 2.4.1.1 Permeability and fluid flow

The infiltration process generally depends on the fact that a fluid is forced into and through a porous structure. Therefore the kinetics of this fluid flow are essential for the process. The ability of a fluid to flow through a porous medium is described as permeability. This character enables the prediction of the flow rate in comparison with a given pressure drop or the other way round, the prediction of a necessary pressure to achieve a determined flow rate. Fluid mechanics has been used to explain the fluid motion and interactions with the tortuous medium path. Topology has supplied the geometric models and parameters of the porous structures that have been used in the fluid mechanical analysis. The result is a vast number of equations and models that attempt to explain permeability [83].

The first one that described the correlation between the pressure drop ($\Delta P$) and the fluid velocity ($V_s$) was produced by Darcy in 1856. For unidirectional flow, neglecting any effect of gravity, Darcy's law may be written as:

$$\frac{\Delta P}{L} = \frac{\mu}{k_1} v_s \qquad\qquad 2.2$$

With  $\Delta P$ – pressure drop

   $L$ – flow distance

   $\mu$ – viscosity of the fluid

   $v_s$ – volumetric flow rate per unit cross sectional area

   $k_1$ – Darcian permeability

Since Darcy's law is only valid for slow flow rates and this is not always given, Reynolds and Forchheimer extended the equation from Darcy to a square dependence of the velocity on the pressure drop. This new equation is known as the Forchheimers equation:

$$\frac{\Delta P}{L} = \frac{\mu}{k_1} v_s + \frac{\rho}{k_2} v_s^2$$

2.3

With  $\Delta P$ – pressure drop

$L$ – flow distance

$\mu$ - viscosity of the fluid

$v_s$ - volumetric flow rate per unit cross sectional area

$\rho$ - density of the fluid

$k_1$ – Darcian permeability

$k_2$ – non-Darcian permeability

The importance of Forchheimers equation is that the fluid and the porous medium are considered to have an influence on the pressure drop independently of each other [84]. However, in most of the articles about the kinetics of infiltration and the fluid flow, only Darcy's law is used and described. This might be because of the complex correlation of the infiltration process, where there are already enough unknown parameters and each simplification may be useful.

However, for both of the two equations the permeability value is connected to the structure of the porous material. The porosity, the pore size, and also the shape of the pores have an influence on the permeability value. Usually this value is calculated by experiments where a medium is pressed through the porous material and the pressure drop for a determined distance is measured. To obtain valid and useful results, these experiments have to be carried out under the same conditions as for the later infiltration. That means that the same materials, pressures, temperatures, and atmospheres should be used to be able to predict the infiltration as early as possible.

A lot of research has been undertaken to try to define the correlation between permeability and a given material structure by mathematical equations. Ergun described the permeability values of Darcy's law and Forchheimers equation for packed columns made of spheres, cylinders, tablets, modules etc. as follows [85].

$$k_1 = \frac{\varepsilon^3 d_p^2}{150(1-\varepsilon)^2}$$

2.4

$$k_2 = \frac{\varepsilon^3 d_p}{1.75(1 - \varepsilon)}$$

2.5

With  $\varepsilon$  – porosity

$d_p$  – mean particle diameter

Since 1952, these types of equations have been used to predict the permeability of porous materials. The main problem of the application of these equations to foam like structures is that they are based on porous materials made of particles that can be described by a geometrical shape. The structure of foams is different. Foams usually consists of cells that are separated by struts. The interconnection between these cells is achieved by smaller windows. The translation of the cell and window sizes to the particle diameters of the Ergun type equations is not easy and the topic of numerous investigations nowadays.

The described laws and equations for the infiltration kinetics are only a small part of the complex process. The porous structure that acts as the basis for the theory changes during an real infiltration process. In case of liquid metals, some parts may solidify and thereby narrow the pores and channels of the material. The same is valid for resin materials, if a very high adhesion of the resin causes higher frictional forces when the resin is flowing through the pores. Further changes could occur because of the deformation and destruction of the porous structure during infiltration. These possibilities are usually not calculable and should be avoided by the right choice of the infiltration parameters, like pressure and viscosity.

## 2.4.1.2 Wettability and surface tension

The pressure required to infiltrate a porous material not only depends on the porous structure and the laws of fluid flow, it also depends on the extent to which the liquid material wets the perform material.

If the liquid wets the solid a spontaneous infiltration occurs to a defined depth. If the solid is not wetted, an external application of pressure is needed to force the liquid into the pores. The external pressure that is required for infiltration can be calculated by the so called capillary law or Laplace equation. If the calculated pressure

is negative, infiltration occurs spontaneously because of wetting.

$$P = A(\sigma_{sl} - \sigma_{sv})\left[\frac{V_r}{(1-V_r)D_r}\right]$$

2.6

Where  $A$ – geometry factor (4 for cylindrical fibres and 6 for spherical particles)

$\sigma_{sl}$ – solid/liquid surface energy

$\sigma_{sv}$ – solid/vapour surface energy

$V_r$ – volume fraction of the reinforcement

$D_r$ – diameter of the reinforcement particles

The difference between the two surface energies is the amount of work that is necessary for immersion. When a solid is immersed into a liquid, as shown in Figure 2.11, immersional wetting occurs and the solid/gas interface is replaced by a solid/liquid interface without changing the area of liquid/gas interface. The free energy of the work performed is called the work of immersion, $W_i$.

$$W_i = \sigma_{sl} - \sigma_{sv}$$

2.7

For the work of immersion the same rules as for the spontaneous infiltration apply. If $W_i < 0$ spontaneous wetting occurs, while if $W_i > 0$ the solid would tend to float and must be forced into the liquid.
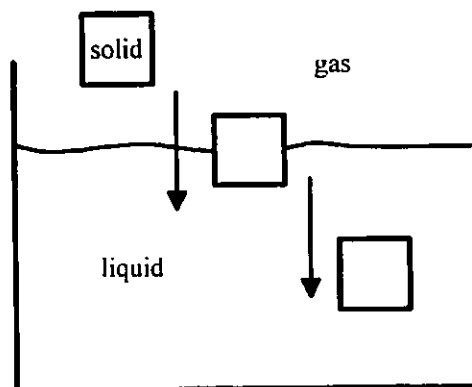


Figure 2.11: Immersion of a solid into a liquid [86].

The wettability of a solid by a liquid is measured by an conventional experimental method, the sessile drop test (see Figure 2.12), in which a drop of the liquid material rests on the solid surface. The measurement of the contact angle and the shape of the drop enables determination of the surface tension of the liquid and the wetting angle, θ, the latter characterising the degree of wetting. The fundamental relationship between the wetting angle, θ, and the surface tension in equilibrium is given by the Young-Dupre equation:

$$\sigma_{sv} = \sigma_{sl} + \sigma_{lv} \cos\theta \qquad\qquad\qquad 2.8$$

With        $\sigma_{sv}$ - solid/vapour surface energy

            $\sigma_{sl}$ - solid/liquid surface energy

            $\sigma_{lv}$ - liquid/vapour surface energy

            $\theta$ - wetting angle
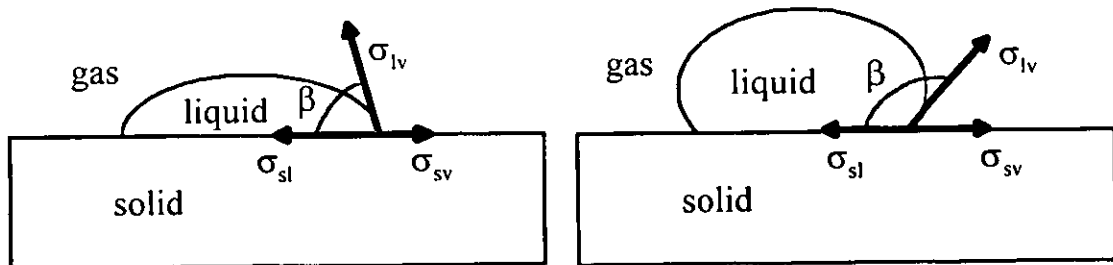


Figure 2.12: Schematic diagram of the sessile drop test. Left: wetting, Right: non-wetting.

Although the results of the sessile drop tests are precise and reliable they can only give a trend for the infiltration process of porous materials. The conditions under which the tests are carried out could be described as equilibrium conditions while the infiltration process is in fact a non-equilibrium situation. The tests are carried out under a determined atmosphere, temperature and time. These parameters vary significantly during an infiltration process. Further, most liquid metals are covered by oxide layers except under high vacuum conditions. These layers prevent the contact of the pure

metal and the solid. During an infiltration process, the oxide layers could be broken by the forces working.

However, the wetting characteristics and the Young-Dupre equation give some ideas for possible solutions to the problem of the generally poor wetting of reinforcements by liquid metals. As seen from the equation, an improvement of the wetting can be achieved by either raising the solid/vapour surface energy, $\sigma_{sv}$, and/or lowering the solid/liquid surface energy $\sigma_{sl}$. Lowering the liquid/vapour surface energy, $\sigma_{lv}$, will not lead to an improvement because the wetting angle will then change as well, leaving the basic entity $\sigma_{sl} - \sigma_{sv}$ unchanged.

Raising the solid/vapour surface energy, $\sigma_{sv}$, can be achieved by either a pre-treatment of the reinforcement material or a coating of the reinforcement with a higher energy element. The pre-treatment changes the chemical nature of the atmosphere prior to infiltration. The adsorption of oxygen or other elements from the atmosphere can modify the reinforcement surface [59]. Within the coating two different types of materials can be distinguished. One reacts with the matrix material and the other type reacts with the oxide layer on the liquid metals and therefore achieves a contact of the metal and the reinforcement. Sometimes both kinds of reaction are possible. Coatings that react with the matrix are mainly metal coatings. Examples for coatings that react with the oxide layer are the fluxing agents known from brazing technology.

A lowering of the solid/liquid surface energy, $\sigma_{sl}$, is often achieved by alloying the metal matrix. Examples are magnesium and lithium in aluminium for alumina reinforcement, titanium in aluminium for SiC fibres and chromium and zirconium in aluminium for carbon fibres [59]. These additional components influence the wetting characteristics in two ways. Some of them react with the reinforcement material while the others change the appearance of the oxide layer of the new alloy.

Another factor that can influence the wetting is the surface roughness. On a rough surface wetting is by the local contact angles, which can differ substantially from the apparent angle. Thus wetting gets worse with an increasing surface roughness [87]. This fact will have a great influence on the infiltration of porous materials, which can be described as materials with a very rough surface. It can be assumed that if this factor is essentially the wetting of a porous reinforcement is even worse than of a solid ceramic. Some wetting tests will be carried out with the ceramic foams during this investigation and hopefully will give some more information about this.

It is important to realise that wettability and bonding are not synonymous terms. Wettability describes the extent of intimate contact between a liquid and a solid. It does not necessarily mean a strong bond at the interface. One can have excellent wettability and a weak van der Waals-type, low-energy bond. A low contact angle, meaning good wettability, is a necessary but not sufficient condition for strong bonding [2].

## 2.4.2 Materials

There is a wide range of materials conceivable for use with the infiltration of porous ceramics. Generally all castable metals and metal alloys can be used. The most common materials are aluminium, magnesium, titanium, nickel and a huge variety of their alloys.

The aluminium alloys are probably the most widely used matrix materials for metal matrix composites, primarily due to their lightweight, low cost and ease of fabrication. Pure aluminium is not suitable for pressure casting processes [88]. This is due to a high shrinkage, low strength and bad casting properties. Within the aluminium alloys there are three main fields that can be distinguished. These are the Al-Si alloys, the Al-Mg alloys and the Al-Cu alloys. The Al-Si alloys are especially suitable for thin and complex castings. The silicon increases the fluidity of the molten alloys while simultaneously strengthening the solid material. Al-Mg alloys provide very good corrosion resistance. The Al-Cu alloys are more used in the USA. Because of the high amount of copper they are more expensive and provide a lower corrosion resistance [88,89].

Magnesium and magnesium alloys are primarily used because of their lightweight. Magnesium alloys have a density about two thirds that of aluminium and about one quarter that of iron-base or zinc-base alloys. A wide range of magnesium alloys is available providing different properties like high strength, high ductility or creep and corrosion resistance.

Titanium and nickel alloys are used mainly for high temperature applications in the aerospace industry. There are also nickel based super alloys. Other metals used for the matrix are copper, zinc and lead.

### 2.4.3 Metal infiltration techniques

A lot of techniques have been developed for the infiltration of porous materials with metals. The most common technique which is in use in the field of metal matrix composites is the squeeze casting process. After the significance of the metal matrix composites increased rapidly the process was further developed to the squeeze infiltration process. The following section outlines this process together with its parameters and characteristics. After the squeeze casting technology there are some other infiltration technique presented that are also used for metal infiltration.

### 2.4.3.1 Squeeze casting

Squeeze casting is a technique that combines the advantages of casting and closed die forging in a single process. The resulting castings combine an excellent microstructure together with a near-net-shape product. The squeeze casting process is widely used for a lot of different alloys and since the development of MMCs it has found a new field of interest.

In the Russian literature the first mention of squeeze casting goes back to 1878 where Chernov is attributed with envisioning the concept. The first squeeze casting experiments were reported in 1937 with the production of brass and bronze cylinders. After the second world war there were a lot of investigations concerning the squeeze casting process and in 1979 Toyota Motor Company introduced squeeze cast aluminium alloy wheels for passenger cars. In 1983 it was again the Toyota Motor Company that presented selectively reinforced squeeze cast composite diesel engine pistons [87,90]. Today squeeze casting is widely used to produce engineering parts with high quality. A few of the parts that have been produced by squeeze casting, include

> - pistons for engines
> - disc brakes
> - automotive wheels
> - truck hubs
> - barrel heads
> - brass and bronze bushings
> - steel missile components

> ➤ differential pinion gears
> ➤ ductile iron mortar shields

After squeeze casting was introduced for the production of composites, especially composites where fibre performs are infiltrated with molten metal, there was a differentiation between the usual squeeze casting process and the squeeze infiltration process. Both processes are available for composites.

For production of a composite via the squeeze casting technique as shown in Figure 2.14, the particles or fibres are already mixed into the alloy before the casting process. The mixture is then poured into the die cavity and solidified at high pressure. After pouring the molten metal mixture into the die there is virtually no further movement of it. The melt stays under hydrostatic pressure until solidification.

Within squeeze casting two variations can be distinguished, viz. the 'direct' and 'indirect' process.

In the 'direct' squeeze casting process a measured quantity of a molten metal alloy is poured into an open preheated mould. The mould is then closed by the means of an upper punch that may be shaped to form part of the casting. After the mould is closed and the punch contacts the molten metal, pressure is applied. The applied pressure is maintained until solidification has taken place. Then the punch opens and the casting is ejected.

In the 'indirect' squeeze casting process the melt is pressed into a closed mould through a lug from below by a smaller punch. After filling the mould, this punch also maintains pressure until solidification of the metal. The process is very similar to the die casting technique and the main difference is the velocity of the molten metal alloy. Within the 'indirect' squeeze casting the velocity usually is about 0.5 m/s while in die-casting it is about 30 m/s [91]. The slow viscosity provides a controlled mould filling without swirling and air inclusions.

In the squeeze infiltration process shown in Figure 2.13, the reinforcement and the molten metal alloy first come in contact when the fixed charge of molten metal is poured into the die cavity where the preform is already placed. Both the die cavity and preform are preheated. After closing the die, the ram first applies a hydrodynamic pressure whereby the liquid metal is forced to infiltrate the preform. Not until the preform is completely filled does the status change to a hydrostatic pressure. Therefore the correct expression for the infiltration of porous ceramics must be squeeze

infiltration process. However, the squeeze infiltration process is based on the squeeze casting technology and it also provides its properties.

The quality of the squeeze casting and infiltration processes depends on the following parameters:

> Melt temperature
> Melt quality
> Die temperature
> Infiltration speed (metal velocity)
> Applied pressure
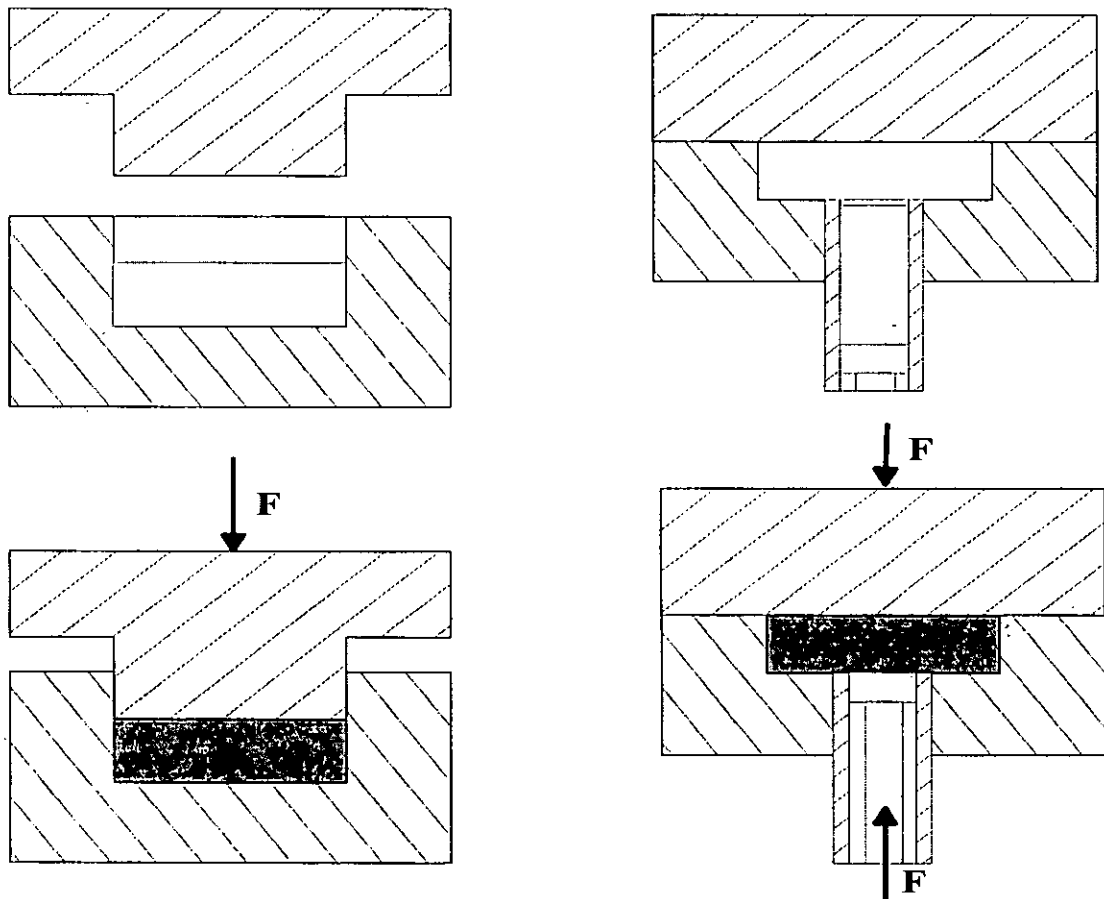


Figure 2.13: The direct (left) and indirect (right) squeeze casting process [92].
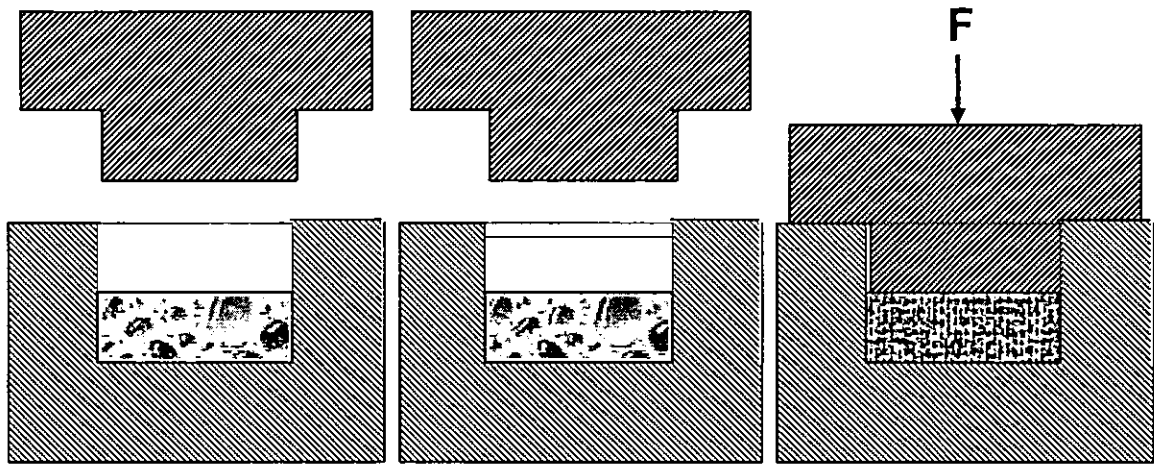
Figure 2.14: The squeeze infiltration process

**Melt Temperature**

The melt temperature affects the casting quality as well as the die life. There is no question that the melt temperature first of all depends on the metal alloy used for the casting. Normally the pouring temperature (melt temperature) lies between 6°C and 55°C above the liquidus temperature of the alloy [92] for squeeze casting, and 50°C to 150°C for squeeze infiltration of metal matrix composites [87]. The temperature further depends on the freezing range (difference between solidus temperature and liquidus temperature), and the shape or complexity of the casting. The narrower the freezing range, the higher must be the degree of superheating of the melt. Materials with a narrow freezing range solidify very quickly after coming into contact with the preform or the mould walls. To make sure that the metal is still liquid when the pressure is applied and further that the preforms and thin sections are completely filled the pouring temperature must be high enough. If the temperature is too low, poorly infiltrated or very porous castings are obtained [93].

On the other hand, a higher melt temperature will cause a shorter die life. If the pouring temperature is too high it can lead to extrusion of liquid metal through the tooling interfaces, causing metal flash or possible jamming of the tooling. It can also result in shrinkage porosity in thick sections of the casting and in reactions between the melt and provided performs. Generally the melt temperature should be chosen to be as low as possible to prevent the disadvantages mentioned above and reach a high

metallurgical quality affected by rapid heat extraction.

Lim [87] investigated the squeeze casting and the investment casting process of the LM25 aluminium alloy in combination with Saffil[TM] alumina fibres which contain 96-97% $Al_2O_3$ and 3-4% $SiO_2$. He further developed a hybrid casting process that combines the advantages of the squeeze and investment casting processes. He found out by his experiments that the higher the melt temperature, the higher the tensile strength due to improved wettability of the fibre reinforcement.

**Melt Quality**

The melt quality affects the casting quality and its mechanical properties. Therefore it is important to ensure a melt that is free of inclusions, gas bubbles and other substances. For this the use of filters, skimming and degassing is recommended. The application of pressure further inhibits gas bubble formation.

**Die Temperature**

The die temperature also influences the die life and the casting quality. If the die temperature is too high it can cause welding between the casting and the die. The casting quality is reduced by hot spots and shrinkage pores. Temperatures above 150°C are used, with the range of 200 to 300°C being most often used for aluminium alloys. To ensure adequate clearance for venting, the punch temperature should be between 15°C and 30°C below that of the die [92].

Lim [87] found an optimum temperature of 250°C for the LM25 aluminium-alloy and Yong [94] received the best ambient and elevated tensile properties for the squeeze casting of MgZn-alloys (RZ25/RZ5DF) also with a die temperature of 250°C.

**Preform Temperature**

The preform temperature influences the casting quality similar to the die temperature. The temperature must be high enough to assure a complete infiltration of the perform and to avoid freezing of the molten metal before the infiltration is completed and the pressure is applied. Therefore the preheat temperature of the preform depends on its dimensions, its porosity, the infiltration speed and the applied pressure. The selection of the metal or alloy and its pouring temperature is the main factor for the choice of the preform temperature. The preheating also provides a better wetting of the

ceramic, due to the thermodynamic rules outlined in earlier chapter. A too high preform temperature can cause metal-ceramic reactions and/or the degradation of the preform.

Lim [87] writes that the fibre preform preheat temperature is of great importance to obtain good infiltration and subsequent fibre/matrix bonding. The highest temperature (400°C) in combination with the highest melt temperature (750°C), during his investigations produced sufficient matrix-fibre wetting but also slightly lower strength due to slower solidification rates. Therefore he suggested a preform temperature of 300°C for Saffil™ alumina fibres combined with LM25 aluminium–alloy as the optimum.

Yong [94] achieved his best results with a preform temperature of 600°C also for Saffil™ fibres but in combination with a MgZn-alloy (RZ5/RZ5DF). The pouring temperatures and the die temperatures were more or less the same in both investigations.

**Infiltration Speed (Metal Velocity)**

The infiltration speed is related to the infiltration pressure by Darcy's law and the Forchheimer equation. Therefore both parameters cannot be controlled at the same time.

Fukunaga [95] found that an infiltration speed ranging between 1 to 5 cm/s has no effect on the tensile strength of the final composite. Generally a slow speed is recommended to get better control of the infiltration process, but too slow on infiltration speed will allow the melt to freeze before it is able to infiltrate the preform completely. On the other hand too fast an infiltration speed can lead to the destruction of parts of the perform, which also decreases the properties of the composite.

**Applied Pressure**

A high pressure applied to the melt and maintained until solidification of the casting has several positive influences on the process.

In the squeeze infiltration process, it first of all serves to infiltrate the liquid metal into the pores of the ceramic preform, giving a sound metal-ceramic composite. The pressure is necessary to overcome frictional forces experienced by the liquid flowing through the preform channels. With pressure the melt front is able to pass quickly through the preform [65]. An additional pressure is necessary to promote the

63

wetting of the ceramic by the liquid metal that is normally prevented by the thermodynamic surface energy. If the pressure is not high enough the preform would not be completely filled and voids would remain in the composite. On the other hand if the applied pressure is too high, deformation or destruction of the preform could occur, which would decrease the composite properties.

The pressure difference necessary for infiltrating the molten metal into a preform can be evaluated by the Laplace equation and Darcy's law. Squeeze casting was used before the squeeze infiltration process was developed. This outlines that the pressure has another important purpose.

The application of high hydrostatic pressure to a pure metal affects its melting point. For alloys it further has an influence on the whole alloy equilibrium phase diagram and shifts it upwards and towards the composition with higher concentrations, whose melting point is least affected [87].

The effect of the pressure on the melt temperature of a pure material is given by the Clausius-Clapeyron equation:

$$\frac{\Delta T}{\Delta P} = \frac{T_m (V_l - V_s)}{Q}$$

2.9

where $\Delta T$ – change in melting temperature

$\Delta P$ – change in pressure

$T_m$ – melt temperature at atmospheric pressure

$V_l$ – specific volume of liquid phase

$V_s$ – specific volume of solid phase

$Q$ – latent heat of freezing

The equation shows that applied pressure raises the melting point of a material in the case material shrinks during freezing which means that the specific volume of the liquid phase is higher than the specific volume of the solid phase. This is true for most metals. If the reverse is true, then an increase of pressure would lead to a decease of the melt temperature. This is valid for silicon and bismuth [87,94].

The effect of an applied pressure of 98.1 MPa on the solidification of the Al-Si system is shown in Figure 2.15. The eutectic point shifts to a higher Si concentration

and simultaneously the eutectic line is shifted to a higher temperature. An alloy with 12% of Si now becomes hypoeutectic. An alloy with the composition X will be completely liquid at the temperature $T_1$. If this composition is now applied to a pressure of 98.1 MPa, the liquidus line will shift above this temperature and this will lead to extensive nucleation and supercooling. Therefore the achieved microstructure of the casting will be very fine.

The increase of the liquidus temperature by the applied pressure during solidification leads to fine microstructures in the castings, coming out of the enforced supercooling combined with extensive nucleation. This high rate of heat extraction is further assisted by the elimination of air gaps between the molten metal and the die. The applied pressure forces the metal against the walls and this results in a higher heat conductivity and therefore in a higher heat transfer at the interfaces between the molten metal and metal die.
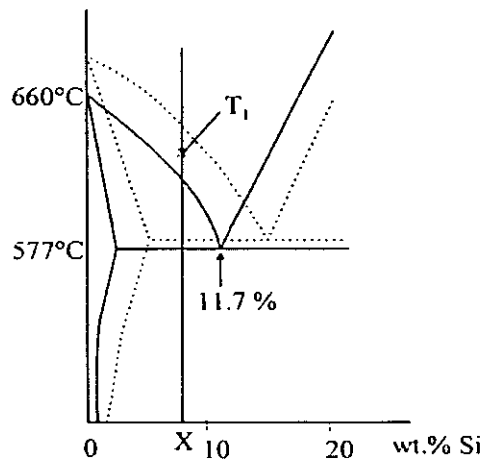


Figure 2.15: Effect of pressure of 98.1 MPa on part of the Al-Si system. Solid lines: equilibrium phase diagram, dotted line: at 98.1 MPa [87].

The pressure is applied with the closing of the die and should be maintained until solidification has finished. The pressurised solidification prevents dissolved gases from nucleating and further feeds the molten metal and/or semi-liquid metal into its voids. This avoids shrinkage and gas porosity and leads to defect free, fully dense materials. Last but not least by forcing the metal against the die walls and into narrow areas during solidification, near-net-shape castings with fine details and an excellent surface finish can be achieved.

Typical infiltration pressures lie in a range between 70 to 200 MPa. Lim [87] received his best results for an LM 25 aluminium-alloy in combination with Saffil$^{TM}$ alumina fibre performs with a MgZn-alloy (RZ / RZ5DF).

The main defects that could occur by choosing incorrect values for the parameters are [96]:

- Oxide inclusions
- Porosity
- Extrusion segregation
- Blistering
- Underfill
- Cold laps
- Hot tearing
- Stickering
- Case bonding
- Extrusion bonding

With a careful selection of the process parameters the squeeze casting technique offers a wide range of advantages for a number of engineering applications and the highest mechanical properties for cast products are attainable. The process has also an excellent potential for automated operation at high rates of productivity and an economical and efficient use of raw materials [96]. The production of composites by using performs and the squeeze infiltration process is simple and receives good results. Metal inserts may also be placed in desired locations and a designer using a computer aided design approach has the flexibility to design castings with specific properties in different areas of casting [90].

A summary of the advantages and disadvantages connected with the squeeze casting and squeeze infiltration process is given below:

**Advantages:**

- Complete elimination of shrinkage and/or porosity

- Fine grain size and excellent microstructure

- Near-net-shape process with high reproducibility complex shapes, thin sections and an excellent surface finish

- Isotropic properties

- Fast solidification leads to fine microstructure, short cycle times and high productivity

- High mechanical properties of the castings

- Economical efficient use of raw materials

- Suitable for a wide range of materials

**Disadvantages:**

- High capital investment

- Careful control of melt quality and quantity required

- Limited aspect ratios

- Limited size of parts

## 2.4.3.2 Investment casting

The investment casting process as shown in Figure 2.16 is designated as a ceramic mould casting process. Moulds are produced by covering an expanded pattern or runner/pattern assembly, almost universally of wax, with a ceramic shell. The shell is produced by dipping the pattern into a ceramic slurry to obtain a coating. The wall thickness can be regulated by dipping and drying several times. Sometimes the pattern is placed into a metal flask which is then completely filled with a ceramic slurry. Once the ceramic mould is produced, the wax pattern is removed by thermal or chemical means (dewaxing). The moulds are then fired to develop a refractory bond. Moulds may subsequently be cast whilst still hot or allowed to cool, depending on section thickness and metallurgical requirements. The mould may be poured under static pressure, or under vacuum pressure or centrifugal assistance. Once the casting has cooled the mould material is typically removed by impact, vibration, grit blasting, high pressure water blasting or chemical dissolution [97].
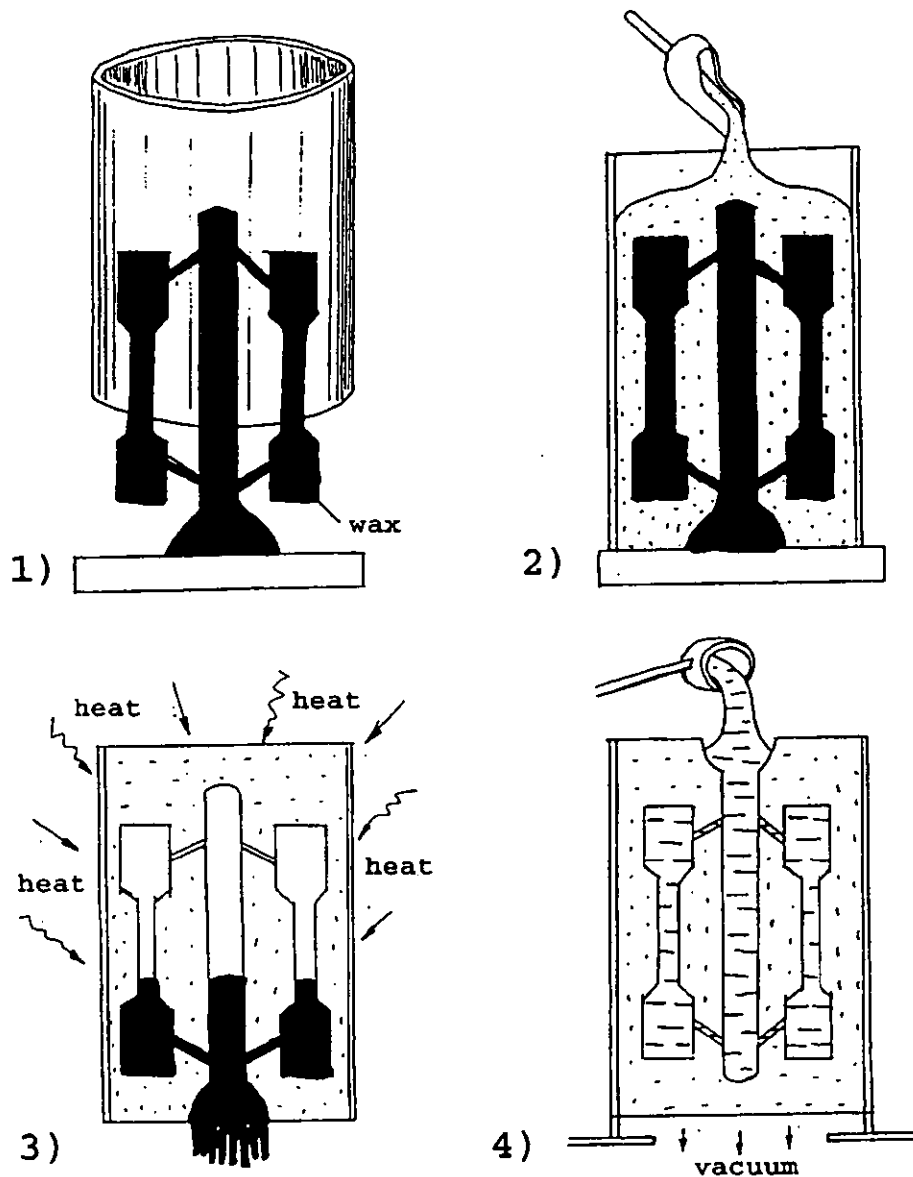
Figure 2.16: The investment casting process [87].

The conventional investment casting process is not suitable for the production of sound metal/ceramic composites by infiltration of preform. Simply pouring molten metal over a fibre preform in a die will not lead to infiltration because of the non-wettability of ceramic materials with liquid metals due to their high surface tensions. The technique is more suitable for premixed short-fibre or particle reinforced alloys. However, the investment casting technique has some interesting advantages in

comparison with the squeeze casting process. Therefore Lim et al [87,98] developed a hybrid casting process for the infiltration of ceramic performs. The process combines the advantages of the investment casting technique with the advantages of the squeeze casting technique.

While the investment casting process is able to produce complex castings it is limited in its ability to produce castings of the highest structural integrity. The squeeze casting process on the other hand provides the advantages that are combined with the applied pressure during the process, but because of the requirement for a metal die there is a limitation to the complexity and section thickness of the castings.

The developed hybrid process uses the wax patterns and block moulds of the investment casting process and combines this with the application of pressure for the infiltration and solidification.
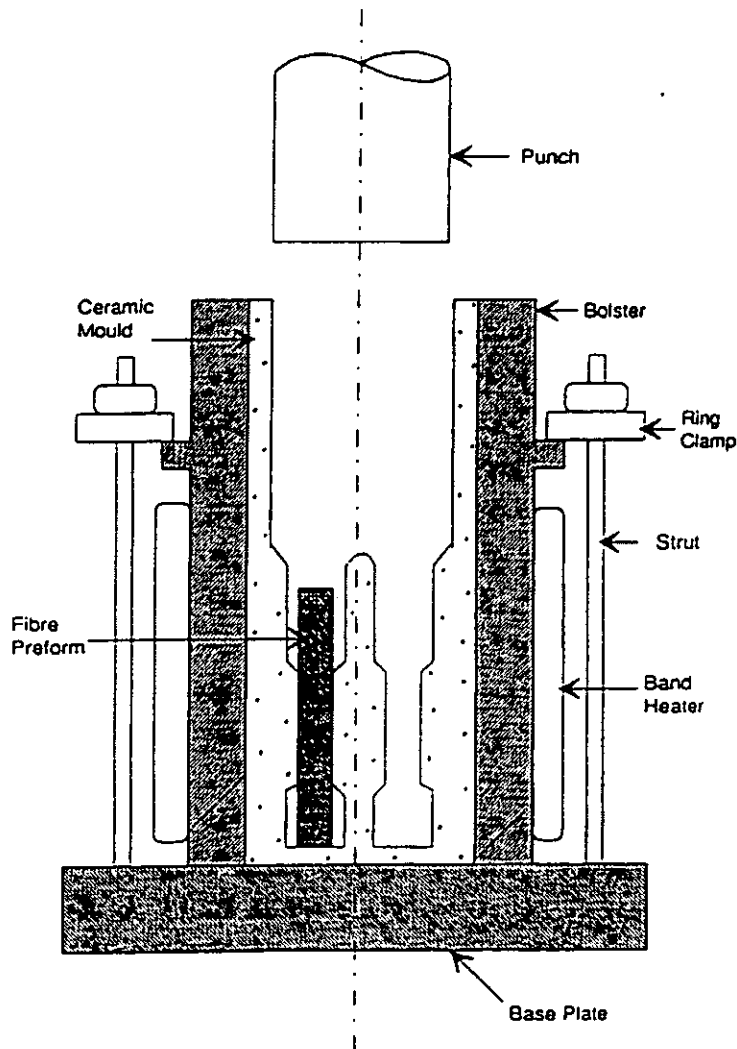


Figure 2.17: Schematic diagram of the hybrid casting equipment [98].

The fibre preforms are incorporated into the wax patterns. It was found out that a non-wetting coating of the ceramic mould must be obtained that permits the escape of air but provides the penetration of the molten metal. Therefore the wax patterns were first coated with an aluminium resistant material and then invested with a ceramic slurry to produce the block mould. After dewaxing and firing, the block mould was placed into a metal bolster. This bolster was necessary to prevent the fracture of the ceramic mould as a result of the applied pressure for infiltration and solidification. The metal was then poured into the mould and pressure was applied by a punch. A schematic diagram of the hybrid casting equipment is given in Figure 2.17.

The hybrid casting process was able to produce metal matrix composites by the infiltration of alumina fibre performs with an LM25 aluminium alloy. The pressure used was 12 MPa and no use of special melt conditions, fibre coatings or gas atmospheres was necessary. The mechanical properties of the composite materials produced were intermediate to those of the squeeze cast and investment cast composites.

## 2.4.3.3 Pressureless metal infiltration

The pressureless metal infiltration or PRIMEX$^{TM}$- process was developed in the late 1980s by the Lanxide Corporation [99]. With this technique a spontaneous infiltration of aluminium alloys into loose beds or compacts of reinforcing materials is achieved. Spontaneous infiltration in this case means without the application of pressure or vacuum but just by choosing the right parameters.

The infiltration parameters that were found to have an influence on the infiltration are:

- The composition of the infiltration alloy
- The process atmosphere
- The process temperature
- The process time

The composition of the infiltration alloy has an influence on the wetting characteristics of the material combination. The wetting and bonding is influenced by

the surface tension of the alloy, the solid-liquid energy and by possible chemical reactions at the solid-liquid interface. Magnesium was found to reduce the surface tension of the aluminium alloy and simultaneously induces interfacial reaction because of its high reactivity. A linear relationship was suggested with an increasing content of magnesium causing an increase in infiltration. Further it was found that a critical minimum value of magnesium must be applied to start infiltration. In this special case the minimum lay between 0.5 wt.% and 1 wt.%.

For the process atmosphere it was found out that a nitrogen atmosphere led to spontaneous infiltration. It was suggested that the nitrogen further reduces the surface tension. While no filtration occurred in a 100% argon atmosphere and only a partial infiltration occurred in a 10% N and 90% Ar atmosphere, 25% nitrogen together with 75 % argon were enough to infiltrate the porous material. The higher the percentage of nitrogen the faster was the infiltration. This further influenced the formation of AlN, which was less with a higher percentage of nitrogen, but possibly because of the faster infiltration.
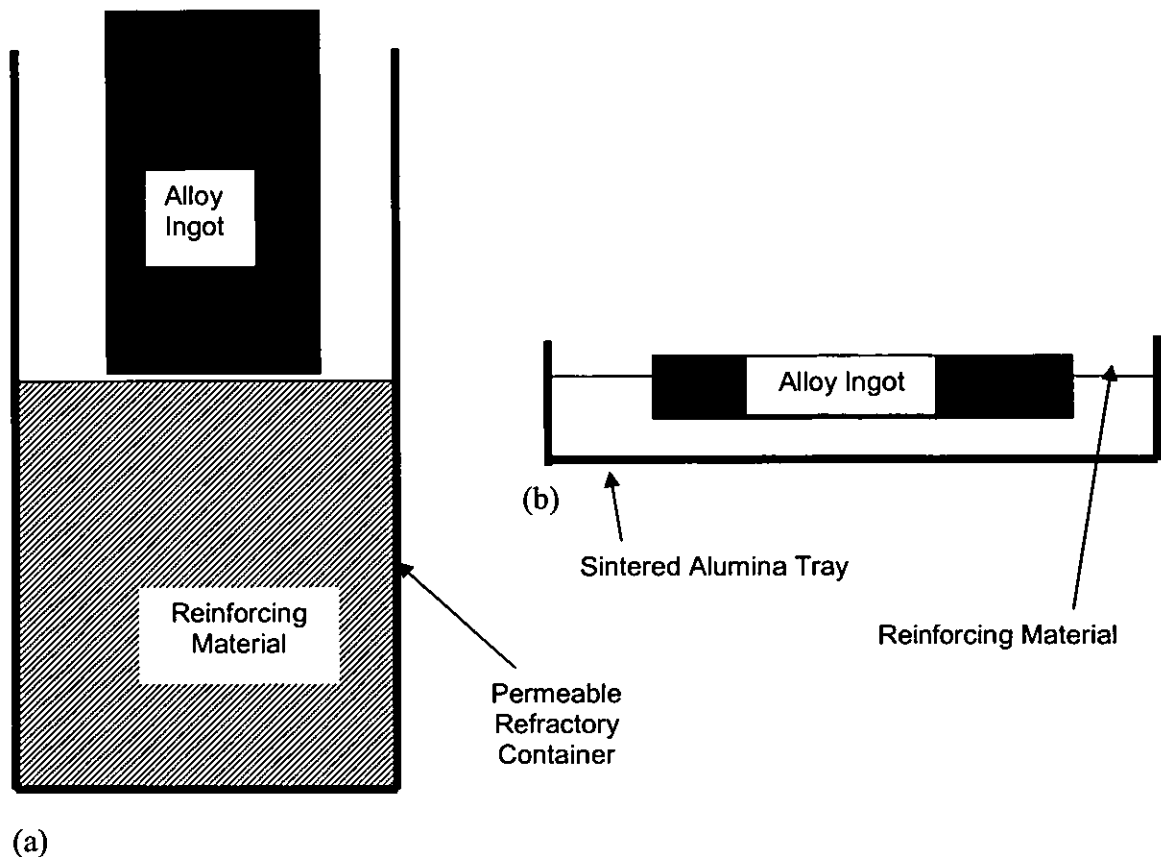


Figure 2.18: Schematic drawing of the pressureless infiltration assembly [99].

71

Infiltration increased in an approximately linear manner with the process temperature. A critical minimum temperature was needed to start the infiltration. The critical temperature in this case was 750°C, with increasing temperature the infiltration depth is increased. Simultaneously an increasing process temperature also increased the formation of AlN. This shows the complex combination of the process parameters and outlines the difficulty to adjust it to receive the best results.

The process time should be as short as possible to prevent the formation of AlN and other unwanted reactions. On the other hand it has to be long enough to allow the alloy to infiltrate the porous material completely and to achieve a sound composite. Therefore the process parameters have to be carefully chosen.

A schematic drawing of the process assembly is given in Figure 2.18. An aluminium alloy ingot is placed on top of the reinforcing material. The alloy/filler pair is then placed into a furnace. The atmosphere in the furnace is evacuated at room temperature and backfilled with the nitrogen atmosphere.

To prevent the entering of unwanted gases entering into the furnace, it is continuously fed with a low flow of nitrogen. The furnace was then ramped to temperature at a rate of 200°C/hr, held at the temperature for the specificied time and then allowed to cool again. If the process parameters have been adjusted correctly infiltration takes place. The pressure less infiltration technique is applicable to the production of composites containing a wide range of reinforcement types [99].

## 2.5 Growth of PMCS & MMCs and the need for this project

The reinforced plastics/composites industry today encompasses a very broad range of materials, products, and manufacturing processes. About 85% of the material used in glass fibre-reinforced polyester resin (often called fibre-reinforced plastic, or FRP). Less than 2% of the material used in the reinforced plastics/composites industry goes into "advanced composites" for use in "high-tech" applications such as aircraft and aerospace [108]. In 1984, the world produced some 22 million pounds of advanced composite materials, mostly in the United States. The total value of fabricated parts was

about $1.3 billion split among four major consuming industries: aerospace (60%), sports equipment (20%), and industrial and automotive (15%).

The market for advanced polymer composites has grown at a relatively high rate of about 15 percent per year during the last few years, with the fastest growing sector being aerospace industry at 22% [109].

For MMCs, a conservative annual market growth rate of between 15 to 20% has been projected through 2004 [110]. This will be led by the ground transportation industry (automotive and rail), and in the high value-added thermal management and electronic packaging sector. Additional applications are expected to result from increased experience and confidence in MMCs, based on prior use and on natural market growth. The growth in the automotive and rail industry is expected from increasing pressure for light weight, fuel economy, and reliability. Unlike the automotive market, MMCs for the electronic packaging sector are high value added. Although electronic packaging is the second-largest MMC market in terms of volume (26.5%) and is by far the largest in terms of volume (66%) [110]. In the thermal management and electronic packaging industry, increased MMC use will result from the dramatic growth in this industry for new networking and wireless communications installations. The largest market by far, and the largest projected growth, is for discontinuously reinforced aluminium (DRA), which is expected to double in production volume between 1999 and 2004 [110]. Figure 2.19 represents MMC market predictions by BCC [64].

This growth is anticipated from existing technologies and applications. However, significant new applications and markets are being pursued vigorously for MMC technologies that are now on the verge of widespread acceptance. A notable example is the relatively low-cost continuously reinforced aluminium MMC produced by 3M. Significant progress has been achieved in the last two years toward the acceptance of this material for overhead power transmission conductors (high tension wires). This application, if successful, will represent a dramatic increase in the worldwide MMC market and may be nearly equal to the entire annual volume of the ground transportation market. The sample, flexible material form (wire and tape) is amenable to use in a wide range of applications. The uniaxial configuration is ideal for hoop and tube or rod configurations, and it can be easily be used as an insert for selective reinforcement of components. Many potential applications are currently being pursued, including flywheel containment, high speed electric motors, and high-

performance automotive components. A novel process using the tape perform is being pursued to produce large cryogen tanks for rocket propulsion, paving the way for building large structures from a simple to-manufacture material form.
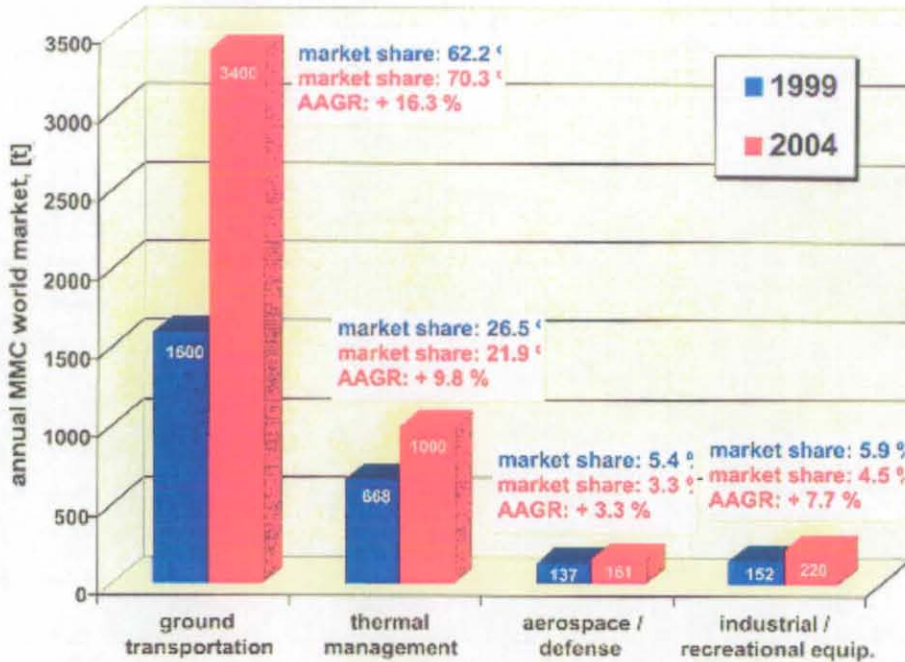


Figure 2.19: MMC Market predictions by BCC [64].

In the longer term, technology innovations leading to new and significantly improved MMC materials can be expected as a result of the robust international activity in MMC research and development. Titanium alloys are specified in many applications, especially aerospace, where the use temperature exceeds the current limit for aluminium alloys, about 150°C. The titanium is more expensive, more difficult to machine, and heavier, yet is required to support the service temperature. Discontinuously reinforced titanium shows very attractive structural properties [61] and is currently used commercially in automotive valves for the Toyota Altezza [63]. However, the approaches taken to ensure that cost goals were met are incompatible with aerospace requirements. Research and development of discontinuously reinforced titanium (DRTi) for aerospace applications show that this MMC has the potential of exceeding the structural efficiency of all metallic materials, and of cross-ply graphite/epoxy. While initial volumes are not expected to be large, the promise

afforded by this material and other advanced MMC technologies makes the future bright for MMCs.

MMCs have tended to dominate in various applications as discussed above and interpenetrating composites in particular are now experiencing steady growth in various sectors due to their unique combination of structural properties (3-3 connectivity). Possibilities exist for a large number of oxide, mixed oxide and non-oxide ceramics to be infiltrated with a wide range of metal alloys and polymeric materials for applications ranging from wear resistant automotive components and armour through to sonar [111]. Hence, there is a need for the industry to understand the characteristics of interpenetrating metal matrix and polymer matrix composites that may influence processability and end product properties.

# CHAPTER 3

# EXPERIMENTAL PROCEDURES

## 3.1 Ceramic foams

As indicated in section 1.4, the aim of the project was to infiltrate ceramic foams with both polymers and metals and then characterise the resultant properties of the composites produced. For the polymer-based composites, it was intended to use both commercial alumina foams and barium titanate foams made in the laboratory, whilst the metal infiltration work only involved the alumina foams.

### 3.1.1 Alumina foams

All the ceramic foams were made by foaming and the in situ polymerisation of organic monomers; the production technique was described in detail in chapter 2. The alumina foams were produced by Hi-Por Ceramics Ltd, Dronfield, UK [100] and had varying density/porosity, cell and window size. The foams were characterised by their density, porosity and mean, smallest and largest cell and window sizes. The foam-density was calculated (after measuring the dimensions and the mass of the samples) using equation 3.1 and the porosity was then calculated from the foam-density and the theoretical density of the ceramic material by using equation 3.2.

$$d_f = \frac{m}{v} \qquad\qquad 3.1$$

$d_f$ = Density of the ceramic preform

$m$ = Mass of the ceramic preform

$v$ = Volume of the ceramic preform

$$P_O = 1 - \frac{d_f}{d_{th}} 100\%$$  3.2

$d_f$ - Density of the foam

$d_{th}$ - Theoretical density of the ceramic material

The theoretical density of alumina was assumed to be 3990 kgm$^{-3}$. The mean, smallest and largest cell and window sizes were calculated from the analysis of scanning electron microscope images as shown in Figure 3.1. The SEM images were taken at four different locations for each ceramic preform sample and the mean was calculated from 40 readings at each location.
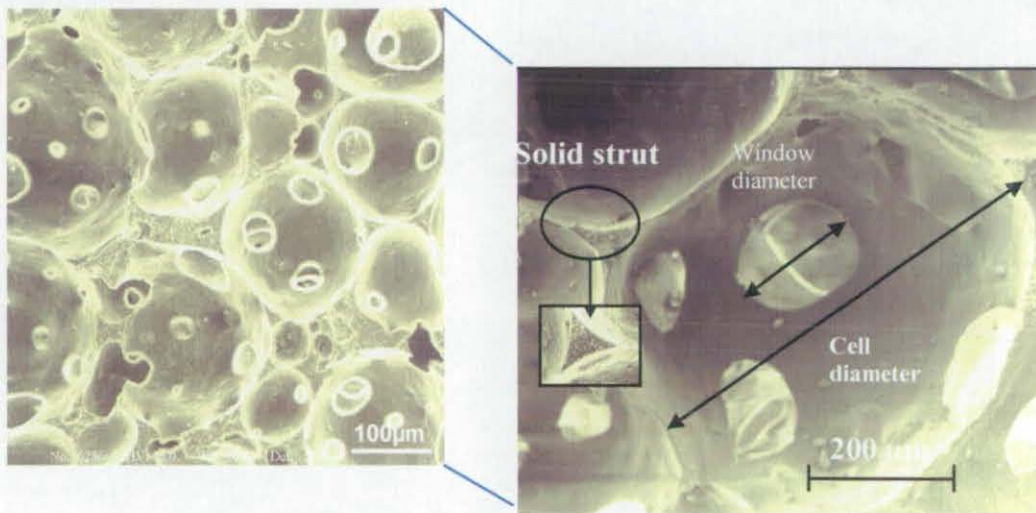


Figure 3.1: Measurement of cell and window size.

## 3.1.2 Processing of BaTiO$_3$ foams

The BaTiO$_3$ foams were made in the laboratory by mechanically agitating ceramic aqueous suspensions to entrain gases and then setting the structure via the *in-situ* polymerisation of organic monomers, see fig 2.1, which resulted in the foams having a very open and interconnected structure.

The aqueous suspension was prepared by blending $BaTiO_3$-HP2 barium titanate powder (Thermograde Process Technology Ltd., Stone, Staffordshire, UK) in concentrations of 76 wt%, a fixed amount (6.5 wt%) of an ammonium acrylate monomer and 2 wt% of Dispex A40 dispersing agent (Allied Colloids, Bradford, UK) in water. The mixture was thoroughly dispersed and homogenised. A foaming agent ($\alpha$-foamer) was added to the barium titanate suspensions and vigorous stirring applied in a sealed vessel under a controlled nitrogen atmosphere in order to generate the foam. During the foaming process 25 wt% of ammonium per sulphate initiator and amine catalyst was added to start the setting process. The volume of the foam produced was measured against stirring time using 246 g samples of 76 wt% of barium titanate slip; the foam volume being expressed in ml (see Table 3.1).

Table 3.1: Values of the volume foamed, foaming agent, initiator and catalyst.

| Sample code | Slurry / g | Volume foamed / ml | Foaming agent / ml | Initiator / ml | Catalyst / ml | Oxygen level / ppm | Induction time / min |
|---|---|---|---|---|---|---|---|
| Foam A | 246 | 500 | 0.7 | 0.7 | 0.05 | 200 | 22 |
| Foam B | 246 | 470 | 0.5 | 0.5 | 0.5 | 100 | 3 |
| Foam C | 246 | 500 | 0.4 | 0.4 | 0.4 | 140 | 4 |
| Foam D | 246 | 550 | 0.4 | 0.5 | 0.15 | 100 | 7 |
| Foam E | 246 | 500 | 0.4 | 0.25 | 0.25 | 100 | 10 |

The time between the addition of the reagents and the beginning of the polymerisation process was characterised by an induction time. The concentration of these reagents was designed to produce an induction period such that polymerisation was initiated immediately after casting of the foam into a mould was completed. Setting of the fluid foam was promoted by the *in situ* polymerisation of the acrylate monomer. Since the polymerisation is intrinsically an exothermic reaction the induction time could be easily evaluated from the change of temperature with time. The induction time is very important during the production process because it describes the time available for the casting of the foamed suspension and also it affects the final cell size, cell size distribution and strut thickness. The induction time was varied by altering the

concentration of the initiator and catalyst in order to obtain different cell sized preforms (see Table 3.1).

After the polymerisation and setting reaction, all the samples were cooled down to room temperature and removed from the moulds. The samples were initially dried at room temperature for 24 h and then in an oven at 110°C. Firing was performed for 3 h at 1300°C using heating schedules of 0.5°C min$^{-1}$ up to 180°C and hold for 1 h, 0.5°C min$^{-1}$ up to 550°C and hold for 2 h and then 1°C min$^{-1}$ up to the sintering temperature and were cooled at a rate of 1°C min$^{-1}$ to room temperature.

## 3.1.2.1 Thermogravimetric analysis (TGA) of BaTiO$_3$ foams

A TA Instruments 2950 Hi-Res Modulated TGA with automatic sample changer was used to study weight losses over the temperature range 25°C to 1000°C. The modulated-temperature capability allows the kinetics of thermal decomposition processes to be studied and a "high resolution" mode can be used to improve the detection of weight loss processes.

The TGA of the barium titanate foam sample was performed at a heating rate of 5°C min$^{-1}$ up to 1000°C in air to know whether the binder (monomer) had completely burnt out and to estimate the % weight loss of the binder as a function of temperature.

## 3.1.2.2   X-ray diffraction

X-ray diffraction analysis was used to detect any phase change occured which might then result in volume change in barium titanate foams which could possibly reveal the reason for cracking of the foams during sintering. The X-ray diffractometer used for the analysis was a Bruker D8 model with a quarter-circle eulerian cradle. In addition to straight-forward powder diffractometry, this permitted stress and texture measurements to be made.

The barium titanate foam material was crushed into a fine powder. The interplanar spacings were calculated by using the following equation;

$$\frac{1}{d_{hkl}} = \sqrt{\frac{h^2}{a^2}} + \sqrt{\frac{k^2}{b^2}} + \sqrt{\frac{l^2}{c^2}}$$

3.3

a=b for tetragonal system.

a=b=c for cubic system.

The resultant data was compared with the [©]JCPDS values to identify the phases present in the materials.

## 3.2 Polymer infiltration

For the polymer infiltration trials, it was intended to use four types of resin systems to study the characterisation properties, whilst the actual infiltration work only involved three resin systems; Crystic 471 PALV polyester resin, Crystic Envirotec LS-451PA polyester resin and Polyvinylidene fluoride resin.

### 3.2.1 Infiltration materials

### 3.2.1.1 Polyester resin-Crystic 471 PALV

Crystic 471 PALV [101] is a pre-accelerated, low viscosity polyester resin with rapid hardening characteristics. It combines rapid impregnation of reinforcements and fillers with a very short mould release time. The resin is recommended for automotive, marine and resin concrete applications. Crystic 471 PALV polyester resin is commercially available from Scott Bader Company Ltd, UK. The properties of the liquid and fully cured resin are given in Tables 3.2 & 3.3. It requires only the addition of catalyst to start the curing reaction. The amount of catalyst added was 2% by volume and the mixture was thoroughly dispersed. The gel time of the resin can be approximately determined from Table 3.4. The first experiments were made to test the curing reactions of the polyester resin. Therefore 40 ml of the resin was mixed with 2 vol% of catalyst. While mixtures were allowed to gel, the gel-time measurement as a function of temperature, Figure 3.2, and the temperature-time profile, Figure 3.3, were recorded.

Table 3.2: Properties of liquid resin [101] – polyester Crystic 471 PALV.

| Property | Liquid Resin | |
|---|---|---|
| Colour | | Cloudy, mauvish |
| Viscosity (25°C) @37.35 s$^{-1}$ | mPa s | 380 |
| Viscosity (25°C) @45.00 s$^{-1}$ | mPa s | 240 |
| Volatile Content | % | 42 |
| Flash Point | °C | 27.5 |

Table 3.3: Properties of fully cured resin [101] - polyester Crystic 471 PALV.

| Property | Fully Cured Resin | |
|---|---|---|
| Tensile Strength | MPa | 68 |
| Tensile Modulus | MPa | 3700 |
| Elongation at Break | % | 2.5 |
| Specific Gravity (25°C) | | 1.22 |

Table 3.4: Gel time of mixed resin with 2 vol% of catalyst [101].

| Temperature / °C | Gel time / min |
|---|---|
| 15 | 18 |
| 20 | 12 |
| 25 | 8 |
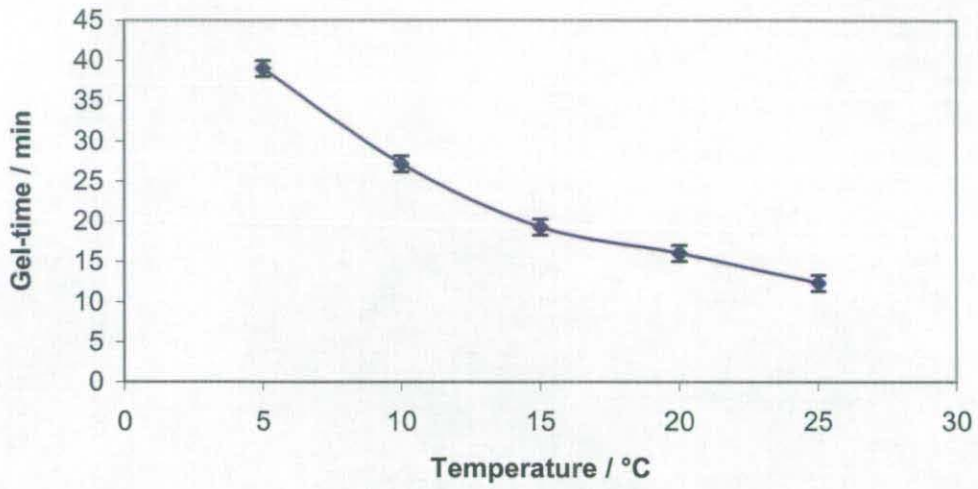
Figure 3.2: Gel-time measurement as a function of temperature with 2 vol% of catalyst.
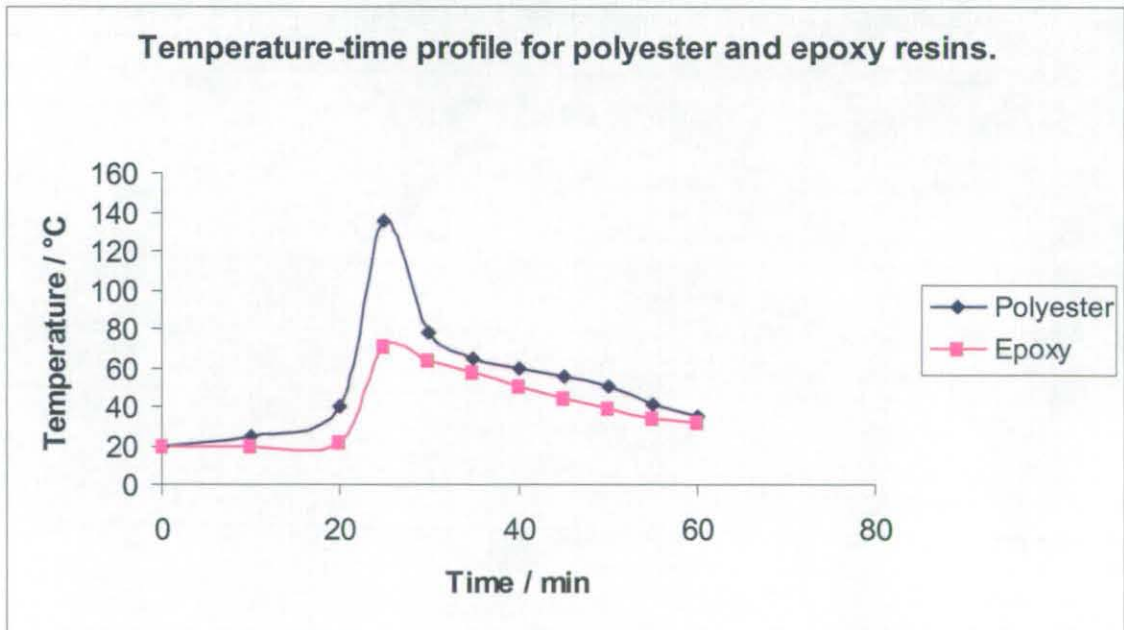


Figure 3.3: Temperature-time profile for polyester and epoxy resin systems.

The testing of the resin revealed that the gel-time under laboratory conditions was about 15 minutes for a mixture with 2 vol% of catalyst. After this time the viscosity increased rapidly and curing started with a rise in the temperature. After 20

minutes the resin was like rubber and could only be deformed elastically. After 25 minutes the temperature had reached its maximum of 138°C. Five minutes later it had already fallen down below 80°C. After 30 minutes, the resin was solid but a little bit sticky and after 45 minutes the colour changed to a transparent brown, like amber, and the resin was not sticky anymore. The experiments revealed that the temperature rise had to be taken into consideration for the next experiments.

## 3.2.1.2 Crystic Envirotec LS-451PA – A low styrene content polyester resin

Crystic Envirotec LS-451PA is a dicyclopentadiene (DCPD) modified polyester resin [102]. It typically contains 25% to 30% styrene. It therefore has a lower styrene emission than standard low styrene emission resins and during the laminating phase, styrene emissions are typically 20% to 30% lower than conventional LSE resins. It is suitable for use in marine industry and for all general moulding requirements. The main features incorporated include:

- Colour change mechanism
- Pre-accelerated
- Thixotropic
- Low viscosity
- Cure rate can be modified by use of different catalysts

It was allowed to attain laboratory temperature (18°C to 20°C) before use. It required only the addition of a catalyst to start the curing reaction. The recommended catalyst is Catalyst M (or Butanox M50) which was added at 2 vol% into the resin and thoroughly dispersed, shortly before use. The gel-time of the resin at different temperatures is given in Table 3.5.

The properties of the liquid and fully cured resin are given in Tables 3.6 & 3.7. There are a number of advantages in using Envirotec LS451PA:

- Low styrene content
- Better cure in the mould
- Easier release from the mould
- Less shrinkage, print through and distortion after components have been released from the mould.

Table 3.5: Gel times of the Crystic Envirotec LS-451 PA polyester resin with 2 vol% catalyst M (Butanox M50) at different temperatures [102].

| Temperature / °C | Gel time / min |
|:---:|:---:|
| 15 | 40 |
| 20 | 25 |
| 25 | 20 |

Table 3.6: Properties of liquid resin – Crystic Envirotec LS-451PA polyester resin [102].

| Property | Liquid Resin | |
|---|---|---|
| Colour | | Blue |
| Viscosity (25°C) @37.35 s$^{-1}$ | mPa s | 400-600 |
| Viscosity (25°C) @45.00 s$^{-1}$ | mPa s | 200-240 |
| Volatile Content | % | 30 |
| Geltime at 25°C using 2% Catalyst M | minutes | 18-22 |

Table 3.7: Properties of fully cured resin – Crystic Envirotec LS-451PA polyester resin [102].

| Property | Fully Cured Resin | |
|---|---|---|
| Tensile Strength | MPa | 46 |
| Tensile Modulus | MPa | 2660 |
| Elongation at Break | % | 2.5 |
| Barcol Hardness | | 38 |

### 3.2.1.3 Epoxy resin-West system 105 resin

Epoxy 105 resin is a clear, light-amber, low-viscosity epoxy, which, when mixed with one of the West system hardeners, is formulated to wet out wood fibre, fibreglass and a variety of metals [103]. It can be cured in a wide temperature range to form a high strength solid with excellent moisture resistance. The 105 resin has a relatively high flash point, which makes it safer to work with than polyesters, and is free from solvent odours and vapours. The resin is recommended for coatings and adhesives for marine applications. West system 105 epoxy resin is commercially available from Scott Bader Company Ltd, UK [103].

Epoxy 105 resin with 205 hardener is used in a majority of situations to produce a rapid cure and results in an epoxy which develops its physical properties quickly. When mixed in the ratio of five parts by weight of 105 resin to one part by weight of 205 hardener, the mixture yields a high-strength, rigid solid, which has excellent cohesive properties and provides an outstanding moisture vapour barrier with excellent bonding and coating properties. The properties of the liquid resin are given in Table 3.8.

Table 3.8: The properties of the liquid resin [103].

| Property | Liquid Resin | |
|---|---|---|
| Colour | | Pale yellow |
| Viscosity (25°C) | mPa s | 450 – 600 |
| Specific Gravity (25°C) | | 1.15 |
| Flash Point | °C | >100 |
| Pot life (25°C) | min | 10-15 |
| Cure to Solid State (21°C) | hours | 5-7 |
| Cure to Maximum Strength (21°C) | days | 5-7 |

## Mixing and cure time

The correct ratio of resin and hardener was dispensed into a mixing vessel. Thorough blending of the two ingredients with a wooden mixing stick was carried for up to 2 to 3 minutes. During mixing, the sides and bottom of the vessel were scraped.

The transition period of an epoxy mix from a liquid to a solid is known as the cure time. It can be divided into three phases described below. The speed of the reaction and the total cure time varied and was independent of the ambient temperature and the mass of the mix.

### 1. Open time

Open time is the period in which the resin/hardener mix is in its liquid state and remains workable.

### 2. Initial cure phase

After its liquid state the epoxy passed into its gelation state (or gel state). Often called the green stage. In this initial cure phase, the solid epoxy feels tack free but it was possible to dent it with a thumb nail and it was too soft to dry and sand.

### 3. Final cure phase

The epoxy had cured to its solid state and had developed about 90% of its ultimate strength.

## Controlling cure time and pot life

The selection of a resin/hardener combination is based on the length of the cure time or the 'pot life'. Pot life is a term used to compare the relative rate of reaction of various resin/hardener combinations and is the amount of time a given mass of mixed resin and hardener will remain in the liquid state at a specific temperature.

The first experiments were made to test the curing reactions of epoxy resin. Therefore small quantities of resin and hardener was mixed by either weight or volume providing the correct ratio was maintained, i.e. 5 parts 105 resin with 1 part of 205 hardener. While mixtures were allowed to set, the gel-time measurement as a function of temperature and the temperature-time profile were recorded. The testing of the resin

revealed that the gel-time under laboratory conditions was about 15-20 minutes for a mixture with the ratio of 5:1 (resin to hardener ratio). While stirring the resin with the hardener, the colour of the mixture changed from colourless liquid to a pale-yellow colour. After 25 minutes the temperature had reached its maximum of 71°C (Figure 3.3). Ten minutes later it was measured to be 57°C and after 60 minutes it had fallen to 32°C. At this stage, the resin was solid but still sticky. As it cured further the colour changed from pale-yellow to pale pink. The resin / hardener mixture was completely cured after 5 hours at room temperature and the resin was no longer sticky.
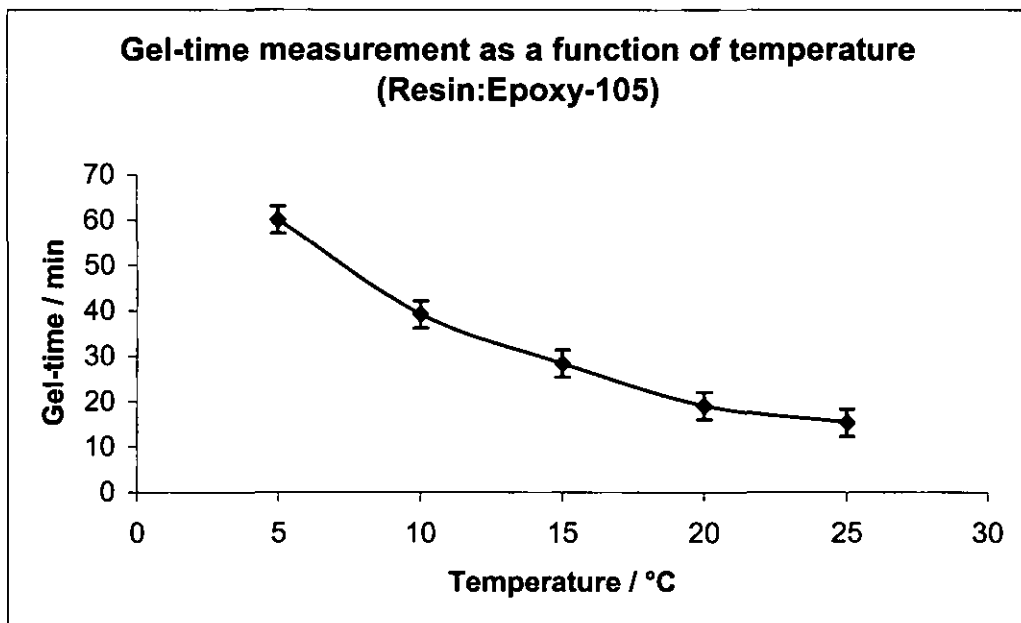


Figure 3.4: Gel-time measurement as a function of temperature with 5:1 resin, hardener ratio.

The experiments suggest that the mixing of the two ingredients should be very slow, gentle and thorough, mixing up to 2-3 minutes to avoid air bubbles in the mixture in order to obtain sound composites after infiltration. The results of gel-time measurement as a function of temperature and temperature – time profile are shown in Figures 3.4 & 3.3. In the present work the primary focus has been on ceramic/polyester composites though some characterisation has also been done on epoxy resin system. The epoxy has been used as another example to study the characterisation properties, but was not actually used for the infiltration trials.

## 3.2.1.4 Polyvinylidene fluoride (PVDF)

### 3.2.1.4.1 KYNAR® PVDF homopolymer

KYNAR® polyvinylidene fluoride (PVDF), the homopolymer of 1,1-di-fluoro-ethene, is a tough, engineering thermoplastic that offers a unique balance of properties [104]. The unique structure of alternating methylene and difluoromethylene units along the chain creates a polymer material having high crystallinity combined with a high polarity resulting in a sharp melting point. Thus KYNAR® PVDF has the characteristic stability of fluoropolymers when exposed to harsh thermal, chemical, and ultraviolet environments, while retaining the properties of a conventional thermoplastic material. KYNAR® resins are readily melt-processed by standard methods of extrusion and injection / compression molding. KYNAR® PVDF resin is commercially available in powder form from ATOFINA UK LTD [104].Important properties of KYNAR® PVDF include:

- Mechanical strength and toughness
- High abrasion resistance
- High thermal stability
- High dielectric strength
- High purity
- Readily melt processible
- Resistant to most chemicals and solvents
- Resistant to ultraviolet and nuclear radiation
- Low permeability to most gases and liquids
- Low flame and smoke characteristics
- Rigid and Flexible versions of KYNAR® PVDF are available.

KYNAR® PVDF offers very good chemical resistance in the presence of a wide variety of different chemicals up to high temperatures of approximately 150°C. However, it has been well established that bases and alkalis can chemically attack PVDF resins leading to chemical embrittlement. The extent of the chemical attack of

PVDF by different bases is greatly governed by temperature, concentration and, in particular, by the type of base [104].

The general mechanism of base attack on PVDF relies on the dehydrofluorination reaction which is initiated by absorbed base molecules. The resultant double bonds formed by the elimination of HF from the polymer backbone give rise to coloration. In case the dehydrofluorination reaction is very pronounced the material becomes brittle [104].

**Molecular mechanism of the base attack:**

Since the absorption of a base is the prerequisite for the chemical attack, the solubility of the base in PVDF becomes a most dominant factor.
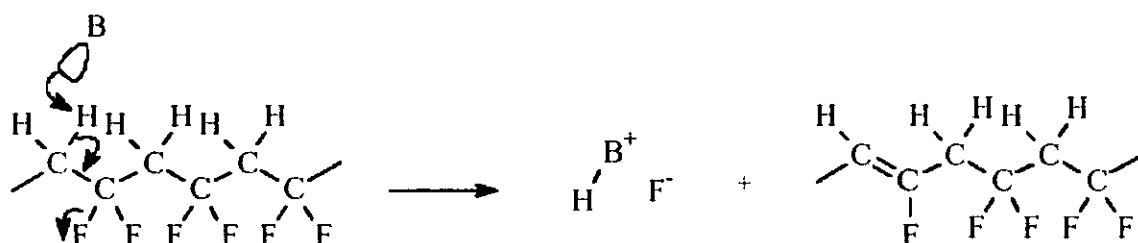


The other important factor is the reactivity of the base. For a given base these factors depend on temperature and concentration [104].

**3.2.1.4.2 KYNAR FLEX® PVDF copolymer**

**I. KYNAR FLEX® PVDF copolymers offer improved base resistance**

KYNAR FLEX®, PVDF copolymers [104], offers a significantly improved chemical resistance due to two effects.

➤ The higher flexibility reduces stress cracking significantly.

➤ The perfluorinated comonomer disrupts the dehydrofluorination process suppressing the embrittlement.

## II. Dehydrofluorination and the blocking of its progress in KYNAR FLEX®
## PVDF copolymers

**PVDF**
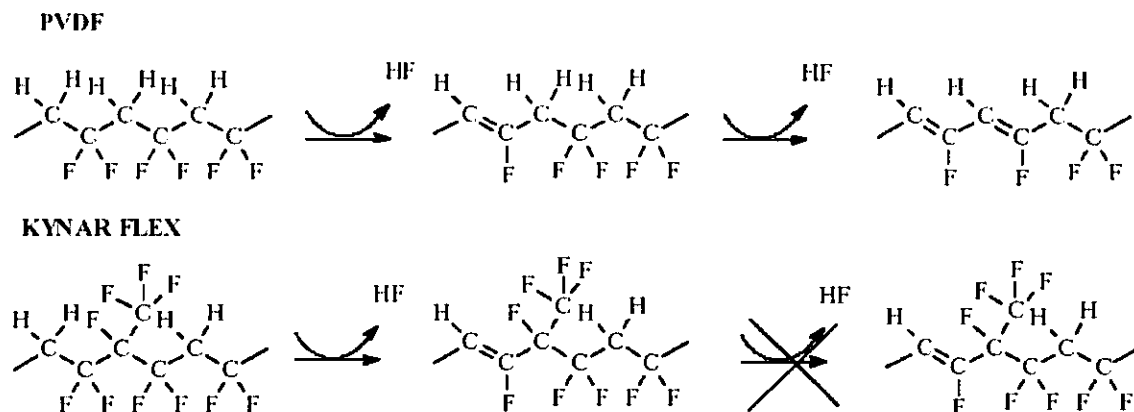


**KYNAR FLEX**



The partial blocking of the dehydrofluorination reaction results in significantly improved colour retention and reduction of material embrittlement. The comonomer used to synthesize the KYNAR FLEX® grades is hexafluoropropene (HFP) which is a completely fluorinated molecule. Thus, the major factor responsible for the outstanding chemical resistance of KYNAR® PVDF is not changed by the incorporation of a comonomer [104].

The main change induced by the incorporation of the HFP comonomer is a reduction in crystallinity of the originally highly crystalline PVDF material. The reduced crystallinity directly results in a decrease of the moduli and hence in a reduced mechanical strength at higher temperatures. Also the reduced crystallinity results in an enhancement of permeation rates which in turn leads to a further decrease in mechanical strength at higher temperatures.

KYNAR FLEX® resins, a series of PVDF based fluoropolymers, possess unique qualities of additional chemical compatibility in high pH solutions, increased impact strength at ambient and colder temperatures, and increased clarity. The improved impact and elongation properties have proven especially beneficial in lining applications.

KYNAR® resins have limited solubility. Table 3.9 lists active solvents which dissolve 5-10% of KYNAR® resin at room temperature. Generally, KYNAR resins are not soluble in aliphatic hydrocarbons, aromatic hydrocarbons, chlorinated solvents,

alcohols, acids, halogens and basic solutions. KYNAR FLEX® tends to be slightly more soluble due to the lower crystallinity attributed to the resin [104].

Table 3.9: Solvents for KYNAR® PVDF [104]

| Solvent | Boiling Point / °C | Flash Point / °C |
|---------|--------------------|--------------------|
| Acetone | 56 | -18 |
| Tetrahydrofuran (THF) | 65 | -17 |
| Methyl ethyl ketone (Butanone) | 80 | -6 |
| Dimethyl formamide (DMF) | 153 | 67 |
| Dimethyl acetamide (DMA) | 166 | 70 |

### 3.2.1.4.3  Preparation of solution of KYNAR FLEX® PVDF copolymer

A free sample of KYNARSUPERFLEX 2500-20 (PLT) resin in powder form was supplied by ATOFINA UK Ltd. For initial trials, 20% by weight of Kynar® PVDF powder was mixed thoroughly with N,N-dimethylformamide and the mixture was dissolved at 60 °C, i.e. lower than the flash point for the solvent. The solvent dimethylformamide is a clear, colourless liquid with a faint, amine odour and is commercially available from Fisher Scientific UK Ltd [105]. The properties of the solvent are given in Table 3.10.

Table 3.10: Properties of dimethylformamide [105].

| Solvent Properties | Values |
|--------------------|--------|
| Viscosity | 0.8 mPa s @ 20°C |
| pH | 6 – 8 @ 20% aq.sol. |
| Vapour Pressure | 4.9 mbar @ 20°C |
| Boiling Point | 153°C |
| Flash Point | 57°C |
| Specific Gravity/Density | 0.9450 |

Mixing of the powder with the solvent resulted in the formation of a lot of air bubbles and subsequent polymerisation. As time passed, the size and quantity of air bubbles reduced and a layer of air bubbles was observed on the top surface. A few minutes later, complete elimination of the air bubbles and the formation of freely flowing transparent resin was obtained. The resin was then placed in an oven at 60°C to dissolve the mixture completely.

## 3.2.1.5 Viscosity measurements

The viscosity of the resin system was an important processing parameter for the infiltration trials, since it affected the ease with which a polymer would penetrate in to the ceramic foam porosity and hence the density of the resulting composite material. Considerable time was spent in looking for low viscosity resin systems to obtain well infiltrated composites. The viscosity measurements of the polyester and epoxy resins were carried out using Haake VT 500 and VT 550 viscometers. Before each of the viscometers was used, they had to be calibrated to ensure that they were giving accurate readings. This was done using a Cannon certified viscosity standard liquid-N350, which has a known viscosity range at 25°C temperature.

In these viscometers, the substance to be measured is located in the measuring gap of the sensor system and the rotor is rotated at a selected speed, n. The substance to be measured exerts a resistance to this rotational movement due to its viscosity, which becomes apparent as a torque value ($M_d$) applied on the measuring shaft of VT 550/500. The cup used was SV1, which is primarily used for viscosity measurements of medium to high viscosity liquids and pastes like greases, creams, ointments, plastisols and working in the low to medium shear rate range.

The speed of rotation was varied to apply a range of shear to the fluid. Recordings of speed of rotation and torque on the inner cylinder were taken in order for calculations of shear rate, shear stress and viscosity to be carried out. The built in computer calculated the relevant measuring values for the following factors from the measured variables of speed, torque and sensor geometry (system factors). The measured viscosity values are given in Table 3.11. The viscosity was calculated by using the following formula:

$$\eta = \tau / \gamma \hspace{8cm} 3.4$$

Where

$\eta =$ Viscosity in mPa s

$\tau =$ Shear stress in Pa

$\gamma =$ Shear rate in $s^{-1}$

Table 3.11: Viscosity measurement values on Haake VT 550 and VT 500.

| Sample | Haake VT 550 | | | Haake VT 500 | | |
|---|---|---|---|---|---|---|
| Specification | Shear rate / $s^{-1}$ | Viscosity / mPa s | T / °C | Shear rate / $s^{-1}$ | Viscosity / mPa s | T / °C |
| N-350 | 100 | 800(±14) | 26.4(±1.5) | 95.94 | 814(±3) | 27.1(±1) |
| Polyester | 37.35 | 470(±6) | 26.4(±1.5) | 40.32 | 440(±10) | 24.9(±0.5) |
| Epoxy | 40 | 647(±14) | 26.6(±1.5) | 40.32 | 747(±11) | 24.9(±0.5) |
| N-350 Cannon Standard Viscosity Liquid – 759.8 mPa s at 25°C. | | | | | | |

## 3.2.2 Vacuum assisted infiltration technique

It was decided to use the vacuum assisted infiltration technique for the infiltration trials of the ceramic foams with polymers. A steel vacuum cylinder with a diameter of 300 mm and a height of about 370 mm was provided. The cylinder had a top plate made of transparent plastic and had two inlets, one inlet with a valve that could be connected to a vacuum pump and a pressure dial gauge. A drawing of the assembly is shown in Figure 3.5. The assembly consisted of a transparent PVC-tube, Figure 3.6, with an inner diameter of 51 mm. The inside of the tube was surrounded by A4 transparency sheets to avoid contact of the resin with the PVC-tube.

The ceramic preforms with a diameter of 48 mm were wrapped using a PTFE-tape to seal the outer surface so that the resin could only flow through the top and the bottom of the preform. The PTFE-tape was held in place with a layer of adhesive tape. Then the preforms were placed into the tube, and fixed and sealed at the right position by two O-rings on top and bottom. Inside the PVC-tube, at the bottom, a flexible PVC-

film with a hole was placed to avoid contact of the resin with the outlet cap. The tube was sealed with an inlet and an outlet cap. A vacuum pipe was connected into the tube through the outlet cap to build the pressure required, where the vacuum was used to suck the resin in to the preform. The other end of the vacuum pipe was connected to the inlet of the vacuum cylinder with a valve.
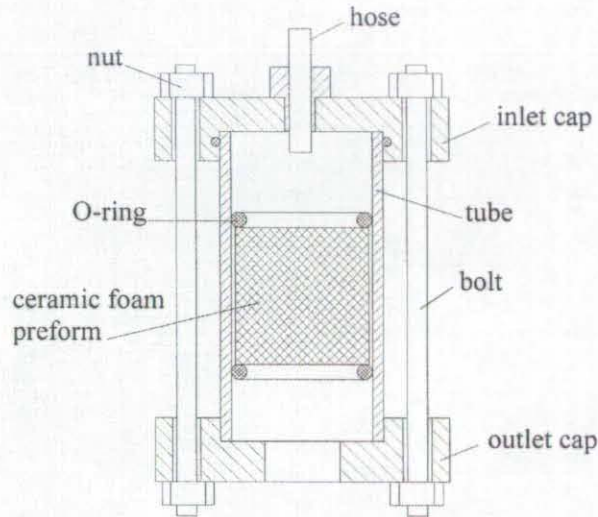


Figure 3.5: A drawing of the assembly for the vacuum assisted infiltration technique.



Figure 3.6: Picture of vacuum assisted infiltration equipment.

The resin was poured on top of the preforms through the inlet cap where it was sucked in to them by capillary and gravity forces. The underpressure in the vacuum

cylinder was adjusted to about 300 mbar. Then the valve was opened slowly and the resin was sucked through the preform. After most of the resin was sucked through it, the valve was closed again and the vacuum pump was switched off. It was made sure that there was at least 10 mm resin left on top of the preform to ensure that no air could enter the preform. After 45 minutes of curing the preform was removed from the assembly and investigated. After this arrangement was tested and the results were satisfactory, for further experiments three more prototypes with the same design were made to carry out a greater number of experiments using this technique.

A number of important parameters have been identified in the vacuum assisted infiltration process. These are: (i) resin viscosity, (ii) resin quality and quantity, (iii) room temperature and (iv) suction pressure. These parameters are discussed in the following paragraphs.

## (i) Resin viscosity

Control of resin viscosity is an effective way of obtaining a refined structure in conventional polymer infiltration processes and will clearly be an important factor in vacuum assisted infiltration process. In general, ceramic preforms with varying cell, window sizes and thick preforms requires low viscosity resins to suck the resin into the preform easily.

## (ii) Resin quality and quantity

Resin quality is always an important factor in infiltration process, as it determines the mechanical properties. Therefore it is important to improve the quality by using such mean as thorough mixing and gentle stirring to avoid the gas entrapment with in the resins system prior to infiltration. In terms of production, precise monitoring of resin poured on to the preform is important in the production of net-shape products by infiltration.

## (iii) Room temperature

Room temperature is another important factor as it affects all other parameters in one or other way. Much higher room temperatures could result in very fast setting times, very low viscosity values, high shrinkage of the resin system, where as very low temperatures could lead to very slow setting time, high viscosity values. Therefore

optimum room temperature is necessary to achieve a sound composite through infiltration.

(iv) Suction pressure

The suction pressure applied must be sufficient to offset shrinkage and gas porosity by sucking the resin through a three dimensional network of ceramic preform. The dissolved gases could either pass through the outlet of the arrangement or dispersed through the micro gaps between the sealed preform and the PVC-tube.

Even though the vacuum assisted infiltration showed encouraging results, it encouraged the entrapment of gas within the polymer in the composite and also shrinkage of the polyester resin under vacuum. To get rid of these problems it was necessary to change the process to positive pressure infiltration and considerable amount of time was spent in designing a suitable die, the location of air vents and to avoid possible sticking problems with the resin system.

## 3.2.3 Development of positive pressure infiltration process

Squeeze infiltration of a metal matrix into a ceramic preform has been used successfully for the fabrication of MMCs. The process is advantageous because metal poured into an impermeable steel die is pressurised during solidification and porosity eliminated by the high squeeze pressures used. Ceramic preform infiltration and ceramic/metal bonding are also enhanced because of high squeeze pressures used. The resultant casting is of high integrity and has a fine equiaxed grain structure. Components that can be cast to near net shape by squeeze casting are however limited to relatively simple shapes. For more complex shapes, complicated split dies have to be used. The high cost of producing such dies is a major disadvantage of the process.

The investment casting process enables wax patterns to be built up to form more complicated shapes especially with the help of special cores. However, there are problems when infiltrating a ceramic preform and casting integrity may not be as good as for castings produced by the squeeze casting process. The main advantage of the process is that it can provide design flexibility.

Thus it would appear logical to combine the two processes and modify them for polymer infiltration in order to develop a positive low pressure process that would exploit the best features of each.

This low pressure process aims to:

- Enable ceramic preforms to be infiltrated with polymers more readily
- Provide the flexibility for polymer resin systems
- Use low pressures and produce complex castings easily
- And provide better casting integrity and thus enhanced mechanical properties

Initial trials were conducted in order to know whether the infiltration using low positive pressure could yield better results and also to establish the minimum squeeze pressure that would infiltrate a ceramic preform completely with the possible elimination of gas entrapment and without shrinkage compared to the use of the vacuum assisted infiltration process. To know the squeeze pressures accurately, a tensile test machine was used.

### 3.2.3.1 Die requirements for the positive pressure infiltration process

The steel die for the positive pressure casting process should provide the following requirements:

- remain impermeable to various resin systems under ceramic preform infiltration pressures
- incorporate air vents to allow air to escape
- be non-reacting with the resin system
- be non-wetting by the resin system

### 3.2.3.2 Die design for positive pressure process

Several ways of incorporating air vents to allow air to escape with a metal die to be pressurized by resin systems were considered. The final design, Figure 3.7, was simple, yet provided easy access for the air to escape from the assembly. Pressure was applied using the top punch, which pushed the air out and then the resin was pushed

down into the preform. The top surface of the base plate was designed in such a way that the air could escape easily without any obstruction. Very thin passages (about 1 mm width) were drilled on the top surface of the base plate in all four directions to let the air vent out uniformly. A drawing of the top view of the base plate with air vents on it is shown in Figure 3.8.
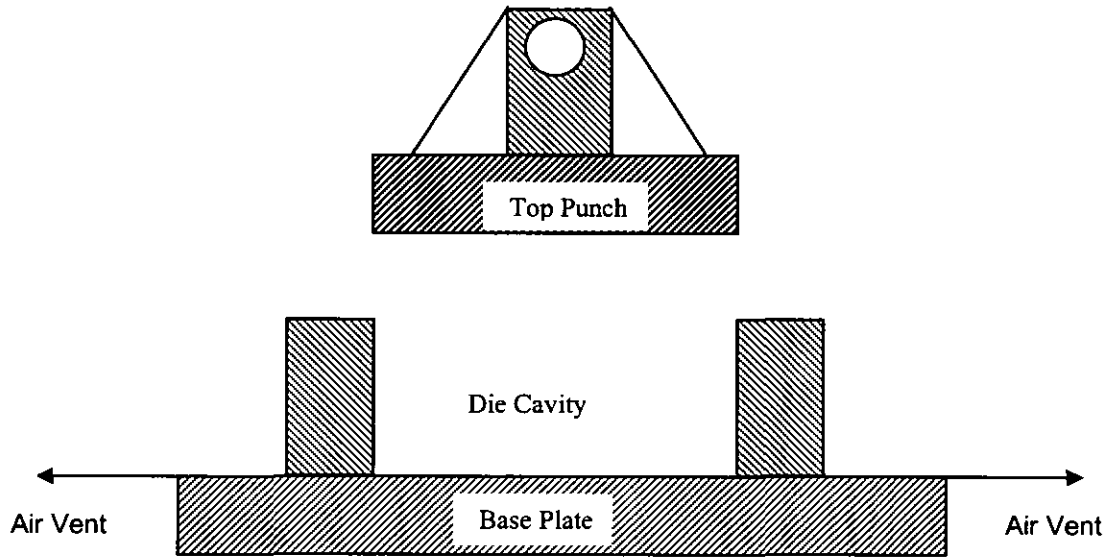


Figure 3.7: Design for the positive pressure infiltration process.
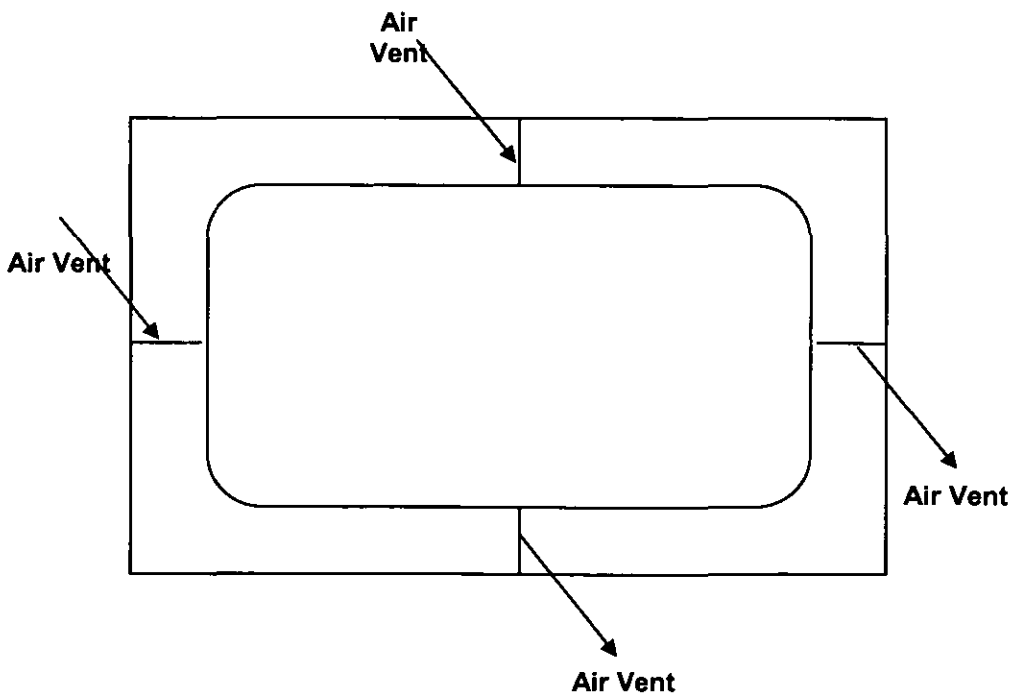


Figure 3.8: Top view of the base plate with air vents on it.

## 3.2.4 Design of experiments for vacuum infiltration trials

A series of experiments were designed to optimise the processing parameters for the infiltration trials with two main variables, pressure and temperature. The following table gives the matrix of experiments and variables.

Table 3.12: Matrix of experiments.

| Material | Variables | | |
|----------|-----------|---|---|
| | Temperature / °C | Pressure / mbar | Gel-time / min |
| Polyester | T1=15 | P1=250 | t1=19.3 |
| | T2=20 | P2=300 | t2=16 |
| | T3=25 | P3=350 | t3=12.3 |

Table 3.13: Set of experiments.

| Set of experiments | | |
|--------------------|---|---|
| Temperature: 15°C, Suction vacuum: 250 mbar | Temperature: 20°C, Suction vacuum: 250 mbar | Temperature: 25°C, Suction vacuum: 250 mbar |
| Temperature: 15°C, Suction vacuum: 300 mbar | Temperature: 20°C, Suction vacuum: 300 mbar | Temperature: 25°C, Suction vacuum: 300 mbar |
| Temperature: 15°C, Suction vacuum: 350 mbar | Temperature: 20°C, Suction vacuum: 350 mbar | Temperature: 25°C, Suction vacuum: 350 mbar |

For initial infiltration trials, 19% dense and 380 µm mean cell size alumina preforms were used. From the cell and window size analysis it could be observed that this particular perform dimensions were matched with the values of the Hi-Por Ceramics Ltd with a small scatter (variation) when compared with the other preforms and sufficient number of preforms were available in stock.

It was assumed that two possible key parameters (e.g. temperature and pressure) could be observed from first set of experiments. One of it was to find out whether it is necessary to carry out all the seven sets of experiments and the effect of parameters (e.g. temperature and pressure) on the density of the received composites. For the first set of experiments vacuum was varied while the temperature was kept constant and vice versa.

Table 3.14: The conditions for series of experiments.

| The conditions for series of experiments | | | | |
|---|---|---|---|---|
| Order of experiments | Variables | | Constant | Samples & Quantity |
| 6 | Temperature / °C | 15 | Suction vacuum: 300 mbar | Foam A & 2 |
| 1 | | 20 | | Foam A & 1 |
| 4 | | 25 | | Foam A & 2 |
| | | | | |
| 2 | Suction vacuum / mbar | 250 | Temperature: 20°C | Foam A & 2 |
| 1 | | 300 | | Foam A & 1 |
| 3 | | 350 | | Foam A & 2 |
| | | | | |
| 7 | Temperature, Suction vacuum | 15°C 350 mbar | Low temperature High suction vacuum | Foam A & 2 |
| | | | | |
| 5 | Temperature, Suction vacuum | 25°C 350 mbar | High temperature High suction vacuum | Foam A & 2 |

The main variables were temperature and pressure as shown in table 3.12. Temperature influences the gel-time or setting time of the particular resin system. High room temperature results in fast setting of the resin system and at low temperatures longer setting times were expected. Viscosity is another important variable which changes according to the change in temperature. At low temperatures high viscosity values could be expected, requiring high pressure to suck the resin through the preform and at high temperatures low viscosity values could be expected which in turn result in low suction pressures. From the design of experiments, at the end it could be possible to predict the optimum processing parameters for different foam structures.

## 3.2.5 Cutting of ceramic-polymer composite specimens

For the first few samples, the specimens were sectioned from the infiltrated samples using a Struers ACCUTOM-5 cutting machine with a diamond cut-off wheel that was operated with a speed of 0.050 mm/s at 3000 rpm from top to bottom surface of the sample along the infiltration direction. This was necessary to obtain a better understanding of the material solidification characteristics, to make it sure that during infiltration trials the resin was passing through the preform and not from the sides of

the preform. The cutting speed was gradually increased to 0.5 mm/s and the cut surface was found to be good enough to carry out microscopic examinations without polishing or grinding.

## 3.2.6 Density measurements of ceramic-polymer composite specimens

The rule of mixtures states that the properties of a composite material are a function of the volume fraction of each material in the composite. Certain properties of a composite depend only on the relative amounts and properties of the individual constituents. The rule of mixtures can accurately predict these properties. The densities of the composite samples were calculated by using the following equation;

$$\rho_c = \sum \rho_i v_i = \rho_1 v_1 + \rho_2 v_2 \qquad\qquad 3.5$$

Where

$\rho_c$ = Density of the composite material

$\rho_1$ = Theoretical density of the ceramic preform (i.e. Alumina – 3990 kgm$^{-3}$)

$v_1$ = Volume fraction of alumina preform

$\rho_2$ = Theoretical density of the resin system (i.e. Polyester – 1180 kgm$^{-3}$)

$v_2$ = Volume fraction of the resin system

## 3.2.7 Microscopic examination

Microscopic examinations were carried out to assess the effect of process parameters on the composites and the quality of the infiltration. For initial examinations a light microscope was used to assess the microstructure of the resulting composites.

Further to light microscopy, incident light fluorescence (reflected light) microscopic examinations were conducted on ceramic-polymer composite samples to differentiate both the phases. This was achieved by using a UV light and the wave length of the light was 365 nm. The microscope used was Zeiss photomicroscope.

## 3.2.8  Impact test

During this test the energy that is needed to cause fracture of a sample is measured. The impact strength is expressed in kilojoules per square metre ($kJ/m^2$). For some applications, e.g. a crash absorber, a high impact resistance is of great importance for the materials. There are a few standard impact tests using either the pendulum or the drop-weight-method.

One of the pendulum-type impact tests is the Charpy Impact Test. It is standardised for plastics under ISO 179 [112] and for metals under EN 10045 [113]. In this impact test method a rod-shaped test specimen, supported near its ends as a horizontal beam, is impacted perpendicularly, with the line of impact midway between the supports, and bent at a high, nominally constant velocity, by the swinging pendulum. The standard test specimen is 55 mm long with a square cross section of 10 mm × 10 mm. Since in the current work the standard test specimen size could not be obtained from the material, test specimens having a rectangular cross section were used.

For materials that behave in a more brittle than ductile manner, unnotched test specimens are usually used. This is because the notch has a great influence on the fracture behaviour of brittle materials. Minor variations in the geometry of the notch can cause major differences in the notch impact value. Further results are affected by the size of the test specimen. An increase in size leads to a decrease in the critical energy per unit area of the fracture. Because of these many influences impact strength values achieved by different samples or techniques can not be compared [114, 115].

Unnotched test specimens were used in the current work and the Charpy impact strength in kilojoules per square metre for these samples was calculated by using the following equation [113]:

$$a_{cU} = \frac{W_B}{bh} \cdot 10^3 \qquad\qquad 3.6$$

Where

$a_{cU}$ - Impact strength (unnotched test specimen)

$h$ – Thickness in mm

$b$ – Width in mm

$W_B$ – Energy at break in J

From the first infiltration trials, see Table 4.2, two composite samples with the highest achieved density and two samples with the lowest achieved density were tested. For comparison, pure Crystic 471 PALV polyester resin samples cured with 2% catalyst were also measured.

The composite test specimens that were made of the infiltrated materials were cut out of the disc shaped samples as described in section 3.2.5. Whilst the pure resin samples were cut out of a cast disc with the diameter of 48 mm and height of approximately 10 mm. To cut them out, a diamond cutting wheel was used. The surface quality of the test specimen after cutting was very good so that further grinding was not necessary. The test specimens were numbered and their dimensions measured. The measurements were carried out using a miniature Charpy Impact testing machine (Figure 3.9) with two different penduli (Table 3.15) to match the fracture energy for the composite samples and the pure resin samples.

Table 3.15: Range of penduli used in charpy miniature impact test.

| Test specimens | Penduli used |
|---|---|
| Composite samples | 1/16 lb |
| Polyester resin samples | 1 lb |
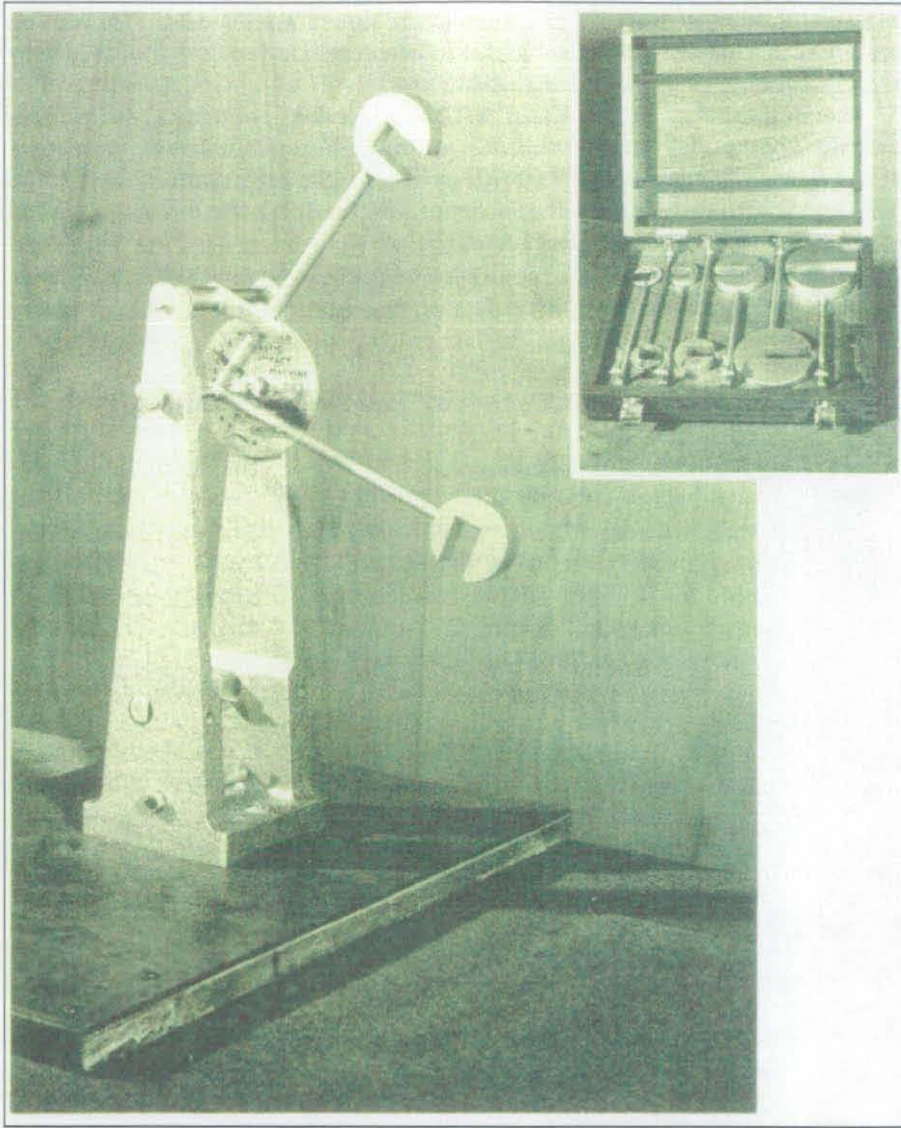
Figure 3.9: Miniature Charpy Impact (2.7 J) machine (double exposure photograph) with range of penduli (inset) [114].

## 3.2.9 Three-point bend test

The axial tensile testing of brittle materials, such as ceramics and glasses, is extremely difficult because of the difficulties associated with the preparation of suitably shaped test-pieces and of effectively holding them within the testing machine. It is customary to determine the fracture strength from a three-point bend test. The flexural strength value determined in this type of test is also known as the modulus of rupture of the material.

When a sample is subjected to bending, as shown in Figure 3.10, a compressive stress is generated in the upper surface and a tensile stress is generated in the lower surface.
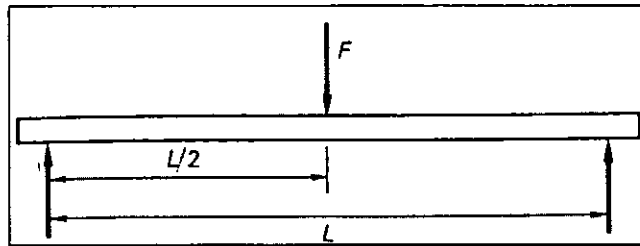


Figure 3.10: Three-point loading arrangement [114].

By applying the load at three points and causing bending, a tensile force acts on the material opposite the mid point. Fracture begins at this location. The flexural strength or modulus of rupture describes the material's strength and was calculated by using the following equation:

$$\text{Flexural Strength} = \frac{3FL}{2BD^2} \qquad\qquad 3.7$$

Where

F = Fracture load

L = Distance between the two outer points

B = Width of the specimen

D = Height of the specimen

The test was performed using a Lloyd instruments 2000R testing machine with a load cell of 5 kN, at a cross head speed of 0.5 mm/min and a span length of 30 mm was maintained for all the samples. For comparison three different materials were tested: two composite samples with the highest and lowest achieved density, an alumina foam with a mean cell size of 380 μm and cured polyester resin samples with 2% catalyst addition. The samples were prepared as explained in section 3.2.5.

# 3.3 Metal infiltration

## 3.3.1 Material - aluminium-silicon alloy LM25

The aluminium-silicon alloy LM25 was used for metal infiltration trials. LM25 alloy is mainly used where good mechanical properties are required in castings of a shape or dimensions requiring an alloy of excellent castability in order to achieve the desired standard of soundness. The alloy is also used where resistance to corrosion is an important consideration, particularly where high strength is also required. It has good weldability.

Table 3.16: Chemical composition of the LM25 casting alloy in wt. % [106].

| Al | Cu | Mg | Si | Fe | Mn | Ni | Zn | Pb | Sn | Ti |
|------|------|---------------|---------------|------|------|------|------|------|------|----------------|
| Rest | 0.20 | 0.20 - 0.65 | 6.50 - 7.50 | 0.55 | 0.35 | 0.15 | 0.15 | 0.15 | 0.05 | 0.05 - 0.25 |

Table 3.17: Properties of the aluminium alloy [106].

| Property | LM25 | |
|-------------------------------|-----------------|-------------|
| 0.2% Proof Strength | MPa | 80 – 260 * |
| Tensile Strength | MPa | 150 – 320 * |
| Modulus of Elasticity | GPa | 71 |
| Brinell Hardness | | 55 – 110 * |
| Elongation at Break | % | 2 – 3 * |
| Coefficient of Thermal Expansion | $°C^{-1}$ | 0.000022 |
| Freezing Range | °C | 615 – 550 |
| Density | $g\,cm^{-3}$ | 2.68 |

* depends on Heat Treatment

Consequently, LM25 finds application in the food, chemical, marine, electrical and many other industries, and, above all, in road transport vehicles where it is used for wheels, cylinder blocks, and heads, and other engine and body castings. Its potential uses are increased by its availability in four conditions of heat-treatment in both sand and chill castings. It is used in nuclear energy installations and for aircraft pump parts. The chemical composition is given in Table 3.16. Table 3.17 outlines the properties of the aluminium alloy. LM25 may be superior for castings, particularly in chill moulds, which are difficult to make to the required standard of soundness. It offers better machinability and mechanical properties than LM6 [106].

## 3.3.2 Squeeze infiltration technique

For the metal infiltration trials the squeeze infiltration technique was used to infiltrate the ceramic foams. The squeeze infiltration process involves the following steps (Figure 3.11);

- Loading the ceramic preform from a preheating furnace into the die cavity
- Pouring molten metal on top of the preform
- Applying pressure to start infiltration and
- Ejecting the composite after solidification

The force that was needed for the process was applied by a 100 tonne Norton squeeze casting press, Figure 3.12. The hydraulic system of the press could be operated manually or controlled automatically. The minimum operation limit was 100 kN. The die cavity of the press had inner dimensions of 125 mm in length and 75 mm in width. The height of the die-cavity was 20 mm. For the first infiltration trials the bottom die temperature was 250°C, the top punch temperature was 175°C and the preforms were pre heated to 800°C. The preforms were then transferred from the oven into the die.

During former investigations at Loughborough University it was calculated by the use of cooling curves that the preforms cool down until the metal is poured on top of them and that they will reach a temperature of approximately 200 to 400°C. The exact temperature depends on the material, the size and the time available for cooling. For further experiments cooling curves could be calculated for each material and

sample size. Immediately after the preform was placed into the die the liquid aluminium alloy with a temperature of 720°C was poured on top of the preform. After the die was filled the press was started and pressure was applied. The pressure applied was 175 kg/cm$^2$ and it was held for two minutes. Then the sample was ejected and allowed to cool down to room temperature. The samples were cut along their axes, mounted, ground and polished to investigate the interface between the metal and the ceramic.
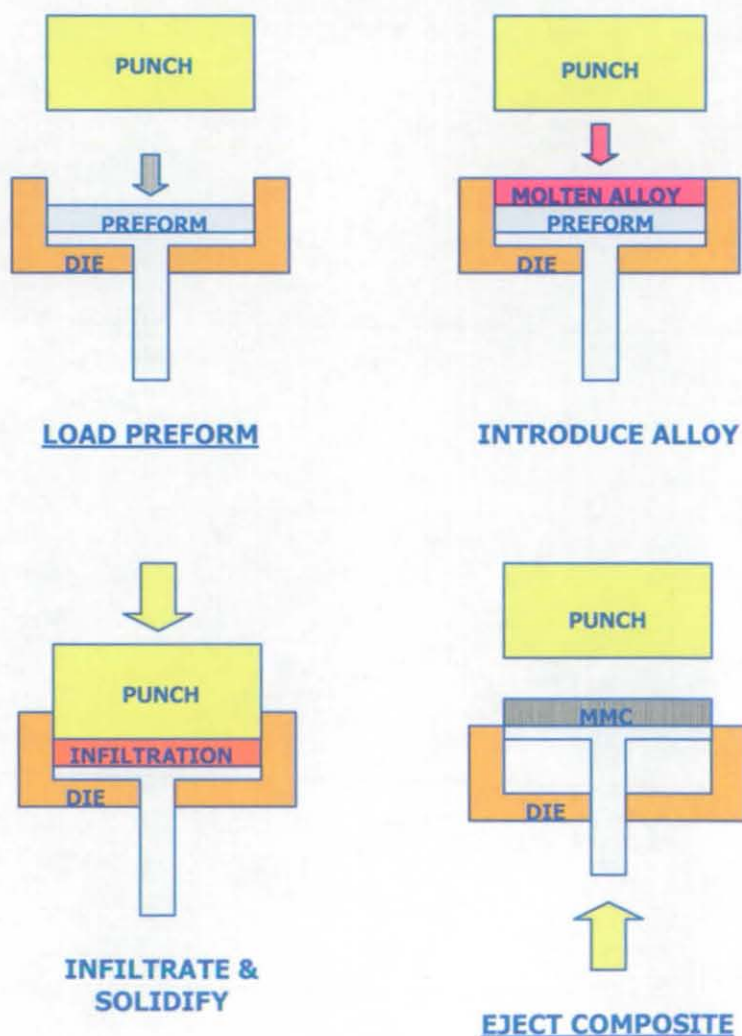
Figure 3.11: Steps involved in the squeeze infiltration process.

Figure 3.12: Picture of the squeeze casting equipment.

### 3.3.3 Metallography

Metallographic examinations were carried out to assess the effect of process parameters on the composites. The procedure for preparing the specimens and microscopic examinations are described in the following sections. For the first few samples, the specimens were sectioned from the casting using a Labotom cutting machine and 31TRE cut-off wheels, on both top and bottom surfaces. This was necessary to obtain better understanding of the material solidification characteristics, to make sure the infiltration characteristics of aluminium passing through the perform during casting and not from the sides. Small sections of the specimens were mounted in a Bakelite powder using a Struers Pronto Press 10 mounting machine. The specimen was placed in the heated mould, resting on the circular support with the relevant surfaces face down. Before starting the mounting process, sufficient mounting compound was poured into the mould to cover the specimen.

The sectioned and mounted specimens were ground initially on a Buehler Linisher which runs at a speed of 300 rpm. The polishing process was carried out

progressively using 320, 400, 600 and 1000 grit silicon carbide papers on a Metaserv hand grinder.

## 3.3.4 SEM examination

The polished surfaces of the specimens were characterised using a scanning electron microscope (SEM) to provide information about the microstructure of the composites and to get more information of the contact area between the ceramic material and the aluminium silicon alloy.

### 3.3.5 Hardness measurement of the ceramic-metal composites

Hardness is a property of the material that enables it to resist plastic deformation, usually by penetration [107]. However, the term hardness may also refer to resistance to scratching, abrasion or cutting. Initially, hardness measurements were conducted on the Vickers hardness scale (HV10 – 10 kg load) for both alloy and composite. The load was increased to 30 kg due to the larger indentation needed to ensure a more consistent measurement on the composite. This is because the area of Vickers hardness indentation is much smaller at 10 kg of load and makes an indent on the surface of the alloy only and this would inevitably cause large variations in the hardness values. When the load was increased to 30 kg it resulted in elongated indentation by covering both the surfaces (alloy and ceramic). For hardness measurements a small part of the specimen was cut from each of the cast specimen across the specimens using a Struers Labotom cutting machine.

# CHAPTER 4:

# RESULTS AND DISCUSSION

## 4.1   Ceramic foams

## 4.1.1 Characterisation of alumina foams

All alumina foams with a range of different density and cell sizes were characterised by remeasuring the density and cell sizes (See table 4.1).

Table 4.1: Comparison of the specifications of ceramic preforms provided by Hi-Por Ceramics Ltd and measured values.

| Hi-Por Specifications | | Measured Values | | | | | | |
|---|---|---|---|---|---|---|---|---|
| Code | Preform Samples | Cell diameter / $\mu$m | | | Window diameter / $\mu$m | | | Porosity / % |
| | | Mean | Smallest | Largest | Mean | Smallest | Largest | |
| A | 20 Al 400 | 380($\pm$143)[a] | 216 | 1020 | 140($\pm$70)[a] | 39 | 333 | 81($\pm$0.2)[b] |
| B | 14 Al 800 | 630($\pm$258) | 193 | 1452 | 198($\pm$113) | 32 | 548 | 87($\pm$1) |
| C | 17 Al 500 | 465($\pm$137) | 258 | 1050 | 107($\pm$52) | 34 | 322 | 84($\pm$0.5) |
| D | 17 Al 700 | 550($\pm$139) | 290 | 903 | 112($\pm$43) | 32 | 258 | 84($\pm$0.2) |

[a] Values in parentheses are standard deviation from at least 100 measurements.

[b] Values in parentheses are standard deviation from at least 20 measurements.

It can be observed from table 4.1 that the variation (scatter) is very high due to high variation in smallest and largest cell and window diameters. The samples used for the infiltration experiments and density and porosity measurements were 48 mm in diameter and 12-16 mm in thickness.

Figures 4.1-1 to 4.1-4 show some SEM-images of foam A, Figures 4.1-5 to 4.1-8 are of foam B, Figures 4.1-9 to 4.1-12 are of foam C and Figures 4.1-13 to 4.1-16 are of foam D. The typical structure of these foams made by foaming and in situ polymerisation of organic monomers can be seen in the figures. The foam consists of spherical cells that are surrounded by dense struts. The cells are interconnected by small windows within these struts.



Figure 4.1-1                           Figure 4.1-2

Figure 4.1-1 & 2: Alumina foam A; mean cell diameter 380 µm; magnification: left 10 times, right 30 times.



Figure 4.1-3                           Figure 4.1-4

Figure 4.1-3 & 4: Alumina foam A; mean cell diameter 380 µm; magnification: left 150 times right 2000 times.
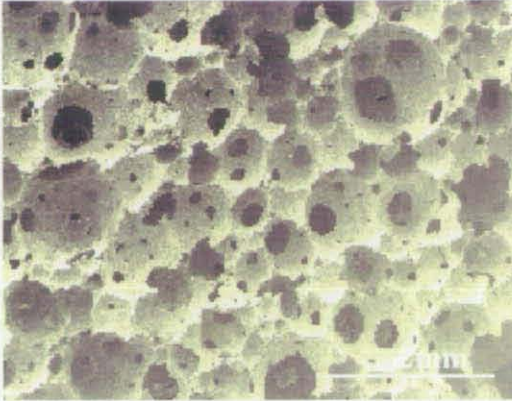
Figure 4.1-5
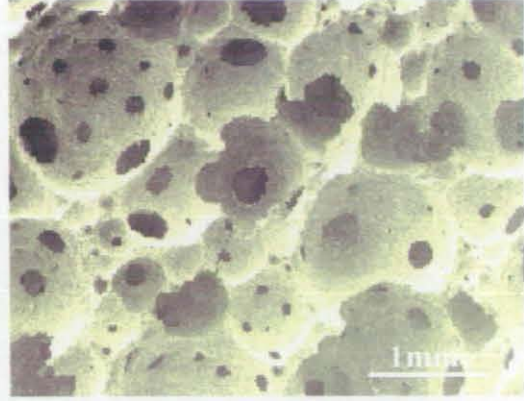
Figure 4.1-6

Figure 4.1-5 & 6: Alumina foam B; mean cell diameter 630 μm; magnification: left 10 times, right 30 times.



Figure 4.1-7
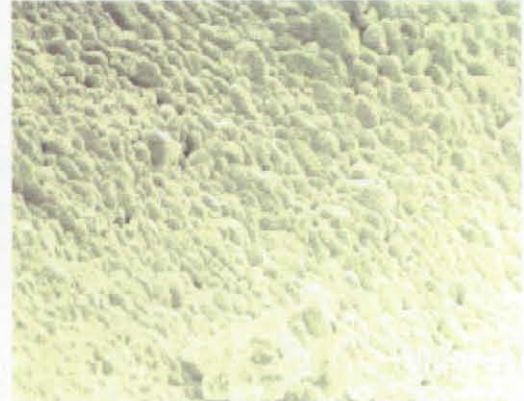
Figure 4.1-8

Figure 4.1-7 & 8: Alumina foam B; mean cell diameter 630 μm; magnification: left 100 times, right 2000 times.
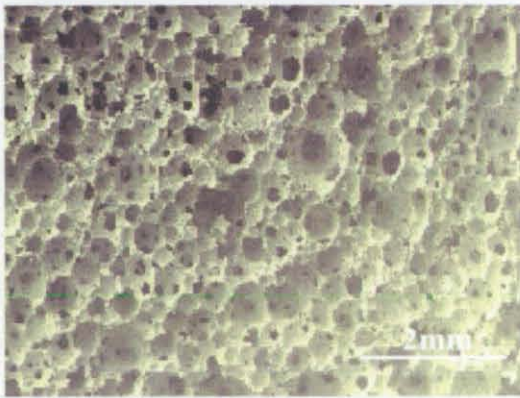


Figure 4.1-9
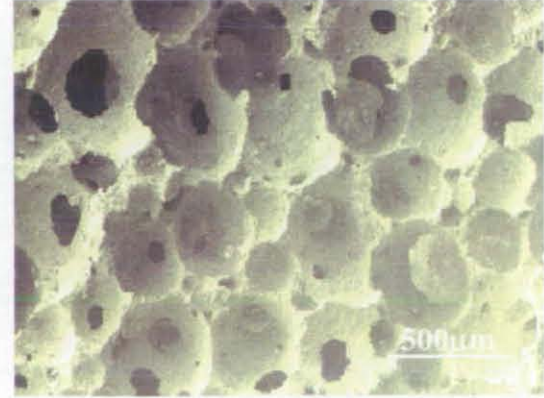
Figure 4.1-10

Figure 4.1-9 & 10: Alumina foam C; mean cell diameter 465 μm; magnification: left 10 times, right 50 times.

113
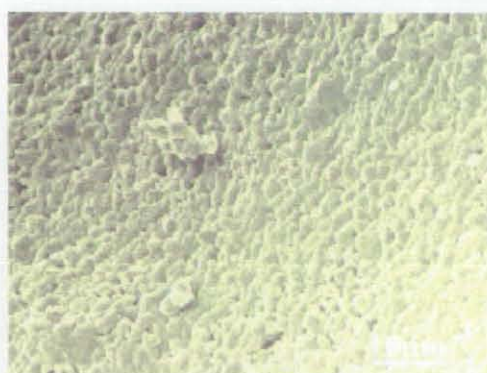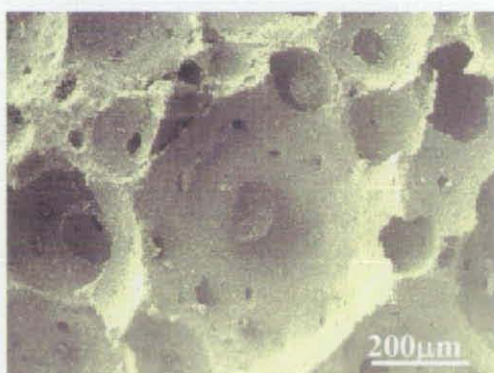
Figure 4.1-11                                    Figure 4.1-12

Figure 4.1-11 &12: Alumina foam C; mean cell diameter 465 µm; magnification: left 100 times, right 2000 times.
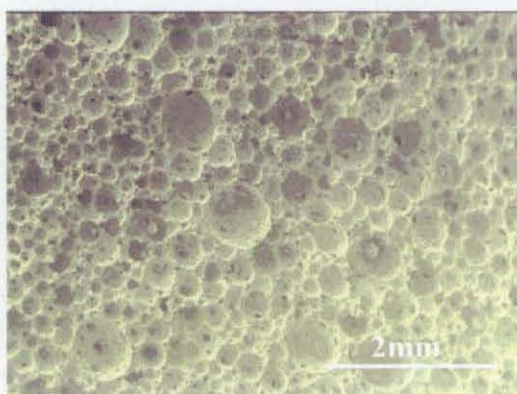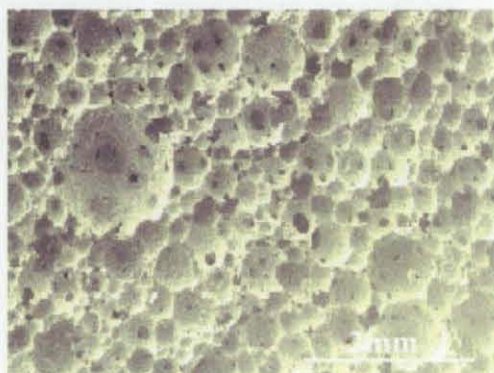


Figure 4.1-13                                    Figure 4.1-14
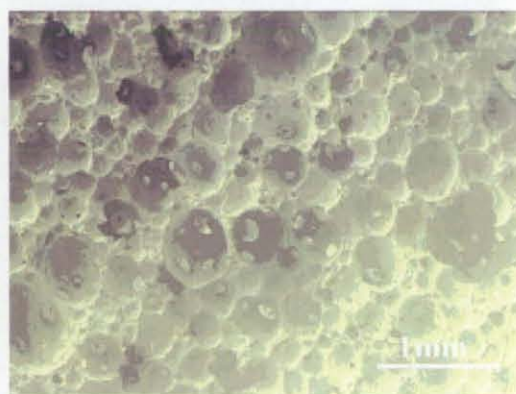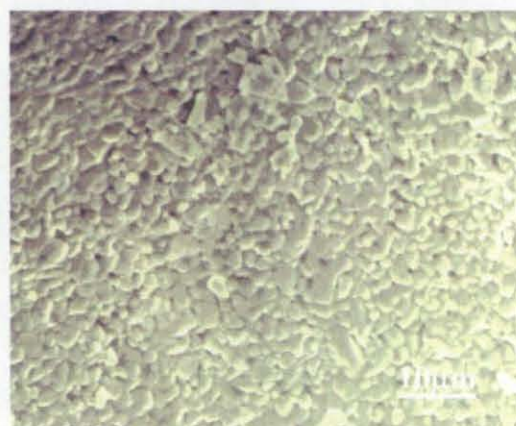
Figure 4.1-13 & 14: Alumina foam D; mean cell diameter 550 µm; magnification: left 10 times, right 50 times.



Figure 4.1-15                                    Figure 4.1-16

Figure 4.1-15 & 16: Alumina foam D; mean cell diameter 550 µm; magnification: left 100 times, right 2000 times.

## 4.1.2 Processing of BaTiO$_3$ foams

The fabrication process of these foams was given in section 3.1.2. The main aim of producing these foams was to infiltrate with polyvinylidenefluoride resin and to measure the piezoelectric properties of the BaTiO$_3$-PVDF composites. Table 4.2 shows the values of the % weight loss of the barium titanate foams after sintering at 1300°C for 3 hours.

Table 4.2: % weight loss of BaTiO$_3$ foams after sintering at 1300°C for 3 h.

| Sample code | Weight loss / % |
|-------------|-----------------|
| Foam A | 7.5 |
| Foam B | 7.2 |
| Foam C | 7.3 |
| Foam D | 7.4 |
| Foam E | 7.4 |

The sintering process resulted in complete cracking of the foams. To know whether these foams were cracking during the binder burn out phase, which occurs from 230-550°C, a few samples were fired at 250, 350, 450, 550 and 600°C for 3 hrs and cooled to room temperature at a rate of 0.5°C. Whilst the foam samples were all very soft after binder burn out, no cracks existed. To determine whether there was any amount of binder left in the foam after firing at 600°C and to see whether there was a volume change because of a phase transformation during sintering, the foams were further characterised using thermo gravimetric analysis (TGA) and x-ray diffraction (XRD).

### 4.1.2.1 Thermogravimetric analysis (TGA)

Figure 4.2 shows the % weight loss of the binder as a function of temperature in a barium titanate foam sample heated at a rate of 5°C min$^{-1}$ up to 600°C in air. The data shows 6.5-7% weight loss with the majority occurring in the range 275-440°C. The monomer used for producing the foams was an aqueous solution containing 35 wt% of ammonium acrylate. This accounts for 7 wt%, approximately matching that lost on heating during both the TGA analysis and sintering studies. It can therefore be concluded that all the monomer was burnt out during the holding stage at 550°C during the sintering schedule and therefore residual polymer in the foams is unlikely to have been the reason for the cracking.
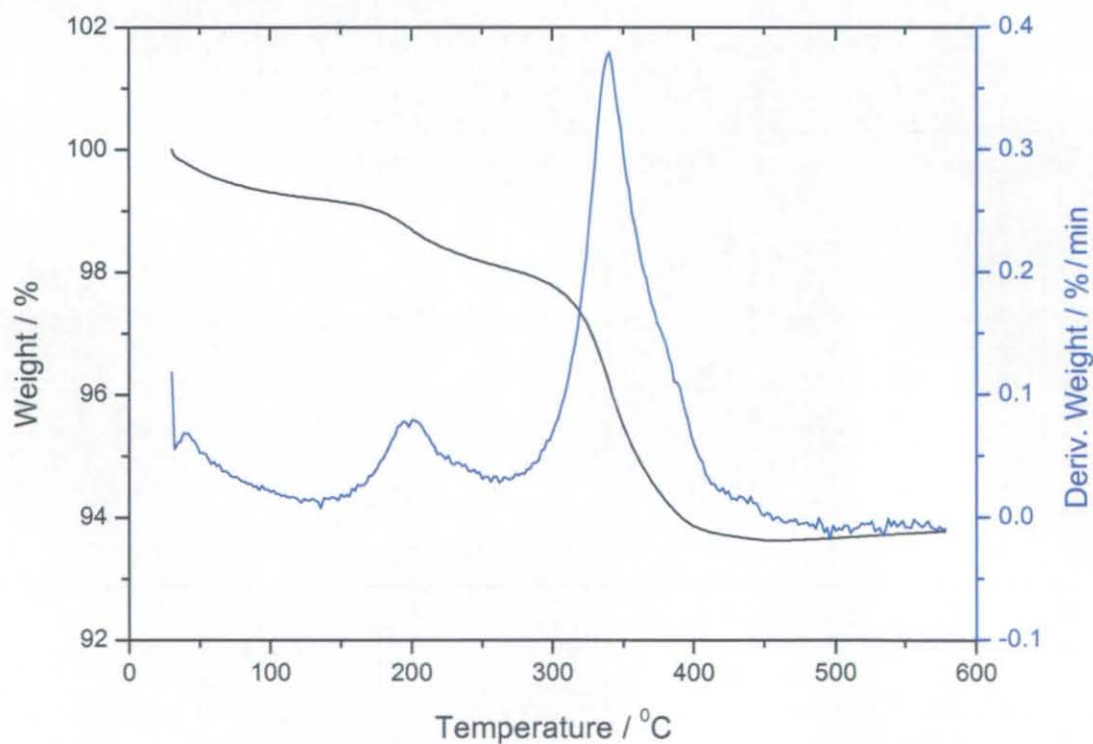


Figure 4.2: TGA of the BaTiO$_3$ foam sample.

## 4.1.2.2 X-ray diffraction

X-ray diffraction analysis was carried out to see whether any volume change occurred in the barium titanate foams as a result of a phase transition that might cause cracking of the foams. The interplanar spacings were calculated as explained in section 3.1.2.2.
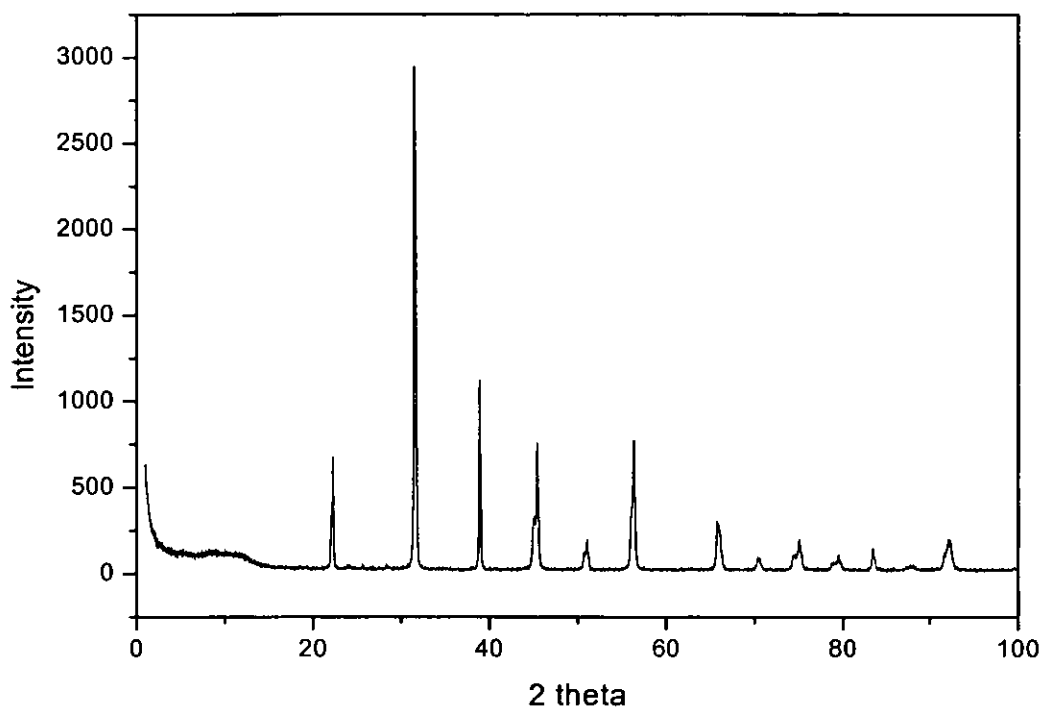


Figure 4.3: XRD pattern of the $BaTiO_3$ powder sample as received.

Table 4.3: XRD values for corresponding peaks of the $BaTiO_3$ powder as received.

| For peaks | | | | | | | |
|---|---|---|---|---|---|---|---|
| 2 theta | Intensity | Theta | sin / theta | d | d / A | Phase | hkl |
| 22.28 | 616 | 11.14 | 0.193207 | 3.99002E-10 | 3.99002125 | t | 100 |
| 31.58 | 2895 | 15.79 | 0.272112 | 2.83302E-10 | 2.83302147 | t | 101 |
| 38.92 | 1125 | 19.46 | 0.333149 | 2.31398E-10 | 2.31398178 | t | 111 |
| 45.42 | 700 | 22.71 | 0.386067 | 1.9968E-10 | 1.99680341 | t | 200 |
| 56.32 | 776 | 28.16 | 0.471935 | 1.63349E-10 | 1.63348633 | t | 211 |
| 65.96 | 266 | 32.98 | 0.544346 | 1.41619E-10 | 1.41619419 | t | 202 |
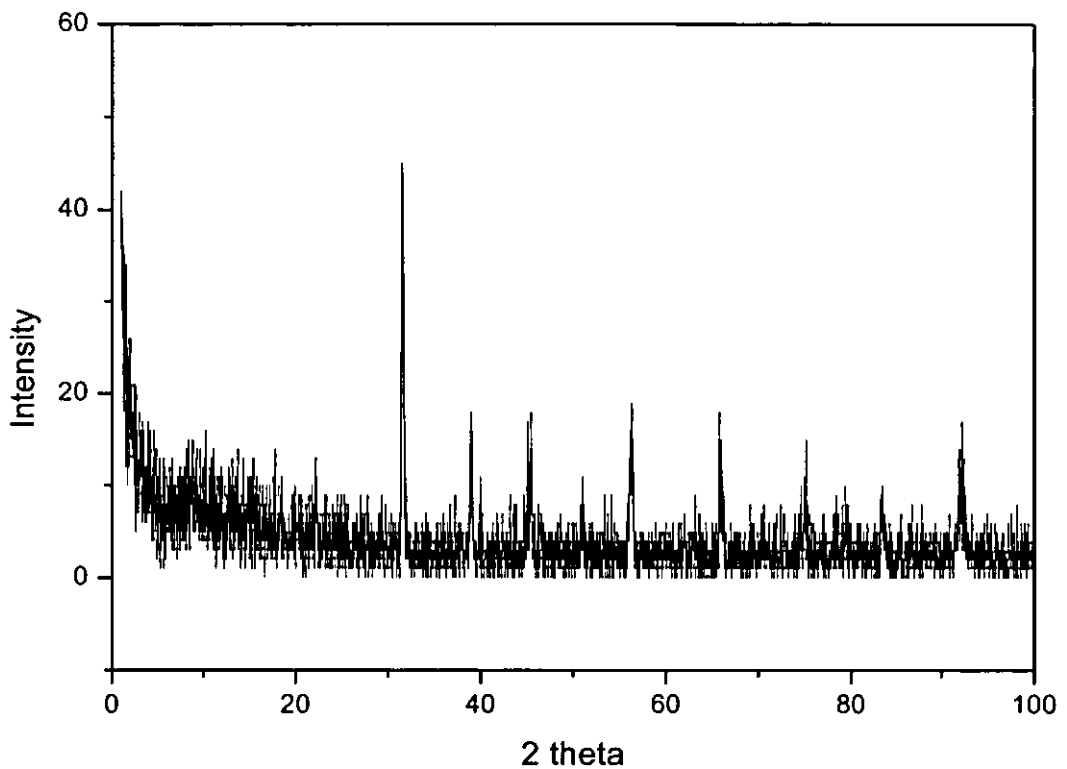
Figure 4.4: XRD pattern of the BaTiO$_3$ foam sample.

Table 4.4: XRD values for corresponding peaks of the BaTiO$_3$ foam.

| For peaks | | | | | | | |
|---|---|---|---|---|---|---|---|
| 2 theta | Intensity | Theta | sin / theta | d | d / A | Phase | hkl |
| 31.68 | 44 | 15.84 | 0.272951936 | 2.82431E-10 | 2.824306772 | t | 110 |
| 38.96 | 18 | 19.48 | 0.333477795 | 2.3117E-10 | 2.311698145 | t | 111 |
| 45.44 | 18 | 22.72 | 0.386228045 | 1.99597E-10 | 1.995971057 | t | 200 |
| 56.34 | 18 | 28.17 | 0.472089251 | 1.63295E-10 | 1.632953936 | t | 211 |
| 56.32 | 19 | 28.16 | 0.471935384 | 1.63349E-10 | 1.633486334 | t | 211 |
| 65.8 | 18 | 32.9 | 0.54317445 | 1.41925E-10 | 1.419249378 | t | 202 |
| 75.22 | 15 | 37.61 | 0.610283435 | 1.26318E-10 | 1.263183556 | t | 310 |
| 92.2 | 17 | 46.1 | 0.720551112 | 1.06988E-10 | 1.069875527 | c | 312 |
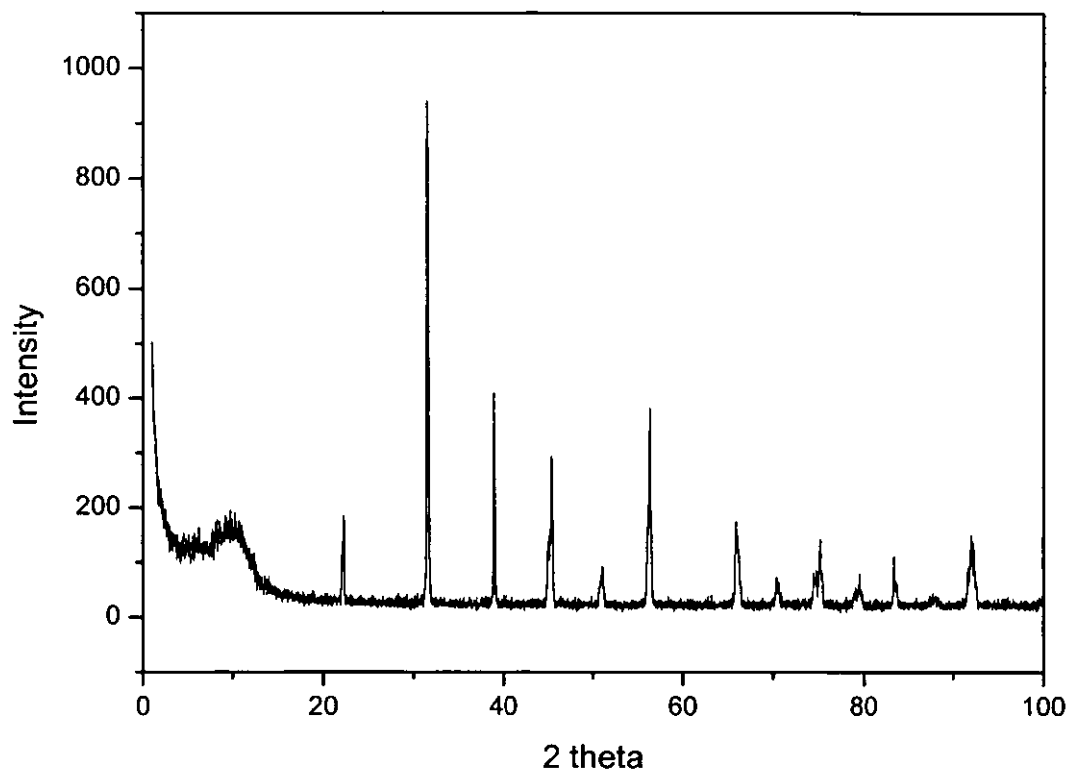
Figure 4.5: XRD pattern of the BaTiO$_3$ foam sample crushed into powder.

Table 4.5: XRD values for corresponding peaks of the BaTiO$_3$ foam crushed into powder.

| For peaks | | | | | | | |
|---|---|---|---|---|---|---|---|
| 2 theta | Intensity | Theta | sin / theta | d | d / angstrom | Phase | hkl |
| 22.24 | 180 | 11.12 | 0.192864491 | 3.99711E-10 | 3.997106973 | t | 100 |
| 31.54 | 940 | 15.77 | 0.271776394 | 2.83652E-10 | 2.836523032 | t | 101 |
| 38.92 | 390 | 19.46 | 0.33314869 | 2.31398E-10 | 2.313981784 | t | 111 |
| 45.4 | 281 | 22.7 | 0.385906042 | 1.99764E-10 | 1.997636511 | t | 200 |
| 56.3 | 381 | 28.15 | 0.471781503 | 1.63402E-10 | 1.634019129 | t | 211 |
| 65.94 | 159 | 32.97 | 0.544199833 | 1.41658E-10 | 1.416575222 | t | 202 |

From the above XRD results it can be concluded that the data and the trend is the same for all the samples. As expected, the only phase present was tetragonal and no phase transformation occurred during sintering. No significant volume change was observed from the above results.

As discussed earlier, no cracks were observed when the foams were heated up to 600°C indicating that the cracking occurred at a higher temperature: since neither residual polymer nor a phase transition appears to be the cause, the reason for the cracking was not determined and further experiments would be needed. On the basis of the results, however, no further work was done on the infiltration of these foams with any of the polymers.

## 4.2 Polymer infiltration trials

## 4.2.1 Vacuum infiltration procedures

The first experiment with the vacuum assisted infiltrated technique and the prototype revealed a few problems with the assembly. The preform was not completely sealed on the outside by the O-ring and therefore most of the Crystic 471 PALV polyester resin was sucked around the ceramic foam sample instead of flowing through it. Only a few millimetres were infiltrated. The second problem was that the resin glued everything together while curing and the sample could not be removed from the tube after cooling. After these results, it was obvious that the sealing of the outside was important to make sure that the resin flows through the foam and further that there will be no resin on the outside to glue the parts together. Another problem was that the assembly could not be easily separated to remove the sample and to load the next sample because of the three long nuts and bolts. It was very difficult and time consuming to loosen and remove all the three nuts and bolts for each trial. To make sure that the foam sample was completely packed outside, a layer of PTFE sealant tape was used, on the top of it another layer of adhesive tape was also used. In order to overcome the problem of resin sticking to the tube, a couple of A4 transparency sheets were folded around the inner diameter of the tube until it sealed the preform tightly. This helped in two ways, it avoided the problem of gluing to the tube and it packs the

sample tightly. With these new arrangements the next trials were satisfactory. The resin, poured on top of the sample, was sucked through the preform. After most of the resin was sucked through the preform it was allowed to cure. The A4 transparencies could be removed after curing. Then the resulting composite was easily separated from the transparency. This way of infiltration seems to be a good possibility to obtain sound results and was used for further polymer infiltration trials.

Table 4.6: Density of the Crystic 471 PALV polyester resin infiltrated composites.

| Sample code | Parameters | Density of composites / kg m$^{-3}$ | % Density of composites | % Avg. density of composites |
|---|---|---|---|---|
| Foam A | 20°C | 1582 | 92.3 | 92.6(±0.3) |
| Foam A | 300 mbar | 1591 | 92.9 | |
| Foam A | 20°C | 1543 | 90.1 | 91(±1) |
| Foam A | 250 mbar | 1576 | 92.0 | |
| Foam A | 20°C | 1538 | 89.8 | 91.7(±1.9) |
| Foam A | 350 mbar | 1604 | 93.6 | |
| | | | | |
| Foam A | 25°C | 1546 | 90.3 | 90.3(±0.1) |
| Foam A | 300 mbar | 1548 | 90.4 | |
| Foam A | 25°C | 1590 | 92.8 | 91(±1.8) |
| Foam A | 350 mbar | 1527 | 89.2 | |
| Foam A | 15°C | 1547 | 90.3 | 89.4(±0.9) |
| Foam A | 250 mbar | 1515 | 88.4 | |

The real achieved density of the composites was calculated for all sets of experiments. A calculation of the theoretical density of a completely filled composite (by taking the theoretical densities of the two components and the porosity of the foam to be 81%, see table 3.1) yielded a density of about 1713 kgm$^{-3}$. The comparison of this theoretical density with real achieved densities, Table 4.6, shows that whilst there was little variation in density, the composites were not completely dense but there was some porosity present in the material. The results also suggest that both the temperature and

suction pressure had a strong influence on the polymer infiltration process, as predicted in the design of experiments. From the above results it could be observed that a temperature of 20°C and suction pressure of 300 mbar achieved the highest density; it also showed better infiltration quality, see section 4.2.1.1. The gel-time at these conditions was 16 mins.

When the pressure was decreased to 250 mbar, the density of the composite was reduced and when the pressure was increased to 350 mbar the % density of the resulting composite increased from 91 to 91.7 %. These results suggest that variation in pressure does affect the infiltration quality. At 20°C, the viscosity of the resin was 470 mPa s, which could be considered as a high viscosity for a pressure of 250 mbar and the pressure was not sufficient enough to suck the resin and resulted in less density, where as a pressure of 350 mbar could be too high to suck the resin and could have sucked the resin too fast, encouraging more gas porosity in the composite material resulting in high scatter of the % density of the resulting composite. At 20°C temperature with a gel-time of 16 mins, a resin viscosity value of 470 mPa s, the optimum pressure required could be 300 mbar and thus resulted in better infiltration quality with a highest density from all the trials.

During the second set of experiments, the temperature was raised to 25°C and pressure was kept at 300 mbar but this did not show any improvement in the density. When the pressure was increased to 350 mbar, it resulted in an increase in % density. These results were obtained with a resin viscosity of 440 mPa s and a gel-time of 12.3 mins. The viscosity of the resin was reduced when the temperature was raised, which in turn resulted in too fast setting of the resin. Under these conditions a pressure of 300 mbar was not high enough to suck the resin with a quick geltime, which in turn resulted in fast setting and the viscosity rose rapidly as the suction process continued. The reverse was true; an increase in the pressure resulted in fast infiltration and encouraged gas entrapment.

From the above results it could be concluded that the parameters, suction pressure and temperature are dependent on each other and are directly dependent on viscosity and gel-time or setting of the resin systems during negative pressure infiltration process.

.

## 4.2.1.1 Light microscopy analysis

From the matrix of experiments, Table 4.6, two composite samples of highest achieved density (best infiltration conditions) and two samples of lowest achieved density (worst infiltration conditions) were investigated using light microscopy.



( a )



( b )



( c )



( d )

( e )                                                    ( f )
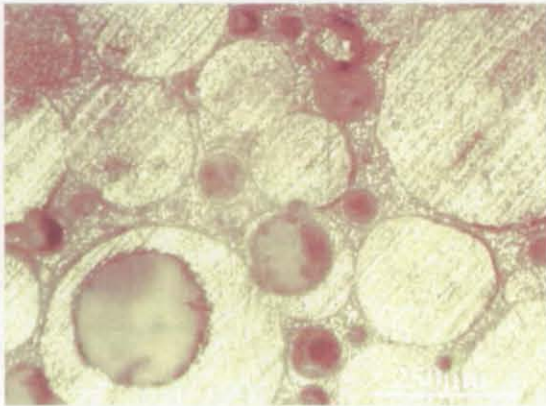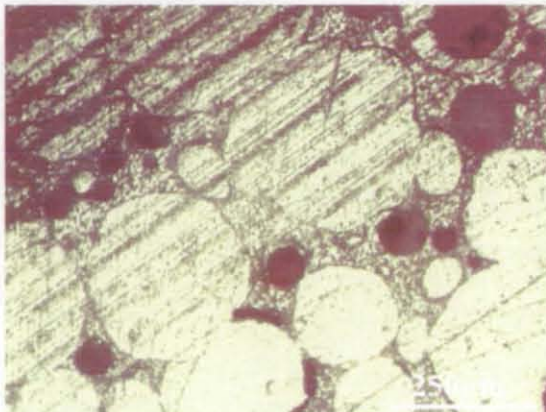
Figure 4.6: Light microscope images of the polyester resin infiltrated alumina foam with a mean cell size of 380 μm (Foam A): a) and b) Near to the infiltration surface, c) and d) halfway to the infiltration surface, e) and f) far from the infiltration surface. The direction of infiltration is from top to bottom. Magnification: 100 times

The above pictures show some light microscope images of the Crystic 471 PALV polyester resin infiltrated ceramic foams. The composite sample shown above was infiltrated under a pressure of 250 mbar and at temperature of 15°C. Figures (a) and (b) were taken near to the infiltration surface. In these pictures the porosity can be observed in the form of big bubbles. These bubbles were observed within the polyester resin phase. The bubbles could be the result of entrapped air that was inside the resin during the infiltration and remained there. Also a few unfilled tiny cells can be observed all over the sample and can be clearly seen in figures (c) and (d). Whether this is a result of closed porosity and hence never having been filled with polymer is difficult to say. Again a comparison of the theoretical density of 1713 kgm$^{-3}$ with the real achieved density of 1515 kgm$^{-3}$ shows that the composites can not be completely dense but there must be air left in the material. All these factors assume that the infiltration is not complete because of the presence of porosity in various forms. The % achieved density of this composite was measured as 88.4%, the lowest achieved density of all the samples and the above images confirms the same thing.

The following pictures show the infiltration quality of an alumina foam sample which is 20% dense and with a mean cell size of 380 μm, infiltrated polyester resin under optimum conditions (20°C, 300 mbar). From these pictures it can be observed

that there are bubbles inside the polyester but the size of the bubbles is small in this sample. Next to the air bubbles there are some tiny unfilled cells in the sample and clearly visible in figures (e) and (f).

As well as the presence of unfilled cells there was a shrinkage problem; the curing and cooling of the resin resulted in high shrinkage. This high shrinkage is the reason for the gaps that appear between the ceramic struts and the polyester inside the cells. The appearance of these gaps is everywhere from the infiltration surface (top) to bottom surface but the width of these gaps shows variations from cell to cell. As can be observed from the SEM images of alumina foam samples and from the cell and window size analysis, section 4.1.1, large variations in cell and window sizes can be observed. If the volume of the infiltrated polyester in one cell is higher then it leads to higher shrinkage. As high the volume of the cell the higher is the shrinkage and therefore the resin debonds at more places as shown in figures (g) and (h).



( a )



( b )



( c )



( d )

( e )

( f )



( g )
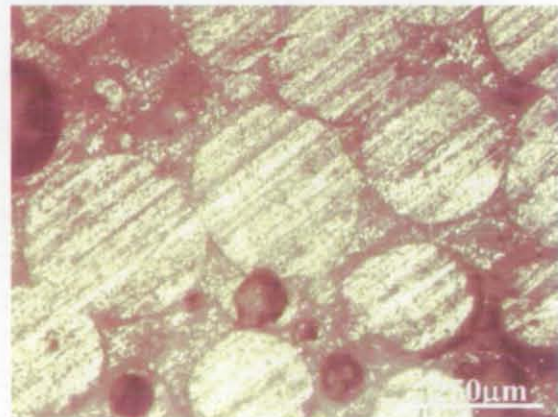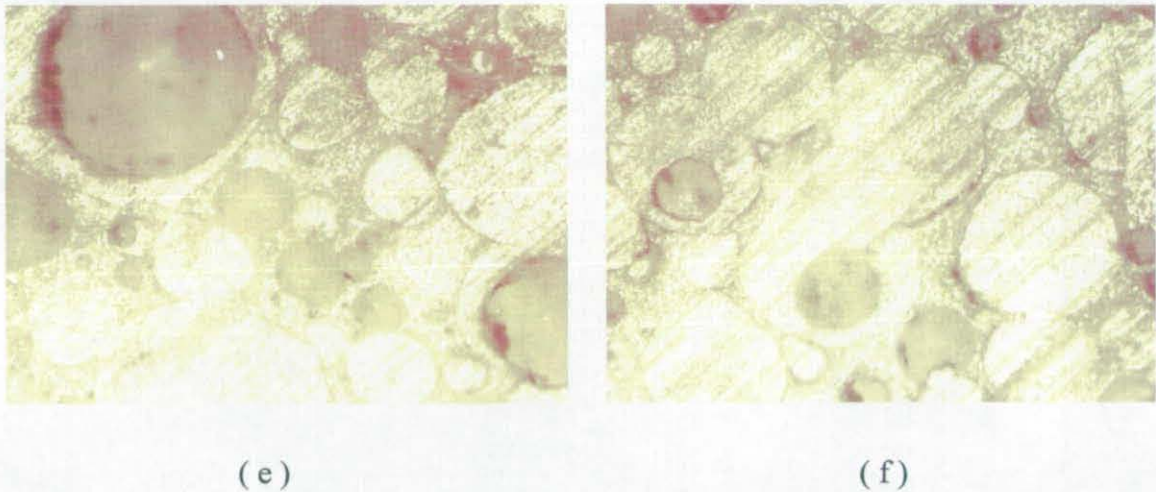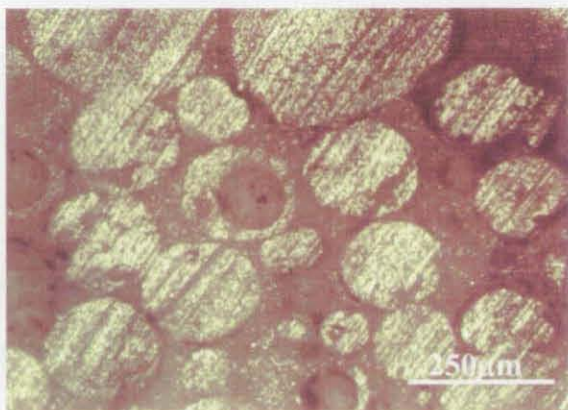
( h )
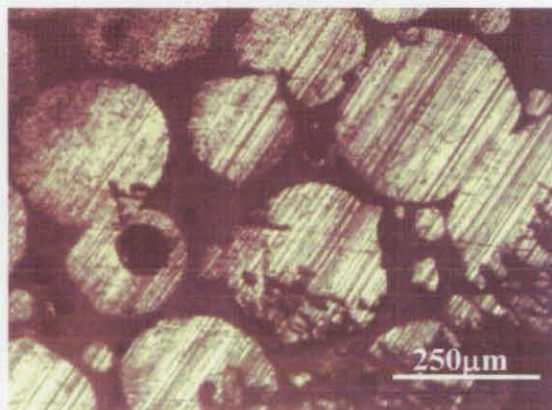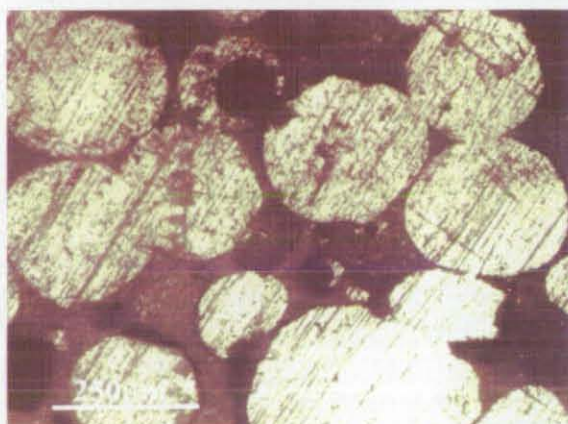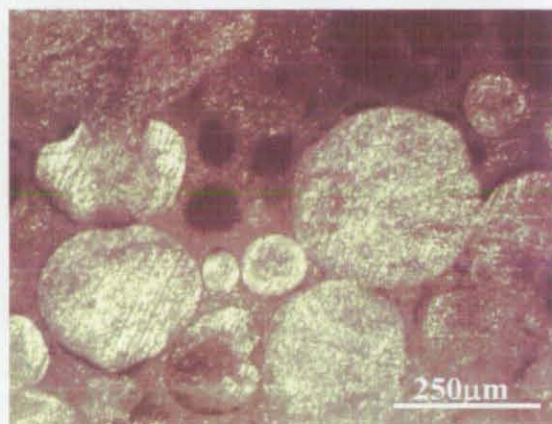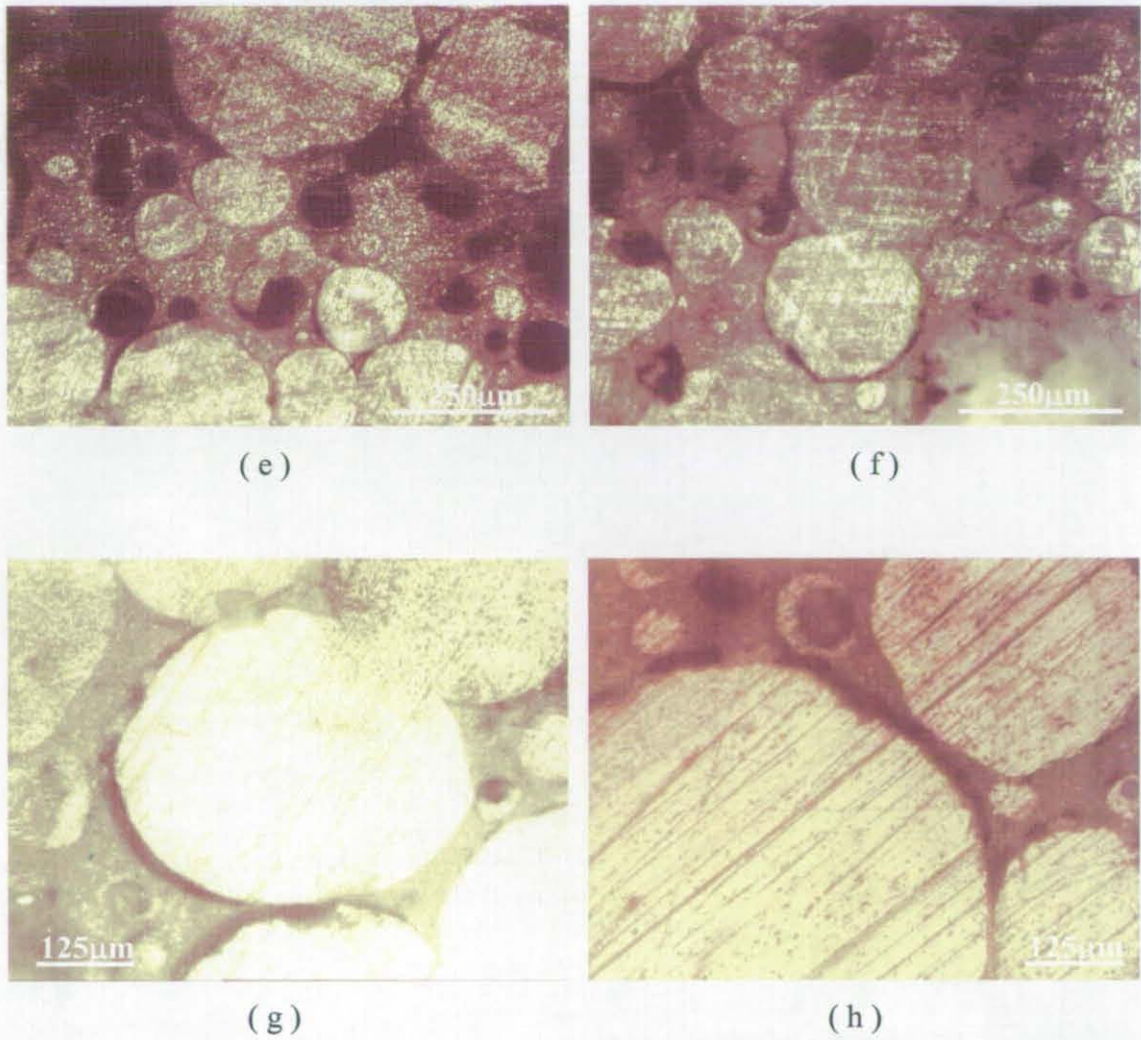
Figure 4.7: Light microscope images of the polyester resin infiltrated alumina foam with a mean cell size of 380 μm (Foam A): a) and b) Near to the infiltration surface, c) and d) halfway to the infiltration surface, e) and f) far from the infiltration surface; The direction of infiltration is from top to bottom. Magnification: 100 times. Figures: g) and h) near to infiltration surface; Foam A; magnification: 500 times.

Another sample with the same porosity and mean cell size was infiltrated under the same conditions to check the reproducibility and the quality of infiltration as shown in figure 4.8.

( a )

( b )

( c )

( d )

( e )

( f )
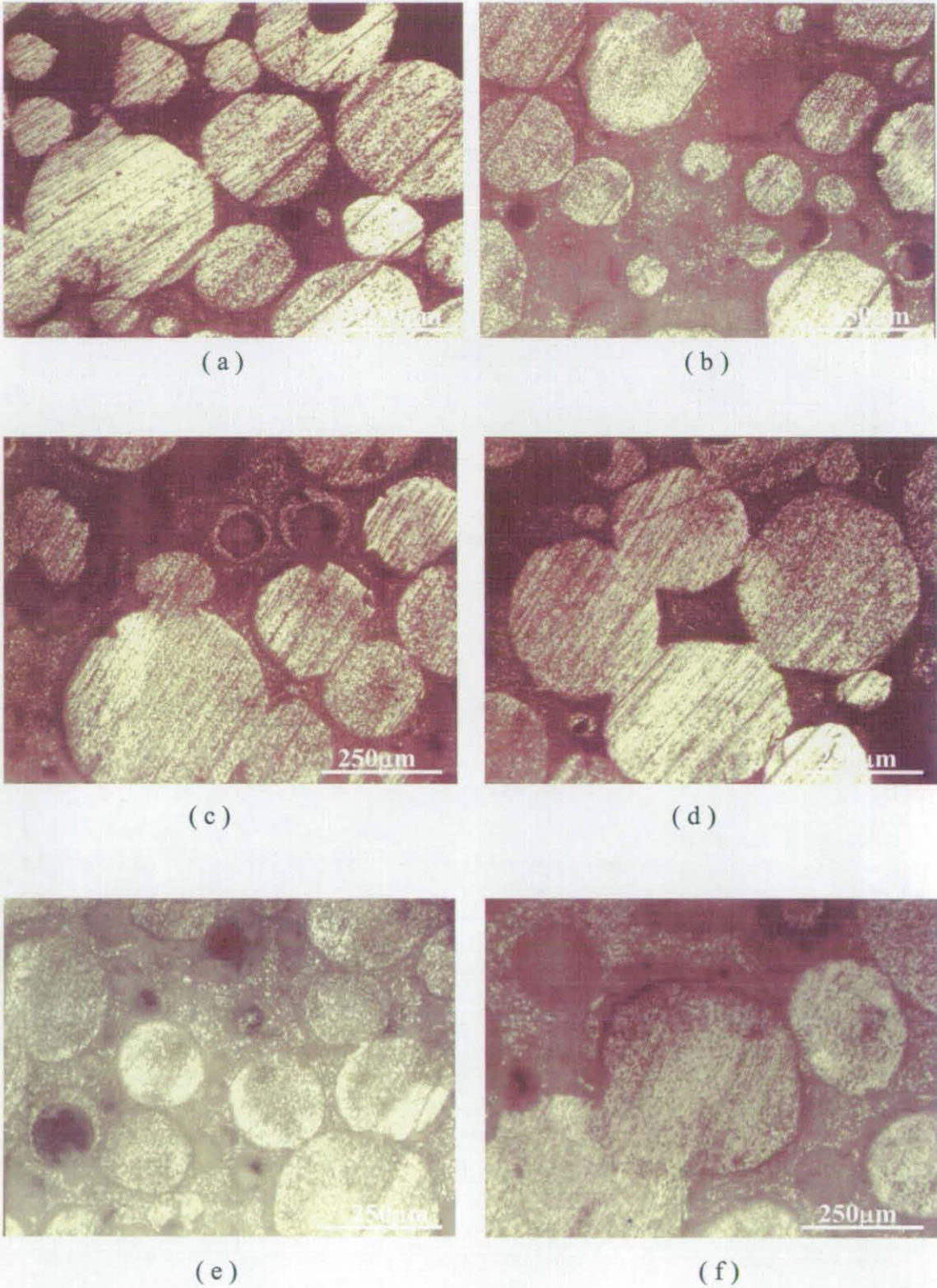
Figure 4.8: Light microscope images of the polyester resin infiltrated alumina foam with a mean cell size of 380 µm (Foam A): a) and b) Near to the infiltration surface, c) and d) halfway to the infiltration surface, e) and f) far from the infiltration surface. The direction of infiltration is from top to bottom. Magnification: 100 times

Figure 4.8 show some light microscope images of the Crystic 471 PALV polyester resin infiltrated alumina foams at 20°C and 300 mbar pressure. From these figures the same trend is observed but the small percentage of air bubbles and unfilled cells resulted in better infiltration with the highest density (92.9%) of the composite achieved.

The shrinkage of the polyester is a problem that has to be taken into account for further investigations to achieve dense composites. Infiltration under vacuum resulted in gas entrapment problems; an infiltration under pressure could help in solving the problem. In order to avoid air bubbles, thorough, gentle and very slow mixing is required.

### 4.2.1.2 Fluorescence microscopy analysis

It was difficult to differentiate the ceramic and resin phases in the light microscopic images. To see whether there was any possibility to differentiate the gas entrapment and unfilled cells/closed porosity, an incident light fluorescence (reflected light) microscopy technique was used. With this technique, when the specimens were focused under reflected light, the ceramic did not fluoresce but the resin did.

Figures 4.9 & 4.10 show some fluorescence microscope images of the Crystic 471 PALV polyester resin infiltrated alumina foams at 20°C and 300 mbar pressure. The direction of infiltration is from left to right. It can be observed from the pictures that there is porosity present in the composite samples and the trend observed is the same as in light microscopy. The region that fluoresced was resin, which has black regions confirming gas entrapment and also shows shrinkage on the corners (debonding) with the same colour.
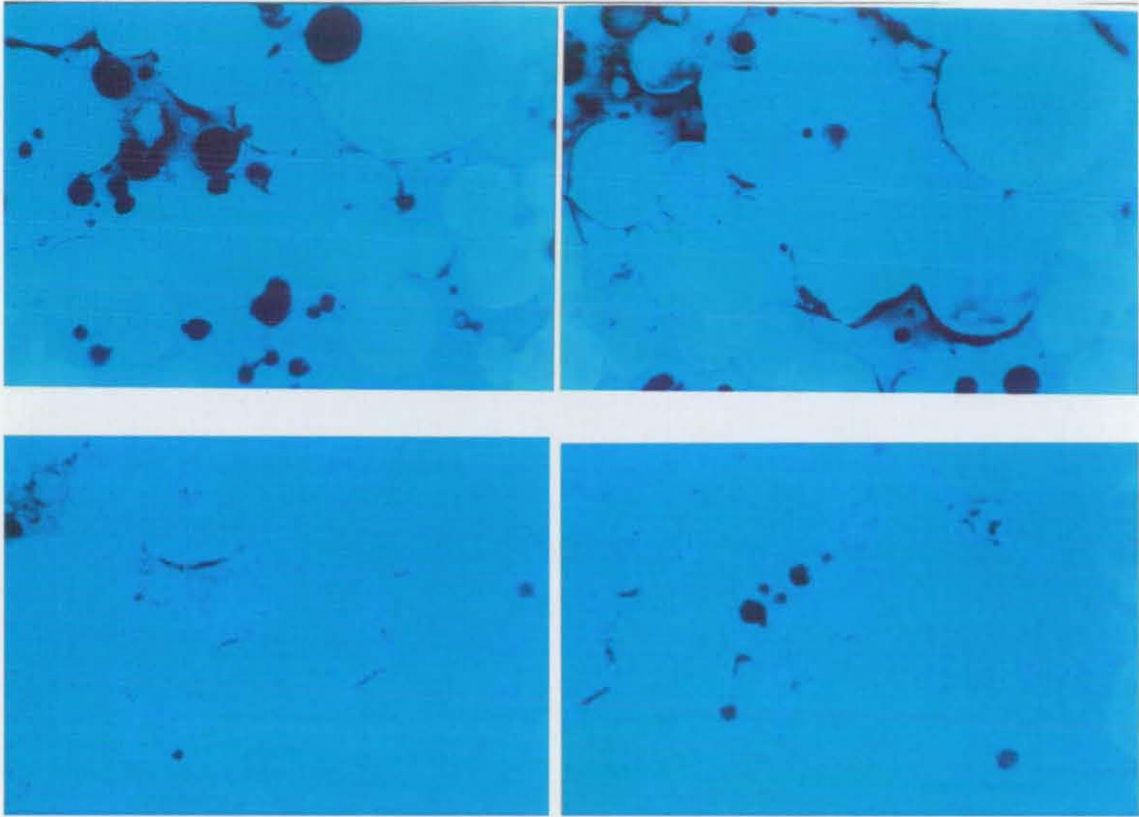
Figure 4.9: Fluorescence microscope images of the polyester resin infiltrated alumina foam with a mean cell size of 380 μm (Foam A); Top pictures –near to infiltration surface, Bottom- far from the infiltration surface. Infiltration direction: from left to right.

From the figures 4.9 and 4.10, it can be concluded that the porosity existed in the vacuum infiltrated composite samples in three different forms. It is difficult to evaluate quantitatively which form of porosity is most extensive. However, it can be qualitatively observed that the maximum porosity arose from gas entrapment within the polyester resin and that high shrinkage was present, resulting in the gaps that appear between the ceramic struts and the polyester inside the cells. There is also a small fraction of closed porosity due to which there are a few unfilled cells left in the composite.
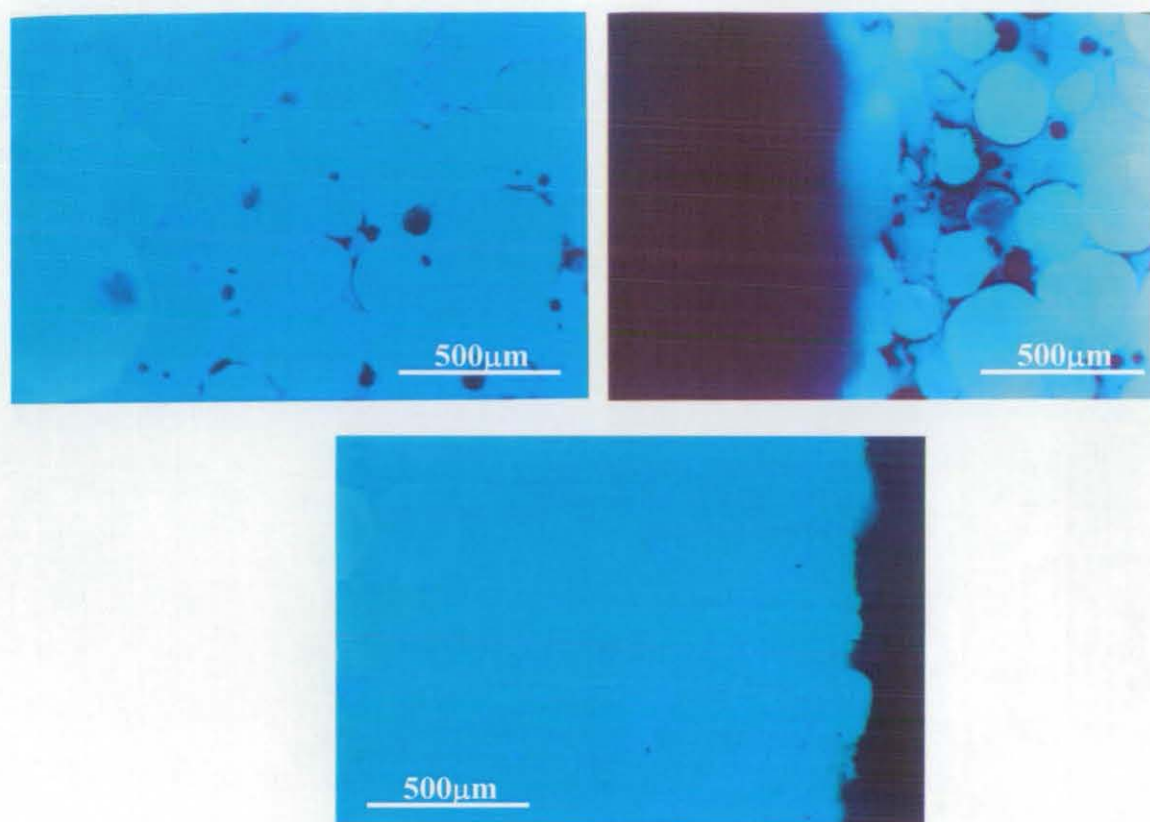
Figure 4.10: Fluorescence microscope images of the polyester resin infiltrated alumina foam with a mean cell size of 380 μm (Foam A); Top right picture–near to infiltration surface, Left- half-way to the infiltration surface, Bottom- far from the infiltration surface.

Figure 4.11, a stained sample, shows different colours representing the existence of three different forms of porosity in the vacuum assisted infiltration process. The stain went into the area between the polyester resin and ceramic strut confirming that there are gaps due to shrinkage.
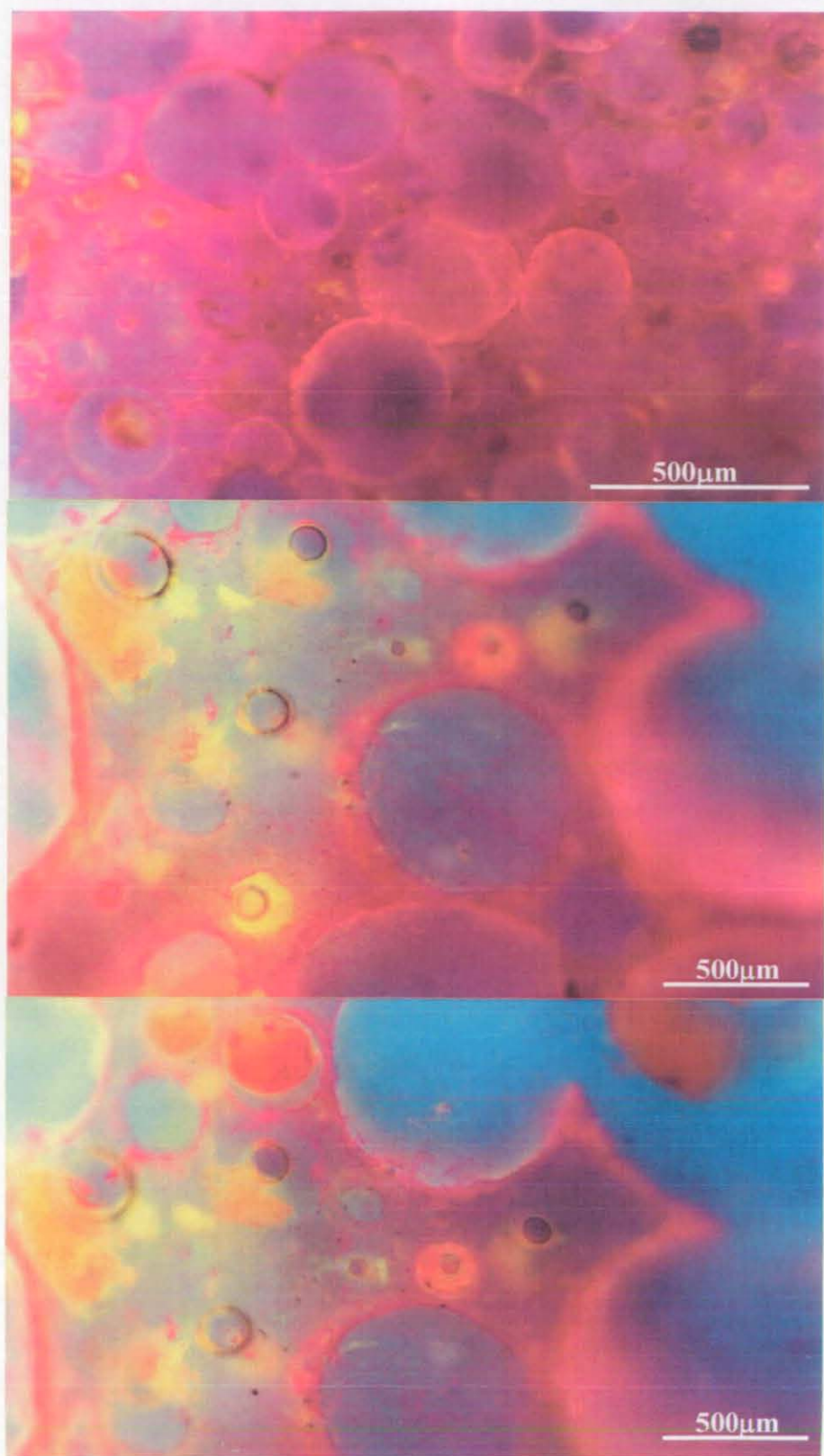
Figure 4.11: Fluorescence microscope images of the polyester resin infiltrated alumina foam with a mean cell size of 380 μm (Foam A); stained sample

A considerable amount of time was spent to overcome the problems that arosed in the vacuum assisted infiltration process. The steps taken to solve two main problems are explained as follows:

## 4.2.1.3 Air entrapment

Entrapment of gas in the resin while mixing, gelling and during the infiltration process was found to be a major drawback. The following steps are considered as options to eliminate or reduce the quantity of air bubbles.

- Avoid air bubble formation during catalyst addition
- Slow injection of catalyst into the resin
- Slow stirring and gentle mixing of resin and catalyst
- Create pressure difference ($\Delta P$) with the help of vacuum

After considering all of the above steps, no great improvement was observed in the infiltration quality of the composite samples. The resin/catalyst mixture was placed in the vacuum assembly for 5-10 minutes to eliminate air bubbles trapped inside the mixture and then it was set to cure at room temperature. A second batch of resin was mixed with the catalyst very slowly and gently and poured via a thin stream, from one container to another container twice to reduce the possibility of air entrapment or eliminate the air bubbles which were already formed. This was then allowed to set at room temperature. After the two mixtures were cured completely, the density (mass/volume) of the cured samples was calculated and % porosity present was calculated using the theoretical density of polyester resin. Table 4.7 gives the approximate quantitative values of % porosity (due to air entrapment) present in the fully cured polyester resin under different poured conditions.

Table 4.7: Approximate quantitative % porosity present in 100% polyester samples cured under different poured conditions.

| Sample | Dia/ mm | Thickness / mm | Mass / g | Density / $kgm^{-3}$ | Porosity % |
|---|---|---|---|---|---|
| Vacuum treated | 52.38 | 10.20 | 25.9 | 1178 | 3.44 |
| Thin stream | 52.24 | 9.75 | 24.8 | 1186 | 2.80 |
| Thin stream | 52.24 | 7.80 | 20.0 | 1187 | 2.70 |

From the above measurements it could be estimated that the approximate amount of porosity present in the form of air entrapment in 100% polyester cured sample could be in the range of 2.5-3.5%.

Two more preforms were infiltrated by following the procedure described above and infiltration was performed under the worst conditions (15°C, 250 mbar) from previous trials to check whether it would be possible to improve the infiltration quality and hence the % density of the composites. Pouring by thin stream and other steps such as thorough and gentle mixing showed an increase in the average % density from 89.4 to 91.7% under the worst infiltration conditions but did not result in any improvement under the best infiltration conditions.

Table 4.8: % density of composites under better mixing conditions.

| Preforms | Infiltration parameters | % Density of composites | % Average density of composites |
|---|---|---|---|
| Foam A | 15°C, 250 mbar | 92.0 | 91.7 |
| Foam A | 15°C, 250 mbar | 91.5 | |
| Foam A | 20°C, 300 mbar | 91.9 | 92.7 |
| Foam A | 20°C, 300 mbar | 93.6 | |

## 4.2.1.4 Shrinkage in polyester

Shrinkage in the polyester resin after curing is considered as the second main problem in producing dense composites using vacuum assisted infiltration process. In practise, the polyester resin, which may vary from a very highly viscous liquid to a brittle solid depending upon composition, is mixed with a reactive diluent such as styrene. Because of its low price, compatibility, low viscosity and ease of use styrene is the preferred reactive diluent in general purpose resins.

According to the concentrations of catalyst and accelerator used, the resin will gel in any time from five minutes to several hours. Gelation will be followed by a rise in temperature. Gelation and the exothermic reaction are followed by hardening and the resin becomes rigid. Hardening is accompanied by substantial volume shrinkage (~8%) and for this reason polyester resins are used only infrequently for casting purposes.

During the curing of the polyester resin, the volatile content, i.e basically the diluent for the resin, styrene (loss of monomer by evaporation) is lost, which usually leads to shrinkage of the cured material. A higher volatile content usually leads to higher % shrinkage. However, 6-8% shrinkage can usually be observed in cured unsaturated polyester resin. The Crystic 471PALV polyester resin used in the infiltration trials has 42% volatile content in liquid resin, which could be considered as high volatile content present in the resin resulting in the high shrinkage of the infiltrated samples.

## 4.2.1.5  Closed porosity/unfilled cells

Apart from gas entrapment and shrinkage in the polyester resin, the third type of porosity which exists on a fine scale (small fraction) could be due to closed porosity and this exists on a macroscopic scale. To overcome this problem, instead of using negative pressure an infiltration under positive pressure, like pressure casting, may yield better results due to the effect of solidification under load.

## 4.2.2 Infiltration trials with no vacuum and with low vacuum

The infiltration of ceramic preforms with polyester resin in the vacuum assisted (negative pressure) process resulted in gas entrapment problems. Even after trying to pour in several ways, using gentle and thorough mixing of the resin and catalyst did not result in complete elimination of these problems. It could be the suction process of the system and exothermic polymerisation reaction causing the entrapment problems. It was decided to investigate whether it is possible to infiltrate without the supply of vacuum or whether better infiltration could be achieved just with low suction vacuum.

In the experiment, the polyester resin was poured on top of a ceramic foam disk 49 mm in diameter. The sample was infiltrated by capillary and gravity forces to a depth of about 5-6 mm. It was assumed that the infiltration depth could be increased if the geltime was increased but would not be suitable to obtain the sound composites with larger dimensions. This also showed that small parts of ceramic foams can be infiltrated without the assistance of pressure or vacuum but that is not suitable for larger parts. The fact that the resin is sucked into the pores of the foam showed further that there is no difficulty in wetting the ceramic with polyester resin. If there were high surface tensions, like with the liquid metals, the resin would not have entered and contacted the ceramic. The reverse is true. The wettability is very good to achieve spontaneous infiltration up to a defined depth. This is due to the hydrophilic character of the resins. The infiltration depth can be further increased by additional gravity force. A series of experiments were carried out at increasing values of suction vacuum to get an idea of whether it could be possible to get better infiltration at low suction vacuum. Table 4.9 gives % achieved density values for low vacuum infiltration trials. From Table 4.9, it can be observed that complete infiltration is not possible with a low suction vacuum system. The % achieved density of the composites for 100 mbar of suction vacuum lies between 76-82%. An increase in another 100 mbar suction vacuum (200 mbar) resulted in better infiltration and 10% increase in % achieved density of the composites. From the matrix of experiments, the highest % density achieved was above 92% and at a suction vacuum of 300 mbar pressure. All these experiments suggest vacuum or pressure need to be high enough to drive the resin in to the windows of the preform structure. Too low a pressure results in incomplete densification and too high a pressure would cause the resin to be pulled out of the preform.

Table 4.9: % density values for no / low vacuum infiltration trials.

| Sample | Specifications | Suction Vacuum | Observations / % density of composites |
|---|---|---|---|
| Foam B | 14Al630(800) | NO | Resin passed up to 5-6 mm in depth |
| Foam E | 11Al530(900) | NO | As above. |
| Foam B | 14Al630(800) | 100 mbar | 81.8 |
| Foam B | 14Al630(800) | 100 mbar | 78.8 |
| Foam E | 11Al530(900) | 100 mbar | 76.6 |
| Foam A | 20Al380(400) | 150 mbar | 91.8 |
| Foam A | 20Al380(400) | 200 mbar | 87.9 |

* All the experiments were conducted at a temperature of 20 ($\pm$1)°C and $\pm$10 mbar of suction vacuum.

For the next infiltration trials an optimum amount of positive pressure needed to be applied to compress and fill the micropores in the preform that had not been filled by the previous vacuum assisted process, and also the amount of pressure that was applied should compress the trapped air bubbles. It was important to solidify under considerable amount of high pressure to avoid the shrinkage of the resin.

All these factors suggest infiltration by using a pressure assisted process would be expected to avoid all the difficulties in the vacuum assisted process. Pressures in the range of 100 MPa are typical for squeeze casting type experiments whereas a gas infiltration setup usually works in the range of 10-30 MPa. In the case of infiltrating ceramic foams with polymer, however it could be possible that a very low pressure starting with 1 bar or more is needed.

## 4.2.3 Pressure infiltration

For the first infiltration trials, a crude piston was designed to push the resin down by applying pressure by hand and the same prototype used for vacuum trials was used with two pistons in it. The height of the PVC tube was reduced to half and two pistons were arranged in such a way that the bottom one would be stationary and the top piston moved up and down. The bottom piston was designed to have a small hole in the centre to let the air escape when pressure was applied from the top. First trial was performed by applying pressure by hand just to check whether it yielded better results. The achieved density of the composite was measured as 93.2%.

For the next infiltration trials the Lloyd's Hydraulic Press with a load cell of 2.5 kN and newly designed steel die with air vents was used to apply the pressure. Two trials were conducted with two different infiltration velocities. The first infiltration was carried at a slow rate of 2 mm/min displacement and the second one at a fast rate of 10 mm/min and the samples were examined using light microscope. During the first trial the resin did not reach the bottom surface of the preform because of the low speed and was solidified. During second trial at a faster rate the resin passed through the preform and could be observed at the bottom surface. The maximum load applied was 234 N for both the trials.



( a )                                ( b )
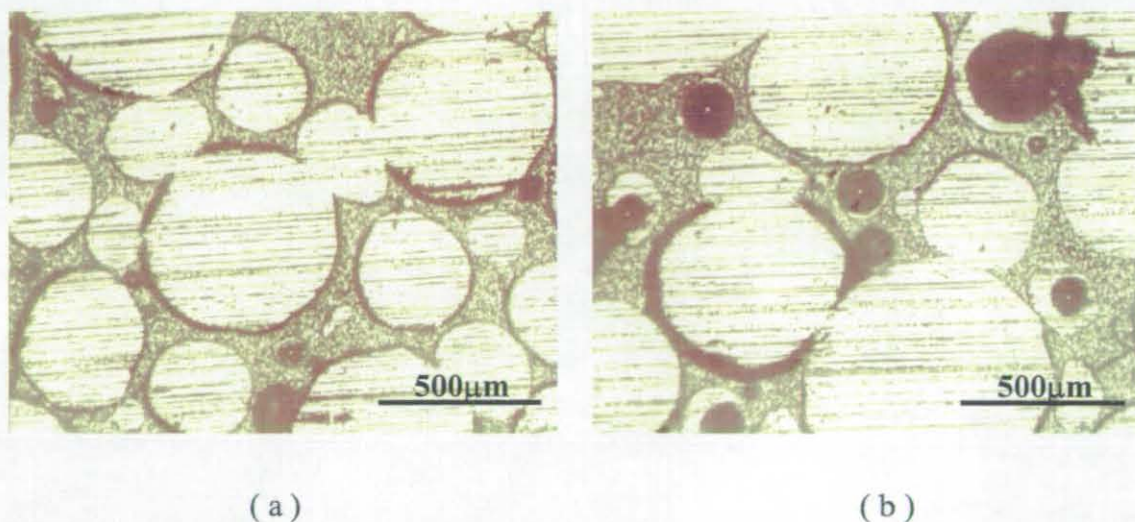
Figure 4.12: Light microscope images of the alumina foam with a mean cell size of 465 μm infiltrated with polyester resin under positive pressure. Magnification: 100 times

Figure 4.12 show the infiltration quality of the sample infiltrated at the faster rate. The achieved density of the sample was measured to be 94.6%. Polymer infiltration trials with positive pressure showed improved infiltration quality and reduced gas entrapment compared to infiltration under negative pressure. There are some tiny air bubbles entrapped in the resin but these could be eliminated with an increase in pressure. The shrinkage is clearly visible in the above pictures. For next infiltration trails, a low styrene content polyester resin was used to see whether the shrinkage could be eliminated.
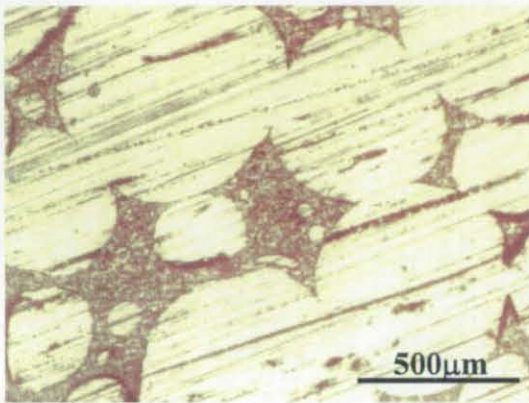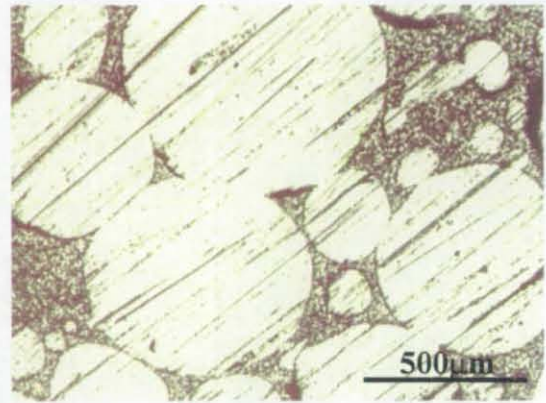


( a )  ( b )
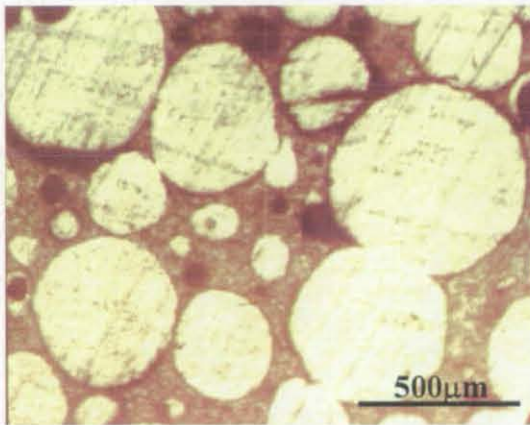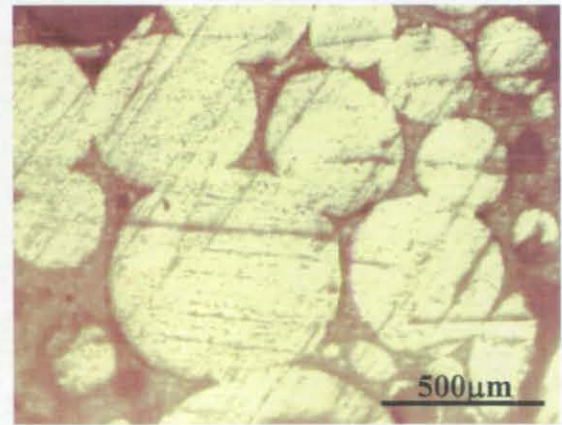


( c )  ( b )

Figure 4.13: Light microscope images of the alumina foam with a mean cell size of 465 μm infiltrated with low styrene content resin under positive pressure. Magnification: 100 times

The infiltration under positive pressure and with low styrene content polyester resin completely eliminated the problem of shrinkage of polyester in the composites. The light microscopy images prove the same point, figure 4.13. There is no peak temperature observed with the low styrene content resin. The low volatile content of the resin resulted in less or no shrinkage in the composite samples. The achieved density was measured to be 95.9% and is the highest density achieved across all the trials. There were a few tiny cells left unfilled. These may have been due to closed porosity of the preform on a macroscopic level or the pressure applied might not have been sufficient to fill the low-volume pores of submicron diameter.

An example of the effect of negative and positive pressures on the microstructure of an alumina-polyester composite is clearly shown in figures 4.7&4.8 (negative pressure infiltration) and in figure 4.13 (positive pressure infiltration). By comparing the microstructure of both the processes, it can be seen that the applied positive pressure process has produced a very fine grained and defect-free structure.

In summary, polymer infiltration trails with positive pressure showed improved infiltration quality. Greater than 95% density was achieved. It reduced the shrinkage of the resin and entrapment problems. Uniform distribution of pressure during the infiltration, a properly designed die to let the air to escape and subsequent optimisation of the process parameters would help in producing sound composites with higher densities.

## 4.2.3.1 Process parameters for the pressure infiltration process

A number of important parameters have been identified in the positive pressure infiltration process. These are (i) room temperature, (ii) applied pressure, (iii) duration of applied pressure and (iv) infiltration speed.

(i) Room temperature

Room temperature has significant effect on all other variables in the infiltration process. Small change in the room temperature could change the resin viscosity and alter the gel-time or setting time of the resin system. High room temperatures lead to faster setting time of the resin system, whereas too low a temperature results in longer setting times. Proper temperature control and accurate temperature measurement would result in better control of infiltration parameters.

(ii) Applied pressure

As observed in the infiltration process applied pressure has a significant effect on the microstructure and mechanical properties of the resulting composites. The pressure applied must be sufficient to overcome the shrinkage and gas entrapment by forcing the resin through ceramic preforms. Too high a pressure could expel the resin from the die cavity and push the resin out of the preform. On the other end too low a pressure could result in gas porosity and high shrinkage due to premature solidification.

(iii) Duration of applied pressure

Pressure duration depends on material use, dimensions of preform or casting, room temperature and resin viscosity and/or gel-time. One second per millimetre of perform thickness was considered as being sufficient to ensure setting of the resin under pressure and resulted in better infiltration in the above trails.

(iv) Infiltration speed

In the above trials, a speed of 2 mm/min did not allow resin to pass through the preform and the resin solidified after reaching half of the infiltration length. A speed of 10 mm/min resulted in complete solidification and avoided the gas porosity which in turn resulted in the highest % density of the composite materials. This could vary a greater extent for the other resin systems.

## 4.2.4 Charpy impact test

The results of charpy impact test are given in Table 4.10. There were always a few tests necessary to adjust the equipment with the right pendulum, to ensure that the results were lying inbetween the measurable range. These tests are not included in the table because it would distort the result.

It can be seen from the table that the calculated impact strengths of the different materials are relatively close together. Therefore the results seem to be reliable and may give a first impression of the impact resistance of the materials.

Table 4.10: Results of Charpy impact test

| Sample | % Achieved density | Height / mm | Width / mm | Length / mm | Energy (absorbed) / Nm | Impact energy / kJm$^{-2}$ |
|---|---|---|---|---|---|---|
| Foam A | 92.9 | | | | | |
| 1 | | 8.67 | 5.72 | 47.39 | 0.03 | 0.6 |
| 2 | | 8.72 | 6.16 | 47.41 | 0.04 | 0.7 |
| 3 | | 8.02 | 6.11 | 45.22 | 0.03 | 0.6 |
| 4 | | 9.09 | 4.99 | 47.42 | 0.03 | 0.6 |
| 5 | | 7.36 | 6.17 | 47.40 | 0.04 | 0.9 |
| 6 | | 7.61 | 5.77 | 47.31 | 0.03 | 0.7 |
| 7 | | 7.45 | 5.11 | 47.42 | 0.03 | 0.7 |
| | | | | | | **0.7** |
| Foam A | 92.3 | | | | | |
| 1 | | 8.25 | 6.44 | 47.49 | 0.03 | 0.6 |
| 2 | | 8.50 | 5.75 | 47.53 | 0.03 | 0.6 |
| 3 | | 8.87 | 6.26 | 46.28 | 0.04 | 0.8 |
| 4 | | 8.49 | 5.66 | 47.10 | 0.04 | 0.8 |
| 5 | | 8.13 | 6.31 | 47.06 | 0.03 | 0.6 |
| 6 | | 8.58 | 6.49 | 46.05 | 0.04 | 0.7 |
| 7 | | 7.54 | 4.87 | 47.02 | 0.02 | 0.7 |
| | | | | | | **0.7** |
| Foam A | 89.8 | | | | | |
| 1 | | 7.87 | 6.94 | 42.29 | 0.03 | 0.5 |
| 2 | | 6.45 | 6.82 | 45.00 | 0.03 | 0.7 |
| 3 | | 7.60 | 6.31 | 47.00 | 0.03 | 0.6 |
| 4 | | 7.37 | 5.82 | 48.73 | 0.02 | 0.5 |
| 5 | | 7.04 | 5.86 | 47.77 | 0.03 | 0.6 |
| 6 | | 6.86 | 5.10 | 47.76 | 0.02 | 0.7 |
| 7 | | 7.48 | 6.53 | 48.15 | 0.03 | 0.6 |
| | | | | | | **0.6** |
| Foam A | 88.4 | | | | | |
| 1 | | 6.75 | 5.96 | 46.48 | 0.02 | 0.6 |
| 2 | | 6.44 | 5.95 | 49.17 | 0.02 | 0.5 |
| 3 | | 6.75 | 5.85 | 46.95 | 0.02 | 0.6 |
| 4 | | 7.80 | 5.68 | 46.48 | 0.03 | 0.7 |
| 5 | | 7.68 | 5.56 | 46.10 | 0.02 | 0.5 |
| 6 | | 7.75 | 5.65 | 44.57 | 0.02 | 0.5 |
| 7 | | 6.58 | 6.02 | 45.00 | 0.02 | 0.6 |
| | | | | | | **0.6** |
| Polyester | 97 | | | | | |
| 1 | | 7.60 | 7.18 | 50.69 | 0.44 | 8.1 |
| 2 | | 9.10 | 6.21 | 50.59 | 0.60 | 10.6 |
| 3 | | 10.04 | 5.59 | 50.65 | 0.68 | 12.1 |
| 4 | | 9.64 | 6.05 | 50.85 | 0.52 | 8.8 |
| 5 | | 8.75 | 4.61 | 50.43 | 0.47 | 11.8 |
| 6 | | 7.75 | 5.68 | 50.61 | 0.62 | 14.2 |
| 7 | | 7.58 | 5.80 | 50.55 | 0.58 | 13.3 |
| | | | | | | **11.1** |

First of all it can be seen that the impact strength of the pure polyester resin is much higher than the composites. The value of about 11.1 kJ m$^{-2}$ is about ten times higher than the value of the composites. This means that the ceramic material inside the polyester resin lowers the amount of energy that can be absorbed during fracture. Although the polyester resin is a brittle polymer the ceramic materials are much more brittle. Therefore the impact strength decreases with an increasing amount of ceramic material within the polyester. For comparison the following table gives the impact strength of some materials together with the results of the tests.

Table 4.11: Impact strength of different materials at room temperature [116,117].

| Material | Impact energy / kJm$^{-2}$ |
|---|---|
| Crystic 471 PALV polyester resin | 11.10 |
| Sintered alumina foam (380 μm) / polyester resin | 0.68 |
| Polyamid 6 | 25 |
| Polyamid 6 filled with 30wt% short glass fibres | 16 |
| PMMA | 15 |
| PS | 20 |
| Al-foam with a relative density of 0.19 | 7.75 |
| Al-foam with a relative density of 0.19 | 36.75 |
| Al-foam with a relative density of 0.19 | 61.25 |
| Al filled with hollow alumina spheres (φ 3.5 mm), relative density 0.6 | 28.25 |
| Mg filled with hollow alumina spheres (φ 3.5 mm), relative density 0.7 | 17.25 |

As can be seen from Table 4.11, the measured impact strength of the pure polyester resin is a little bit lower than the strength of the other given polymers polyamid 6, PMMA and PS. The polyester resin is a duroplastic polymer that is more brittle than the thermoplastic polymers. Therefore, the value of 11.1 kJ m$^{-2}$ seems to be realistic. It can be observed that the values of the ceramic foam/polyester composites are much lower than the values of the other materials. However, it should be noted that the values may be increased with optimised infiltration techniques and a variation of

142

the foam structure, material and the infiltration material. The values of the hollow alumina spheres filled with aluminium and magnesium, which are most comparable to metal infiltrated ceramics foams, let assume that the impact strength values of these infiltrated foams may be similar. This has to be investigated in further experiments. Generally, the composites based on the ceramic foams have the advantage that the energy absorption behaviour can be adjusted by changing the density, cell size and infiltration material. By doing this, the material could be adjusted to behave more like an ideal absorber that is characterised by a rectangular force-distance course. This means that the deformation force is constant over the whole deformation distance. Ceramic based impact materials could gain their advantage in the area where higher deformation forces are required, for example if the deformation distance is limited because of reduced space. To characterise the impact behaviour of infiltrated ceramic foams and to find out which structure and material combination will receive good results there is a need for a lot of further investigations.

## 4.2.5 Three-point bend test

The results of the three-point bend test are given in Table 4.12. For comparison, the bend strength of uninfiltrated ceramic foams produced by the same technique is given as 2 to 25 MPa [15]. The bending strength of dense alumina is about 410 MPa [118] and that of fully cured polyester resin is given as 68 MPa [101]. This means that the resin strengthens the ceramic foam, but that the values of the composite will never reach the values of the pure dense materials. The alumina/polyester composite has an average strength of 18 MPa. For comparison, the tensile strength of similar pure reticulated alumina foams is given by Sepulveda et al. [15] at about 10 MPa. This also shows the foam is strengthened by the polymer. The results of alumina/polyester composites therefore fit into the scheme that the resin strengthens the ceramic foam. The measured results provide a first impression of these composites. It is believed that the strength can be increased by optimising the ceramic microstructure and improving the quality of the infiltration to make sure that there are no bubbles, shrinkage in the resin and voids in the resin and the composite. Changing the ceramic and/or polymer material could also be a possible option.

Table 4.12: Results of Three-point bend test.

| Sample code | Density / kgm$^{-3}$ | Width / mm | Thickness / mm | Max. load / N | 3-Pt Bend strength / MPa | Increase % |
|---|---|---|---|---|---|---|
| Polyester | 1180 | | | | | |
| 1 | | 4.93 | 6.70 | 738.9 | 150 | |
| 2 | | 5.56 | 5.89 | 554.3 | 129 | |
| 3 | | 5.40 | 6.78 | 709.5 | 129 | |
| 4 | | 4.94 | 6.80 | 680.5 | 134 | |
| 5 | | 5.32 | 7.21 | 844.2 | 137 | |
| 6 | | 5.88 | 7.11 | 870.5 | 132 | |
| | | | | | **135** | |
| Foam A | 860 | | | | | |
| 1 | | 10.01 | 10.97 | 321.6 | 12 | |
| 2 | | 11.45 | 11.64 | 473.4 | 14 | |
| 3 | | 11.68 | 10.27 | 338.9 | 13 | |
| 4 | | 11.63 | 11.04 | 332.1 | 11 | |
| 5 | | 11.27 | 11.00 | 312.6 | 10 | |
| 6 | | 10.60 | 11.23 | 337.8 | 11 | |
| | | | | | **12** | |
| Composite | 1591 | | | | | |
| 1 | | 6.47 | 7.04 | 117.5 | 17 | 29 |
| 2 | | 6.13 | 6.44 | 87.36 | 16 | 24 |
| 3 | | 6.48 | 6.51 | 94.22 | 15 | 24 |
| 4 | | 6.41 | 6.31 | 86.68 | 15 | 23 |
| 5 | | 5.50 | 6.35 | 108.7 | 22 | 47 |
| 6 | | 5.46 | 6.21 | 96.51 | 21 | 43 |
| | | | | | **18** | **32** |
| Composite | 1605 | | | | | |
| 1 | | 5.40 | 7.22 | 118.60 | 19 | 38 |
| 2 | | 5.45 | 6.23 | 88.12 | 19 | 37 |
| 3 | | 6.08 | 6.98 | 124.70 | 19 | 38 |
| 4 | | 6.12 | 6.66 | 101.90 | 17 | 31 |
| 5 | | 4.73 | 6.51 | 86.59 | 19 | 40 |
| 6 | | 4.64 | 7.12 | 92.70 | 18 | 34 |
| | | | | | **18** | **36** |
| Composite | 1547 | | | | | |
| 1 | | 6.38 | 7.10 | 120.50 | 17 | 30 |
| 2 | | 5.70 | 5.90 | 67.40 | 15 | 23 |
| 3 | | 5.97 | 6.48 | 94.60 | 17 | 31 |
| 4 | | 6.99 | 7.08 | 129.30 | 17 | 29 |
| 5 | | 6.66 | 6.81 | 121.30 | 18 | 34 |
| 6 | | 6.34 | 6.49 | 100.70 | 17 | 31 |
| | | | | | **16** | **25** |
| Composite | 1515 | | | | | |
| 1 | | 5.70 | 5.90 | 67.40 | 15 | 23 |
| 2 | | 5.40 | 6.31 | 108.30 | 23 | 48 |
| 3 | | 6.12 | 6.66 | 101.90 | 17 | 31 |
| 4 | | 4.89 | 6.55 | 81.25 | 17 | 33 |
| 5 | | 5.11 | 5.37 | 39.67 | 12 | 3 |
| 6 | | 6.30 | 6.52 | 102.80 | 17 | 32 |
| | | | | | **16** | **14** |

## 4.2.6  Al$_2$O$_3$ - Polyvinylidene fluoride (PVDF) infiltration trails

The preparation of solution of Kynar$^{\circledR}$ PVDF resin was explained in chapter 3 (see section 3.2.1.4.3). The Kynar$^{\circledR}$ PVDF resin solution with 20% by weight of solid content was poured on top of the alumina preform several times; pouring was stopped when it passed through the bottom of the preform. The preform sample was placed in an oven at a temperature of 130°C for 10 min to drain out the solvent. This whole procedure was repeated 4-5 times to fill the preform completely. After this the sample was taken out of the oven and the quality of infiltration was examined.

Experiments showed that the viscosity of the resin with only 20% by weight of solid content was too low and easily passed through the preform and the presence of porosity was observed. A series of experiments with increasing solid content are recommended for future work to estimate the correct proportion of solid content required to yield a viscosity that compares favourably with that of the polyester and could lead to a better infiltration quality of the alumina-polyvinylidene fluoride composites.

## 4.3  Metal infiltration trials

### 4.3.1 Infiltration procedures

During squeeze infiltration trials the molten metal was poured into the mould on top of the ceramic preform and pressure was applied to create the infiltration. To get a basic understanding of the effects of preheating temperature of preforms, pouring temperature and squeeze pressure applied, different sets of experiments were carried out; Table 4.13 summarises the conditions of each set of experiments and quality of infiltration.

All the experiments were carried out with alumina foams with varying cell, window size and % porosity using squeeze casting equipment. Before doing the first experiments there were many break downs and technical problems with the squeeze casting equipment. New tools for the entire die solved most of the technical problems.

145

The first experiment was carried out in a series of sessions. The first experiment was carried out with two alumina foams, one with a mean cell size of 381 μm, 20% dense and the other 13% dense with a mean cell size of 509 μm. The first trial to infiltrate the alumina foams with the LM25 aluminium alloy was successful. The processing parameters used for infiltrating the first preform were: molten metal temperature 720°C, squeeze pressure applied 175 kg/cm$^2$ and a preheating temperature of 1000°C. The first preform infiltrated successfully but another preform with the same specifications was partially crushed at the bottom surface. The preform with a mean cell size of 509 μm was infiltrated successfully without any crushing. The metal temperature used for infiltrating the above preform was measured as 741°C. No attempt was made to infiltrate any preforms further and it was decided to section the sample already made before continuing. After the samples were cut through the middle along their axis, it could be seen that they were infiltrated completely with the aluminium-silicon alloy from top to the bottom surface. For the second infiltration trials, 13% dense alumina preform with a mean cell size of 649 μm, a metal temperature of 756°C, squeeze pressure of 175 kg/cm$^2$ and the preheating temperature the same as before (1000°C) was used. Up to five preforms with the same specifications were infiltrated successfully in which one was crushed at the bottom surface and the equipment was broken during removal of fifth sample.

For further trials, 15% dense alumina preforms with a mean cell size of 489 μm, a metal temperature of 743°C and same squeeze pressure, preheating temperature as before were used. Eight out of nine preforms with the same specifications were infiltrated successfully without any difficulty but one was crushed at the bottom surface. Another two alumina performs, 13% dense with a mean cell size of 643 μm, were infiltrated successfully with the same processing parameters.

For the third infiltration trials, 20% dense alumina preforms (which have the same specification as the ones in first trials but were picked from a different batch) with a mean cell size of 381 μm, a metal temperature of 800°C, squeeze pressure of 175 kg/cm$^2$ were used. The first sample was infiltrated successfully but the diaphragm broke while trying to infiltrate the second sample. After repairing, hydraulic valves were out of sequence and hence the next sample was not infiltrated. Squeeze pressure was then increased to 185 kg/cm$^2$. 15 preforms with the same specifications were infiltrated, but 10 preforms out of 15 were crushed at the bottom surface and another

three preforms partially crushed at the bottom surface. It was assumed that the reason for crushing could be the amount of squeeze pressure applied was too high or the preform did not fit the die dimensions (This was due to the damage caused to the die during previous investigations. The die was re machined and the dimensions of the die were increased further).

For the next infiltration trials the performs used were with new dimensions which exactly fitted to the die, 11% dense alumina preform with a mean cell size of 532 $\mu$m, the squeeze pressure was reduced to 160 kg/cm$^2$, a metal temperature of 823°C, and a preheating temperature of 1000°C was used. Five out of five preforms with the same specifications and with the above processing parameters were infiltrated successfully with out any crushing or any other processing difficulties. It could be assumed that the low pressure and using preforms which fits to the die dimensions resulted in better infiltration trials and avoided the problem of crushing.

Table 4.13: The conditions of each set of experiments and the quality of infiltration.

| No. | Variables | | Constant | Remarks |
|---|---|---|---|---|
| First trials | Metal temperature | 720°C | Preheating temperature 1000°C Squeeze pressure 175 kg/cm$^2$ | Partially crushed |
| | | 741°C | | Good |
| | | 756°C | | Partially crushed |
| | | 743°C | | Good |
| Second trials | Squeeze pressure 185 kg/cm$^2$ Metal temperature 800°C | | Preheating temperature 1000°C | Crushed at the bottom surface. |
| | Squeeze pressure 165 kg/cm$^2$ Metal temperature 715°C | | Preheating temperature 1000°C | Slightly crushed on the corner at the bottom surface |
| · | Squeeze pressure 173 kg/cm$^2$ Metal temperature 793°C | | Preheating temperature 1000°C | Crushed at the bottom surface |
| Third trials | Metal temperature | 823°C | Preheating temperature 1000°C Squeeze pressure 160 kg/cm$^2$ | Good |
| | | 815°C | | Good |
| | | 803°C | | Good |

The set of experiments in Table 4.13 suggests that the squeeze pressure has a strong influence on the infiltration process. When the squeeze pressure was >165 kg/cm$^2$, the performs were found to be crushed. The squeeze pressure level of 160 kg/cm$^2$, pouring temperature of 803-825°C and at a preheating temperature of 1000°C have shown better infiltration and could be considered as suitable conditions for infiltration. This suggests that pressure needs to be high enough to drive molten Al in to the windows, while too high a pressure causes crushing of the preform or causes the molten metal to pass through the preform completely. Better results could be achieved at the pressure of 160 kg/cm$^2$.

### 4.3.2  SEM analysis of the composite samples

The successful infiltration of preform samples by using squeeze infiltration technique and after the first visual examination the samples were sliced, mounted, ground and polished. To get information of the microstructure of the resulting composites and the contact area between the ceramic material and the aluminium-silicon alloy, polished samples of the metal-ceramic composites were subjected to examination under an SEM-microscope. Figures 4.14-1 to 4.14-6 shows an overview of the LM25 aluminium-silicon infiltrated alumina foams with different mean cell sizes.
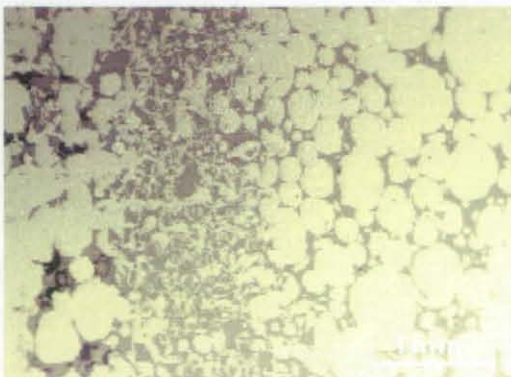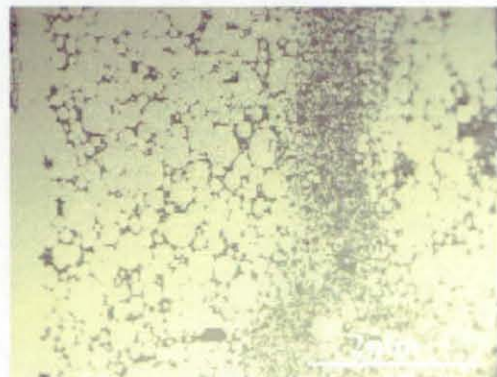


| Figure 4.14-1 | Figure 4.14-2 |

Figure 4.14-1 & 2 SEM image of LM25 aluminium-silicon alloy infiltrated alumina foam with the mean cell sizes of 509 μm (left) and 643 μm (right); magnification: left 30 times, right 10 times.
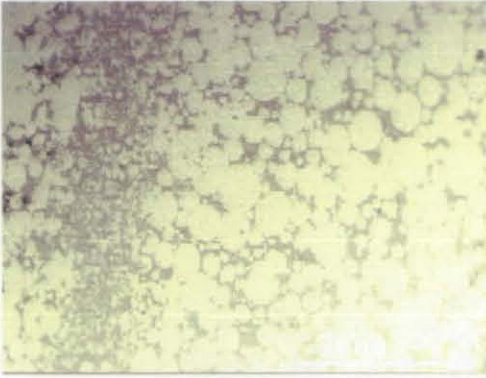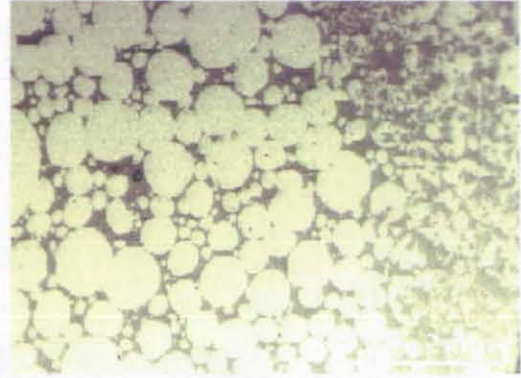
| Figure 4.14-3 | Figure 4.14-4 |

Figure 4.14-3 & 4: SEM image of LM25 aluminium-silicon alloy infiltrated alumina foam with the mean cell sizes of 489 µm (left) and 622 µm (right); magnification: 10 times.
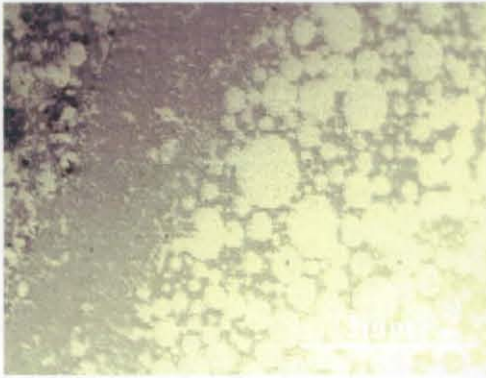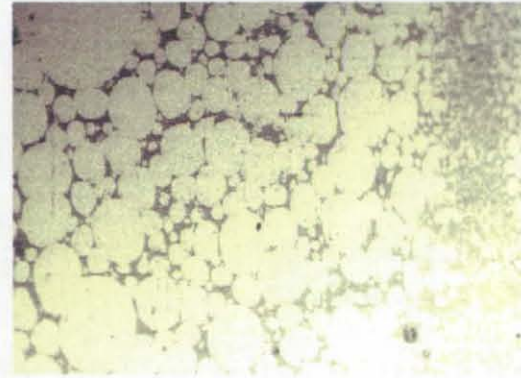


| Figure 4.14-5 | Figures 4.14-6 |

Figure 4.14-5 & 6: SEM image of LM25 aluminium-silicon alloy infiltrated alumina foam with the mean cell sizes of 488 µm (left) and 532 µm (right); magnification: 10 times.

The direction of infiltration is from left to right. All preforms shown above are infiltrated satisfactorily from top to the bottom, in other words the melt has passed through the interconnected network of cells. But it is clearly visible in all the above SEM images there is layer of entrapment which occurred at various locations. In some of the preforms it starts near to the infiltration surface, half-way to the infiltration surfaces and also far from the infiltration surface. For instance in squeeze infiltration technique, apart from the liquid phase, such as a molten metal, has a zero wetting angle with the preform material, an external pressure needs to be applied to force the liquid into the preform. Under the applied pressure, crushing or breaking up of the preform

may occur that, in turn, changes the size distribution of the remaining cells and thereby alters the penetration rate constant.

## 4.3.3 Density measurements

Table 4.14: Density measurements of composite samples.

| Density of Composite Samples | | | | |
|---|---|---|---|---|
| Sample code | Preform porosity / % | Density of composites / $kg/m^3$ | Theoretical density of composites / $kg/m^3$ | Achieved density / % |
| 20Al400 | 80 | 2872 | 2933 | 98 |
| 20Al400 | 78 | 2749 | 2885 | 95 |
| 20Al300 | 78 | 2857 | 2892 | 99 |
| 20Al300 | 77 | 2778 | 2870 | 97 |
| 13Al1mm | 87 | 2735 | 2851 | 96 |
| 13Al1mm | 87 | 2869 | 2858 | 100 |
| 13Al1mm | 87 | 2684 | 2854 | 94 |
| 13Al1mm | 86 | 2764 | 2836 | 97 |
| 13Al1mm | 88 | 2815 | 2869 | 98 |
| 13Al400 | 87 | 2842 | 2857 | 99 |
| 13Al400 | 87 | 2741 | 2857 | 96 |
| 13Al400 | 87 | 2717 | 2858 | 95 |
| 13Al400 | 87 | 2747 | 2838 | 97 |
| 13Al500 | 87 | 2788 | 2839 | 98 |
| 13Al500 | 87 | 2803 | 2840 | 99 |
| 15Al500 | 84 | 2757 | 2849 | 97 |
| 15Al500 | 84 | 2767 | 2856 | 97 |
| 20Al700 | 81 | 2857 | 2965 | 96 |
| 20Al700 | 80 | 2887 | 2949 | 98 |
| 17Al800 | 83 | 2803 | 2895 | 97 |
| 17Al800 | 82 | 2845 | 2874 | 99 |

Table 4.14 shows the calculated densities of the composites produced. As can be seen the calculated densities of each composite shows little variation. This suggests that the infiltration quality could be similar all over the sample. For comparison, in Table 4.14 there are theoretical densities of the different composites given. The theoretical density is calculated from the density of the two components in relation to the porosity of the ceramic foam. As can be seen, the theoretical densities are always a little bit higher than the measured ones except one particular composite which has shown 100% theoretical density. This means that most of the composite materials are not completely dense and there are unfilled pores. The SEM images of the materials confirmed this behaviour.

## 4.3.4 Hardness measurement results

The resulting composites have shown up to 44% increase in hardness when compared with the component alloy. The results of hardness tests are given in Table 4.15.

Table 4.15: Hardness measurement results.

| Vickers Hardness (HV30 - 30 kg load) | | |
|---|---|---|
| Sample code | HV VK | % Increase in hardness |
| 20Al400 | 94 | 36 |
| 20Al300 | 92 | 35 |
| 13Al1mm | 78 | 23 |
| 13Al500 | 99 | 39 |
| 17Al400 | 107 | 44 |
| 17Al800 | 98 | 39 |
| 20Al700 | 93 | 35 |
| 15Al500 | 76 | 21 |
| 11Al900 | 100 | 40 |
| 11Al1mm | 95 | 37 |
| 13Al400 | 91 | 34 |

# CHAPTER 5:

# CONCLUSIONS

The development of interpenetrating composites is a logical and inevitable step in the continuing evolution of materials that began with the fabrication of the first particulate composites. The typical structure of these 3-3 connected composites enables the combination of completely different phases with their own properties put together to form a new material with multi functional properties. For example, a ceramic phase could serve as the load-bearing structure whilst a metal phase could serve as electrical conductor, or a piezoelectric ceramic phase could be the functional part whilst a polymer phase could serve as isolator or provide flexibility.

The primary aim involved in this research was to learn how to infiltrate the ceramic foams successfully with one polymer and one alloy and optimise the processing conditions, investigating the effect of the structure and properties of the ceramic foams, i.e. cell size and density, on the vacuum/pressure assisted infiltration parameters (polymer viscosity, gel time, temperature, etc.) and squeeze infiltration parameters (pressure, temperature, molten metal viscosity, preform preheating temperature, etc.).

The $BaTiO_3$ foams were produced by mechanically agitating ceramic aqueous suspensions to entrain gases and then setting the structure via the *in-situ* polymerisation of organic monomers. This resulted in the foams having a very open and interconnected structure that should be easily infiltrated by using a simple low pressure system. The main aim of producing these foams was to infiltrate with polyvinylidenefluoride resin and to measure the piezoelectric properties of the $BaTiO_3$-PVDF composites. The sintering process resulted in complete cracking of the $BaTiO_3$ foams. The results of TGA and XRD indicate that neither residual polymer nor a phase transition appears to be the cause. The reason for the cracking was not determined and further experiments would be needed. On the basis of the results, however, no further work was done on the infiltration of these foams with any of the polymers.

Ceramic-polymer interpenetrating composites were successfully produced by infiltrating alumina foams with polyester resins using a simple, low pressure system. Both positive and negative pressures have been investigated. The main problem of the

process whilst using negative pressure was the entrapment of gas within the polymer system. The high shrinkage and high temperature due to the exothermic curing reaction caused problems with voids in the polymer phase.

The infiltration of ceramic foams with polymer resins was observed to be much easier compared to the metal infiltration. The wetting of the ceramic by the resins was not a problem. This could be shown by the spontaneous infiltration of all the different foams, irrespective of cell size, at atmospheric conditions. The infiltration depth could be increased by the use of a positive pressure infiltration process.

It was shown that suitable design of the die with air vents to let the gas escape yielded higher final densities. A suitable polymer squeeze casting process was developed for the positive pressure infiltration trials. To date, ceramic-polymer composites of >95% theoretical density have been produced and it is expected that this can be improved further as the processing is increasingly optimised. The resulting composites have been characterised by the light and fluorescence microscopy techniques followed by mechanical testing.

Some initial mechanical characterisation of the polymer/ceramic foam composites could be achieved by the charpy impact test, and the three-point bend test, see section 4.2.5. The bend strength of the composites was between 15 and 18 MPa. For comparison, the tensile strength of similar pure reticulated alumina foams was given by Sepulveda et al. [15] to be about 10 MPa. This shows that the foam is generally strengthened by the polymer, especially if it is taken into account that these results were achieved with out fully optimised processing parameters in the infiltration trials. It is believed that the strength can be increased by optimising the ceramic microstructure and improving the quality of the infiltration to make sure that there is no gas entrapment and voids in the resin and in the composite. Changing the ceramic and/or polymer material is also a possible option.

The impact strength of the composites was about ten times lower than the impact strength of the pure polyester resin and with values around 1 kJ m$^{-2}$ are not very high. For comparison, the impact strength of polyamid 6 filled with 30 wt.% short glass fibres was about 16 kJ m$^{-2}$ [116] and the impact strength of an Al-foam with a relative density of 0.19 was about 7.75 kJ m$^{-2}$ [117]. It can be seen that the values of the alumina foam/polyester composite are much lower than the values of other materials. However, it has again to be taken into account that the results were obtained with not

fully optimised processing parameters and a variation of the structure and change of infiltration material could improve the results.

Experiments with PVDF showed that the viscosity of the resin with only 20% by weight solid contents was too low and easily passed through the foam and the presence of porosity was observed in the alumina-polyvinylidenefluoride infiltrated composite. A series of experiments with increasing solid content are recommended for future work to estimate the correct proportion of solid content required to yield a viscosity that compares favourably with that of the polyester and could lead to a better infiltration quality of the alumina-polyvinylidenefluoride composites.

With the metal/ceramic composites the main problem in the production is the wettability of ceramic materials by liquid metals and pressure entrapment at various stages during infiltration. With the optimisation of the squeeze infiltration parameters it might be possible to receive much better infiltration qualities and sound composites. The mechanical evaluation and microstructure of the produced composites revealed some useful information. The pressure used in the squeeze casting trials was very high; values in the range of 100-150 MPa were required. Whilst this resulted in successful infiltration with molten alloy, it also resulted in crushing of the preform.

# CHAPTER 6:

# FUTURE WORK

The literature survey outlined the high potential for ceramic/polymer and ceramic/metal composites. The special interest in three-dimensional interpenetrating phase composites could also be shown. The examples that were presented proved the possibility to use ceramic foams as reinforcement within composite materials. A lot of further applications are conceivable with ceramic foams used as a reinforcement, load bearing structure and functional phase, e.g. piezoelectric composites. It would be desirable to produce, characterise and optimise composites for each of the possible applications outlined to determine commercial opportunities. Especially for the ceramic foam/polymer and/or metal composites more combinations of different ceramics and some further special resin systems/alloys should be evaluated. The variation of the pressure, the melt temperature, the die temperature and the preform temperature for metal infiltration must also be examined. The infiltration of fibre preforms is well established in the industry and the problems of shrinkage, voids and by-products of the curing reactions are under control. The variation of pressure, melt viscosity and preform dimensions must also be examined. As mentioned before, few experiments could be sufficient enough to find out these relevant parameters for the respective use. Therefore, it could be possible to infiltrate ceramic foams with optimised parameters and production techniques, such as pressure casting or squeeze infiltration. Sound ceramic/polymer foam composites are producible by replacing fibre preforms and adjusting the right parameters.

Once each of the composite materials has been optimised for the different application, more basic properties and parameters, e.g. strength, wear resistance, thermal expansion coefficient, must be investigated to receive detailed information about the resulting composites and to outline the benefits of these materials. For example, to produce piezoelectric composites some piezoelectric foams (like $BaTiO_3$ and PZT)must initially be produced without any processing difficulties and then infiltrated with suitable polymers. Measurements can then be performed to determine

the composites piezoelectric properties. Ultimately, prototypes need to be produced for the more promising commercial applications.

All in all there is a lot of further research that has to be done until these kind of composites could be used for the first applications. However, this investigation revealed the high potential for ceramic foams used in combination with polymer and metal matrix composites and above all interesting structure of the three-dimensional interpenetrating composites.

Future work should mainly focus on the following objectives:

> The reason for cracking of the $BaTiO_3$ needs to be determined.
> Find a suitable route for infiltrating $BaTiO_3$ foams with PVDF resin.
> Optimise the processing parameters.
> Perform piezoelectric property testing and mechanical testing of resulting composites.
> Evaluate other preform materials, e.g. PZT, spinel, SiC.
> Evaluate the ease of ceramic-polymer composite production with complex shapes.
> Investigate opportunities for selective reinforcement of engineering components.

# REFERENCES

[1] http://www.compositesatlantic.com/pdf/vol1_2.pdf

[2] K. K. Chawla, *"Ceramic Matrix Composites"*, Chapman & Hall, London, UK, 1993, pp. 1-3.

[3] T-W. Chou, R. L. McCullough, R. B. Pipes, *"Composites"*, Scientific American, 255, 4, pp. 167-177, 1986.

[4] B. Harris, *"Engineering Composite Materials"*, IOM Communications Ltd, London, UK, 1999.

[5] R. E. Newnham, D. P. Skinner, L. E. Cross, *"Connectivity and Piezoelectric-Pyroelectric Composites"*, Materials Research Bulletin, 13, pp. 525-536, 1978.

[6] D. R. Clarke, *"Interpenetrating Phase Composites"*, Journal of the American Ceramic Society, 75, 4, pp. 739-759, 1992.

[7] S. R. Broadbent and J. M. Hammersley, *"Percolation Processes. I, Crystals and Mazes"*, Proc. Cambridge Philos. Soc., 53, 629, 1957.

[8] R. Zallen, "The Physics of Amorphous Solids", Wiley, New York, 1983.

[9] S. Kirkpatrick, *"Percolation and Conduction"*, Rev. Mod. Phys., 1973, 45 [4], pp. 574-588.

[10] http://www.soilmoisture.com/ceramics.html.

[11] K. Schwartzwalder, A. V. Somers, *"Method of Making Porous Ceramic Articles"*, US Pat. No. 3 090 094, 1963.

[12] http://www.keram.se/eng/pdf/Porous%20ceramics.pdf.

[13] E. A. Barringer and H. K. Bowen, *"Formation, Packing, and Sintering of Monodisperse TiO₂ Powders"*, J. Am. Ceram. Soc., 65 [12], C-199-C-201, 1982.

[14] F. F. Lange, "Powder Processing Science and Technology for Increased Reliability", J. Am. Ceram. Soc., 72[1] 3-15, 1989.

[15] P. Sepulveda, J. G. P. Binner, *"Processing of Cellular Ceramics by Foaming and in situ Polymerisation of Organic Monomers"*, Journal of European Ceramic Society, 1999, 19, pp. 2059-2066.

[16] Dytech Corporation LtD, Sheffield, UK, *"Porous Articles"*, International Patent, WO 93/04013, 1992.

[17]   K. Schwartzwalder, A. V. Somers, *"Method of Making Porous Ceramic Articles"*, US Pat. No. 3 090 094, 1963.

[18]   Foseco International Ltd., Birmingham, UK, *"Verfahren zur Herstellung von porosen keramischen Materialien"*, Deutsches Patentamt, DE 2 301 662, 1973.

[19]   Schweizerische Aluminium AG, CH-3965, *"Chippis Keramischer Schaum und Verfahren zu dessen Herstellung"*, Europaisches Patentamt, EP 0 341 203, 1989.

[20]   A. J. Sherman, R. H. Tuffias, R. B. Kaplan, *"Refractory Ceramic Foams: A Novel, New High-Temperature Structure"*, American Ceramic Society Bulletin, 1991, 70, 6, pp. 1025-1029.

[21]   H. R. Maier, C. E. Scott, W. P. Minnear, *"Verfahren zur Herstellung poroser keramischer Strukturen, Deutsches Patentamt"*, DE 196 05 149, 1997.

[22]   E. J. A. E. Williams, J. R. G. Evans, *"Expanded ceramic foam"*, Journal of Material Science, 1996, 31, pp. 559-563.

[23]   C. Tuck, J. R. G. Evans, *"Porous ceramics prepared from aqueous foams"*, Journal of Material Science Letters, 1999, 18, pp. 1003-1005.

[24]   E. Sundermann and J. Viedt, *"Method of Manufacturing Ceramic Foam Bodies"*, U. S. Pat. No. 3 745 201, July 10, 1973.

[25]   L. L.Wood, P. Messina, and K. Frisch, *"Method of Preparing Porous Ceramic Strucutres by Firing a Polyurethane Foam that is Impregnated with Organic Material"*, U. S. Pat. No. 3 833 386, Sept.3, 1974.

[26]   H. Motoki, *"Process for Preparing a Foamed Body"*, U. S. Pat. No. 4 084 980, Apr. 18, 1978.

[27]   G. Jackson and W. Meredith, *"Inorganic Foams"*, U. S. Pat. No. 4 547 469, Oct. 15, 1985.

[28]   H. Nakajima, T. Ito, and Y. Muragachi, *"Alumina Porous Body and Production of the Same"*, U. S. Pat. No. 4 965 230, Oct. 23, 1990.

[29]   T. Meek, R. Blake, and T. Gregory, *"Low-Density Inorganic Foams Fabricated Using Microwaves"*, Ceram. Eng. Sci. Proc., 6 [7-8] 1161-70 (1985).

[30]   High Performance Composites Source Book 2001, Ray Publishing, www.hpcomposites.com.

[31]   http://www.spsystems.com/pdfs/SP%20Guide%20to%20Composites.pdf.

[32]   R. Kotte, *"Der Resin-Transfer-Molding-Process"*, Dissertation, RWTH Aachen, 1991.

[33] H, Tengler, *"Erkenntnisse bei der Weiterentwicklung des Vakuum-Injektionsverfahrens zur Herstellung hochleistungsfahiger Bauteile aus CFK Kunststoffe"*, 1985, 75, 2, pp. 73-75.

[34] J. Kretschmer, *"Composites in automotive applications-state of the art and prospects"*, Material Science and Technology, 1998, 4, Sep, pp. 757-767.

[35] J. Humphreys, *"Composites For Automotive On-Engine Applications"*, Materials & Design, 1987, 8, 3, pp. 147-151.

[36] *"Phenolic resin plates"*, Plastic Industry News, 1985, 31, 1, pp. 2.

[37] *"Phenolic foam tile system"*, Euopean Plastics News, 1987, 14, 12, pp. 3.

[38] *"Fire-safe flooring materials non-conductive and strong"*, Reinforced Plastics, 1996, May, pp. 7.

[39] *"Cladding material for fire protection"*, Reinforced Plastics, 1994, Feb, pp. 10.

[40] *"DSM opens door o recycling"*, Reinforced Plastics, 1994, Jun, pp. 42.

[41] *"Synthetic takes on cast iron"*, Reinforced Plastics, 1996, Jul/Aug, pp. 16.

[42] *"Mineral-filled polyester sounds better"*, Reinforced Plastics, 1995, Dec, pp. 4.

[43] A. J. Moulson, J. M. Herbert, *"Electroceramics: Materials, Properties, and Applications"*, Chapman and Hall, London, UK, 1990.

[44] J. Runt, E. C. Galgoci, *"Polymer/Piezoelectric Ceramic Composites: Polystyrene and Poly(methyl methacrylate) with PZT"*, Journal of Applied Polymer Science, 1984, 29, pp. 611-617.

[45] D. P. Skinner, R. E. Newnham, L. E. Cross, *"Flexible composite transducers"*, Materials Research Bulletin, 1978, 13, pp. 599-607.

[46] Q. M. Zhang, H. Wang, L. E. Cross, *"Piezoelectric tubes and tubular composites for actuator and sensor applications"*, Journal of Materials Science, 1993, 28, pp. 3962-3968.

[47] J. N. Weber, E. W. White, *"Replamineform: A New Process for Preparing Porous Ceramic, Metal, and Polymer"*, Prosthetic Materials Science, 1972, 176, May, pp. 922-924.

[48] T. R. Shrout, W. A. Schulze, J. V. Biggers, *"Simplified Fabrication of PZT/Polymer Composites"*, Materials Research Bulletin, 1979, 14, pp.1553-1559.

[49] General Electric Company, Schenectady, NT, USA, *"Piezoelectric composite with anisotropic 3-3 connectivity"*, US Patent, 1997.

[50]    General Electric Company, Schenectady, NY, USA, *"Method for fabricating lamellar piezoelectric preform and composite"*, US Patent, 1997.

[51]    General Electric Company, Schenectady, NY, USA, *"Piezoelectric composite with anisotropic 3-3 connectivity"*, Europlastics Patent, 1996.

[52]    A. Safari, V. F. Janas, A. Bandyopadhyay, R. k. Panda, M. K. Agarwala, S. C. Danforth, *"Method for producing novel ceramic composites"*, US Patent, 1999.

[53]    Bandyopadhyay, R. K. Panda, V. F. Janas, M. K. Agarwala, S. C. Danforth, A. Safari, *"Processing of Piezocomposites by Fused Deposition Technique"*, Journal of American Ceramic Society, 1997, 80, 6, pp. 1366-1372.

[54]    *"Polymeric Composite Materials"*, http://www.mpg.de/pdf/europeanWhiteBook/wb_materials_216_218.pdf.

[55]    *"Brite Euram project: Assessment of Metal Matrix Composites for Innovations"*: http://mmc-assess.tuwien.ac.at/.

[56]    *"Metal Matrix Composites: Challenges and Opportunities"*, http://www.mpg.de/pdf/europeanWhiteBook/wb_materials_210_213.pdf

[57]    T. W. Clyne, and P. J. Withers, *"An Introduction to Metal Matrix Composites"*, Cambridge University Press, Cambridge, 1993.

[58]    S. Suresh, A. Mortensen and A. Needleman Eds., *"Fundamentals of Metal Matrix Composites"*, Butterworths, Boston, 1993.

[59]    A. Mortensen, J. A. Cornie, M. C. Flemings, *"Solidification Processing of Metal-Matrix-Composites, Materials & Design"*, 1989, 10, 2, pp. 68-75.

[60]    C. Liu, S. Pape, J. J. Lewandowski, *"Effect of Matrix Microstructure and Interfaces on Influencing Monotonic Crack Propagation in SiC/Al Alloy Composites"*, Interfaces in Polymer, Ceramic and Metal Matrix Composites, pp. 513-524.

[61]    B.Harris, *"Engineering Composite Materials"*, IOM Communications Ltd, London, UK, 1999.

[62]    T. W. Clyne, M. G. Bader, G. R. Cappleman, P. A. Hubert, *"The use of d-alumina fibre for metal-matrix composites"*, Journal of Material Science, 1985, 20, pp. 85-96.

[63]    M. Taya, R. J. Arsenault, *"Metal Matrix Composites"*, Pergamon Press, Oxford, UK, 1989.

[64]    A. Mortensen, *"Metal Matrix Composites in Industry: an overview"*,

http://mmc-assess.tuwien.ac.at/index1.htm.

[65]    Z. Zhu, "*A Literature survey on fabrication methods of cast reinforced metal composites*", Cast Reinforced Metal Composites, Proceedings of the International Symposium on Advances in Cast Reinforced Metal Composites, 1988, pp. 93-99.

[66]    M. K. Aghjanian, M. A. Rocazella, J. T. Burke, S. D. Keck, "*The fabrication of metal matric composites by a pressureless infiltration technique*", Journal of Material Science, 1991, 26, pp. 447-454.

[67]    A. Brown, "*Metal matrix composites on the road*", Materials World, 1993, Jan, pp. 20-21.

[68]    G. Curran, MMCs: "*The future*", Materials World, 1998, Jan, pp. 20-21.

[69]    J. A. Hooker, P. J. Doorbar, "*Metal Matrix Composites for aeroengines*" Materials Science and Technology, 2000, 16, Jul/Aug, pp. 725-731.

[70]    J. Goni, I. Mitxelena, J. Coleto, "*Development of low cost metal matrix composites for commercial applications*", Materials Science and Technology, 2000, 16, Jul/Aug, pp. 743-746.

[71]    C. Baker, "*Metal Matrix Composites VI*", Material World, 1998, Jan, pp. 22-23.

[72]    A. Mortensen, L. J. Masur, J. A. Cornie, M. C. Flemings, "*Infiltration of Fibrous Preforms by a Pure Metal*": Part 1. Theory Metallurgical and Material Transactions A, 1989, 20A, Nov., pp. 2535-2547.

[73]    L. J. Masur, A. Mortensen, J. A. Cornie, M. C. Flemings, "*Infiltration of Fibrous Preforms by a Pure Metal*": Part II. Experiment Metallurgical and Material Transactions A, 1989, 20A, Nov., pp. 2549-2557.

[74]    A. Mortensen, T. Wong, "*Infiltration of Fibrous Preforms by a Pure Metal*": Part III. Capillary Phenomena, Metallurgical and Material Transactions A, 1990, 21A, Aug., pp. 2257-2263.

[75]    A. Mortensen, V. J. Michaud , J. A. Cornie, M. C. Flemings, L. J. Masur, "*Kinetics of fibre preform infiltration, Cast Reinforced Metal Composites*", Proceedings of the International Symposium on Advances in Cast Reinforced Metal Composites, 1988, pp. 7-13.

[76]    J. Narciso, A. Alonso, A. Pamies, C. Garcia-Cordovilla, E. Louis, "*Factors Affecting Pressure Infiltration of Packed SiC Particulates by Liquid Aluminium*", Metallurgical and Material Transactions A, 1995, 26A, Apr., pp. 983-990.

[77] A. Alonso, A. Pamies, J. Narciso, C. Garcia-Cordovilla, E. Louis, "*Evaluation of the Wettability by Liquid Aluminium with Ceramic Particulates (SiC, TiC, $Al_2O_3$ ) by Means of Pressure Infiltration*", Metallurgical and Material Transactions A, 1993, 24A, Jun., pp. 1423-1431.

[78] T. R. Jonas, J. A. Cornie, K. C. Russel, "*Infiltration and Wetting of Alumina Particulate Preforms by Aluminium and Aluminium-Magnesium Alloys*", Metallurgical and Material Transactions A, 1995, 26A, Jun., pp. 1491-1497.

[79] F. A. Acosta, A. H. Castillejos, "*A mathematical Model of Aluminium Depth Filtration with Ceramic Foam Filters : Part 1, Validation for Short-Term Filtration*", Metallurgical and Material Transactions B, 2000, 31B, pp. 491-502.

[80] F. A. Acosta, A. H. Castillejos, "*A mathematical Model of Aluminium Depth Filtration with Ceramic Foam Filters: Part 2, Application to Long-Term Filtration*", Metallurgical and Material Transactions B, 2000, 31B, pp. 503-514.

[81] G. P. Martins, D. L. Olson, G. R. Edwards, "*Modelling of Infiltration Kinetics for Liquid Metal Processing of Composites*", Metallurgical and Material Transactions B, 1988, 19B, Feb., pp. 95-101.

[82] E. Lacoste, M. Davis, F. Girot, J. M. Quenisset, "*Numerical simulation of the injection moulding of thin parts by liquid metal infiltration of fibrous performs*", Materials Science and Engineering A, 1991, A135, pp. 45-49.

[83] M. D. M. Innocentini, V. R. Salvini, V. C. Pandolfelli, J. R. Coury, "*The Permeability of Ceramic Foams*", American Ceramic Society Bulletin, 1999, Sep, pp. 78-84.

[84] M. D. M. Innocentini, V. R. Salvini, V. C. Pandolfelli, J. R. Coury, "*Assessment of Forchheimr's Equation to Predict the Permeability of Ceramic Foams*", Journal of American Ceramic Society, 1999, 82, 7, pp. 1945-1948.

[85] M. D. M. Innocentini, V. R. Salvini, V. C. Pandolfelli, J. R. Coury, "*The Permeability of Ceramic Foams*", American Ceramic Society Bulletin, 1999, Sep, pp. 78-84.

[86] S.- Y. Oh, J. A. Corne, K. C. Russel, "*Wetting of Ceramic Particulates with Liquid Aluminium Alloys: Part I. Experimental Techniques*", Metallurgical and Material Transactions A, 1989, 20A, pp. 527-532.

[87] C.-S. Lim, "*The Production and Evaluation of Fibre Preform Infiltrated Metal-Matrix-Composite Castings Produced by a Development of Pressure Assisted Investment casting process*", Doctoral Thesis at Loughborough University of

Technology, 1995.

[88]   J. Gerber, "*Druckguss*", Verlag Technik, Berlin, 1991.

[89]   E. Brunhuber, "*Praxis der Druckgussfertigung*", Schiele & Schoen, Berlin, 1991.

[90]   M. A. H. Howes, "*Ceramic-Reinforced Metal Matrix Composites Fabricated by Squeeze Casting Advanced Composites*", Conference Proceedings, Dearborn, Michigan, American society for metals, Pennsylvania, US, 1985, pp. 223-230.

[91]   K. U. Kainer, E. Boehm, "*Pressgiessen (Squeeze-Casting) von Magnesium Legierungen*", VDI-Berichte, 1995, Vol. 1235, pp. 117-125.

[92]   A. J. Clegg, "*Precision Casting Processes*", Pergamon Press, Oxford, UK, 1991.

[93]   P. K. Rohatgi, R. Asthana, "*Solidification Processing of Metal – Matrix – Composites*", Proceedings of the International Symposium on Advanced Structural Materials, pp. 43-51.

[94]   M. S. Yong, "*Process Optimisation of Squeeze Cast Magnesium-Zinc-Rare Earth Alloys and Short Fibre Composites*", Doctoral Thesis at Loughborough University of Technology, 1999.

[95]   H. Fukunaga, "*Squeeze casting process for fibre reinforced metals and their mechanical properties*", Cast Reinforced Metal Composites, Proceedings of the International Symposium on Advances in Cast Reinforced Metal Composites, 1988, pp. 101-107.

[96]   S. K. Verma, J. L. Dorcic, "*Manufacturing of composites by squeeze castingCast Reinforced Metal Composites*", Proceedings of the International Symposium on Advances in Cast Reinforced Metal Composites, 1988, pp. 115-126.

[97]   L. Siaminwe, "*Optimisation of the Mechanical Properties in an Investment Cast Aluminium Alloy*", Doctoral Thesis at Loughborough University of Technology, 1997.

[98]   C. S. Lim, A, J. Clegg, "*A Hybrid Investment Casting Process for the Production of Metal Matrix Composites*", Foundryman, 1996, Sep, pp. 279-285.

[99]   M. K. Aghjanian, M. A. Rocazella, J. T. Burke, S. D. Keck, "*The fabrication of metal matric composites by a pressureless infiltration technique*", Journal of Material Science, 1991, 26, pp. 447-454.

[100]  "*HI-POR company brochure*", Hi-Por Ceramics Ltd, Sheffield, UK.

[101]   Crystic 471 PALV, *"Data sheet of polyester resin"*, Scott Bader Company Ltd, Wollaston, Wellingborough, Northamptonshire, UK, November 2000.

[102]   Crystic Envirotec LS451PA, *"Data sheet of polyester resin"*, Scott Bader Company Ltd, Wollaston, Wellingborough, Northamptonshire, UK, September 2001.

[103]   West System Epoxy Resin, *"Data sheet of epoxy resin"*, Scott Bader Company Ltd, West Midlands Regional Centre, Brierley Hill, UK, July 2003.

[104]   *"KYNAR® Chemical resistance tables"*, ATOFINA UK LTD.

[105]   *"KYNAR® & KYNAR Flex® PVDF Performance Characteristics & Data"*, http://www.atofinachemicals.com/kynarglobal/kynar-literature.cfm

[106]   *"LM25 aluminium casting alloy, British and European Aluminium Casting Alloys – Their properties and Characteristics"*, The Association of Light Alloy Refiners, Birmingham, UK, 1992, pp. 119-122.

[107]   http://www.gordonengland.co.uk/hardness/index.htm.

[108]   R. B. Stoops & Associates, Newport, RI, *"Manufacturing Requirements of Polymer Matrix Composites"* contractor report prepared for the Office of Technology Assessment, December 1985.

[109]   According to the market research firm, Strategic Analysis (Reading, PA) as reported in *"High Technology"*, May 1986, p. 72.

[110]   M. N. Rittner, *"Metal Matrix Composites in the 21$^{st}$ Century: Markets and Opportunities"*, Report GB-108R, Business Communications Co., Inc., Norwalk, CT, 2000.

[111]   http://www.azom.com/details.asp?ArticleID=1869.

[112]   EN ISO 179-2, *"Determination of Charpy impact properties – Part 2: Instrumented impact test"*, European Standard, 1990.

[113]   EN 10045, *"Metallic materials – Charpy impact test – Part 1: Test method"*, European Standard, 1990.

[114]   V. John, *"Testing of Materials"*, MacMillian Education Ltd, London, UK, 1992, pp. 60-66.

[115]   K. G. Budinski, *"Engineering Materials – Properties and Selection"*, Prentice – Hall Inc, US, 1996, pp. 38-39.

[116]   W. Michaeli, *"Werkstoffkunde II – Kunststoffe"*, IKV der RWTH Achen, 1993.

[117]   S. Kohler, T. J. Fitzgerald, R. F. Singer, *"Herstellung und Eigenschaften von Zellularem Magnesium"*, VDI-Berichte, 1995, Vol. 1235, pp. 305 – 319.

[118]  http://www.mkt-intl.com/ceramics/alumina.html.

[119]  F. F. Lange, K. T. Miller, *"Open-cell, low density ceramics fabricated from reticulated polymer substrates"*, Journal of the American Ceramic Society, 1987, 70, 4, pp. 827 – 831.

[120]  R. Brezny, D. J. Green, *"Fracture behaviour of open-cell ceramics"*, Journal of the American Ceramic Society, 1989, 72, 7, pp. 1145 – 1152.

[121]  R. Lenormand and C. Zarcone, *"Percolation in an Etched Network: Measurement of Fractal Dimension"*, Rev. lett., 1986, 54, pp. 2226.